



**British
Geological Survey**

NATURAL ENVIRONMENT RESEARCH COUNCIL

Contaminant mobility as a result of sediment inundation: Literature review and laboratory scale pilot study on mining contaminated sediments

Groundwater Science Programme

Open Report OR/11/051



BRITISH GEOLOGICAL SURVEY

GROUNDWATER SCIENCE PROGRAMME

OPEN REPORT OR/11/051

Contaminant mobility as a result of sediment inundation: Literature review and laboratory scale pilot study on mining contaminated sediments

The National Grid and other Ordnance Survey data are used with the permission of the Controller of Her Majesty's Stationery Office.
Licence No: 100017897/2011.

Keywords

Sediment, flooding, mining, contamination, laboratory experiment, Rookhope Burn, Weardale, lead contamination.

Front cover

Rookhope Burn at Wolf Cleugh, North Pennine, UK.

Bibliographical reference

WRAGG, J AND PALUMBO-ROE, B. 2011. Contaminant mobility as a result of sediment inundation: Literature review and laboratory scale pilot study on mining contaminated sediments. *British Geological Survey Open Report*, OR/11/051. 101pp.

Copyright in materials derived from the British Geological Survey's work is owned by the Natural Environment Research Council (NERC) and/or the authority that commissioned the work. You may not copy or adapt this publication without first obtaining permission. Contact the BGS Intellectual Property Rights Section, British Geological Survey, Keyworth, e-mail ipr@bgs.ac.uk. You may quote extracts of a reasonable length without prior permission, provided a full acknowledgement is given of the source of the extract.

Maps and diagrams in this book use topography based on Ordnance Survey mapping.

J Wragg and B Palumbo-Roe

BRITISH GEOLOGICAL SURVEY

The full range of our publications is available from BGS shops at Nottingham, Edinburgh, London and Cardiff (Welsh publications only) see contact details below or shop online at www.geologyshop.com

The London Information Office also maintains a reference collection of BGS publications, including maps, for consultation.

We publish an annual catalogue of our maps and other publications; this catalogue is available online or from any of the BGS shops.

The British Geological Survey carries out the geological survey of Great Britain and Northern Ireland (the latter as an agency service for the government of Northern Ireland), and of the surrounding continental shelf, as well as basic research projects. It also undertakes programmes of technical aid in geology in developing countries.

The British Geological Survey is a component body of the Natural Environment Research Council.

British Geological Survey offices

BGS Central Enquiries Desk

Tel 0115 936 3143 Fax 0115 936 3276
email enquiries@bgs.ac.uk

Kingsley Dunham Centre, Keyworth, Nottingham NG12 5GG

Tel 0115 936 3241 Fax 0115 936 3488
email sales@bgs.ac.uk

Murchison House, West Mains Road, Edinburgh EH9 3LA

Tel 0131 667 1000 Fax 0131 668 2683
email scotsales@bgs.ac.uk

Natural History Museum, Cromwell Road, London SW7 5BD

Tel 020 7589 4090 Fax 020 7584 8270
Tel 020 7942 5344/45 email bgs_london@bgs.ac.uk

Columbus House, Greenmeadow Springs, Tongwynlais, Cardiff CF15 7NE

Tel 029 2052 1962 Fax 029 2052 1963

Maclean Building, Crowmarsh Gifford, Wallingford OX10 8BB

Tel 01491 838800 Fax 01491 692345

Geological Survey of Northern Ireland, Colby House, Stranmillis Court, Belfast BT9 5BF

Tel 028 9038 8462 Fax 028 9038 8461

www.bgs.ac.uk/gsni/

Parent Body

Natural Environment Research Council, Polaris House, North Star Avenue, Swindon SN2 1EU

Tel 01793 411500 Fax 01793 411501
www.nerc.ac.uk

Website www.bgs.ac.uk

Shop online at www.geologyshop.com

Foreword

This report is the published product of a study by the British Geological Survey (BGS) with funding from the Natural Environment Research Council. The study reports the findings of a literature review for soil and sediment inundation methodologies and the results of a laboratory scale pilot study, undertaken as a result of the literature review, to characterise the mobility of potentially harmful elements from mining contaminated sediments during flooding. The work described herein forms part of a larger project aiming to characterise the environmental effects of historical mining in the Rookhope catchment, Upper Weardale, North Pennine.

Acknowledgements

The authors gratefully acknowledge the assistance of Vanessa Banks, Simon Chenery and Ben Klinck during the field work and BGS Analytical Geochemistry for chemical analysis of water and sediment samples.

Contents

Foreword	i
Acknowledgements	i
Contents	i
Summary	vi
1 Introduction	1
1.1 Contaminated land and inundation events.....	1
1.2 Impact of mining contaminated sediments in response to flood disturbance.....	2
2 Inundation Methodology Literature Search	3
3 Sampling of Rookhope Burn River Bank Sediments and Stream Water	6
4 Inundation Pilot Experiment	13
4.1 Experimental set-up.....	13
5 Analytical Techniques	15
5.1 Characterisation of sediments by X-ray Diffraction analysis (XRD).....	15
5.2 Mixed acid digestion of Sediments	15
5.3 Analysis of the rookhope stream water, of the inundation water and bulk pore water	17
6 Results	20
6.1 Rookhope sediments characterisation	20
6.2 Inundation experiments	21
6.3 Pore water composition	36
6.4 Saturation indices	37
6.5 Zn/SO ₄ and Cd/Zn molar ratios	41
7 Discussion	42
8 Conclusions	45

Appendix 1	Water and Sediment Quality Standards	46
Appendix 2	XRD Sediment Characterisation data	48
Appendix 3	Sediment Characterisation data, Organic Matter (OM, %), pH and total elemental concentrations (mg kg⁻¹).....	49
Appendix 4	Inundation water characterisation data	50
Appendix 5	Inundation Experiment Information and Laboratory Measurement Data	51
Appendix 6	WDS 16, Inundated water data	53
Appendix 7	WDS 23, Inundated water data	56
Appendix 8	WDS 45, Inundated water data	59
Appendix 9	WDS 46, Inundated water data	62
Appendix 10	WDS 47, Inundated water data	65
Appendix 11	Residual bulk pore-water data	68
Appendix 12	Release rate curves for analysed elements in the study where sediment information has been determined	71
	Aluminium	71
	Arsenic	72
	Barium.....	73
	Calcium	74
	Cadmium	75
	Cobalt	76
	Chromium	77
	Lithium.....	78
	Magnesium.....	79
	Nickel	80
	Potassium	81
	Selenium.....	82
	Sodium	83
	Strontium.....	84
	Sulphur	85
	Vanadium	86
References		87

FIGURES

Figure 1	Sampling locations.....	7
Figure 2	Sampling location 1: Wolf Cleugh (sample WDS 46).	8
Figure 3	Detail of river banks at Wolf Cleugh (sample WDS 46).....	8

Figure 4	Sampling location 2: Tailrace Level (sample WDS 45).....	9
Figure 5	Details of river banks at Tailrace Level (sample WDS 45).....	9
Figure 6	General view of Rookhope Burn near the Rookhope Arch (Sampling location 3)...	10
Figure 7	Sampling Location 3: Rookhope Burn near Rookhope Arch (sample WDS 16).	10
Figure 8	Sampling location 4: Rookhope burn near Church House (sample WDS 23).....	11
Figure 9	Detail of sampling location 4 of Rookhope burn riverbank sediments near Church House (sample WDS 23).	11
Figure 10	Sampling location 5: Rookhope Burn at South Smailburn plantation (sample WDS 47).....	12
Figure 11	Schematic of the laboratory based inundation experiment.	14
Figure 12	pH changes during the flooding of the Rookhope sediments, the errors are calculated as the difference between the two replicates divided by two.	23
Figure 13	Iron release rate curve, $\mu\text{g l}^{-1}$	25
Figure 14	Lead release rate curve, $\mu\text{g l}^{-1}$	26
Figure 15	Expanded lead release rate curve, $\mu\text{g l}^{-1}$ for the 0-10 day time period.	26
Figure 16	Lead release rate curve, % of the original sediment concentration.	28
Figure 17	Copper release rate curve, $\mu\text{g l}^{-1}$	29
Figure 18	Copper release rate curve, % of the original sediment concentration.	29
Figure 19	Manganese release rate curve, $\mu\text{g l}^{-1}$	32
Figure 20	Manganese release rate curve, % of the original sediment concentration.	32
Figure 21	Zinc release rate curve, $\mu\text{g l}^{-1}$	33
Figure 22	Zinc release rate curve, % of the original sediment concentration.	35
Figure 23	SO_4^{2-} release rate curve, mg l^{-1}	35
Figure 24	Box and Whisker plots showing the range of selected analyte concentrations in the inundation waters collected at 88 days (IW) and the sediment bulk pore waters (PW) for the sites under investigation.	37
Figure 25	Plots of Zn/SO_4 and $\text{Cd (x100)}/\text{Zn}$ molar ratios across the inundation period.	41
Figure 26	Aluminium rate release curve, $\mu\text{g l}^{-1}$	71
Figure 27	Aluminium release rate curve, % of the original sediment concentration.....	71
Figure 28	Arsenic rate release curve, $\mu\text{g l}^{-1}$	72
Figure 29	Barium release rate curve, $\mu\text{g l}^{-1}$	73
Figure 30	Barium rate release curve, % of the original sediment concentration	73
Figure 31	Calcium release rate curve, mg l^{-1}	74
Figure 32	Calcium release rate curve, % of the original sediment concentration.....	74
Figure 33	Cadmium release rate curve, mg l^{-1}	75
Figure 34	Cadmium release rate curve, % of the original sediment concentration	75
Figure 35	Cobalt release rate curve, $\mu\text{g l}^{-1}$	76
Figure 36	Cobalt release rate curve, % of the original sediment concentration.....	76
Figure 37	Chromium release rate curve, $\mu\text{g l}^{-1}$	77

Figure 38	Lithium release rate curve, $\mu\text{g l}^{-1}$	78
Figure 39	Lithium release rate curve, % of the original sediment concentration	78
Figure 40	Magnesium release rate curve, mg l^{-1}	79
Figure 41	Magnesium release rate curve, % of the original sediment concentration	79
Figure 42	Nickel release rate curve, mg l^{-1}	80
Figure 43	Nickel release rate curve, % of the original sediment concentration.....	80
Figure 44	Potassium release rate curve, mg l^{-1}	81
Figure 45	Potassium release rate curve, % of the original sediment concentration.....	81
Figure 46	Selenium release rate curve, mg l^{-1}	82
Figure 47	Selenium release rate curve, % of the original sediment concentration	82
Figure 48	Sodium release rate curve, mg l^{-1}	83
Figure 49	Sodium release rate curve, % of the original sediment concentration.....	83
Figure 50	Strontium release rate curve, $\mu\text{g l}^{-1}$	84
Figure 51	Strontium release rate curve, % of the original sediment concentration	84
Figure 52	Sulphur release rate curve, mg l^{-1}	85
Figure 53	Sulphur release rate curve, % of the original sediment concentration.....	85
Figure 54	Vanadium release rate curve, mg l^{-1}	86
Figure 55	Vanadium release rate curve, % of the original sediment concentration.....	86

TABLES

Table 1	Rookhope Burn Sediment Samples (upstream to downstream sequence).....	7
Table 2	Volume and colour of bulk pore water (pre and post filtering)	14
Table 3	ICP-MS calibration ranges for elements listed in Table 1, after Breward et al. (2009)19	
Table 4	Particle size distribution in Rookhope river bank sediment samples	20
Table 5	Summary of concentrations of selected environmentally sensitive elements in Rookhope Burn stream sediments, mg kg^{-1} , ordered from upstream to downstream (PHEs that are above the TEL are highlighted in italics and those PHEs above both the TEL and the PEL are denoted by bold italics).....	21
Table 6	Summary of concentrations of selected environmentally sensitive elements in Rookhope Burn stream water sample	22
Table 7	Average iron concentrations in the inundation water during flooding. Concentrations in bold are above the EQS.	24
Table 8	Average lead concentrations in the inundation water during flooding. Concentrations in bold are above the EQS.	27
Table 9	Average copper concentrations in the inundation water during flooding. Concentrations in bold are above the EQS	30
Table 10	Average manganese concentrations in the inundation water during flooding.....	31
Table 11	Average zinc concentrations in the inundation water during flooding. Concentrations in bold are above the EQS.	34

Table 12	Average sulphate concentrations in the inundation water during flooding.....	36
Table 13	Calculated SI for WDS 16, 23 and 45.....	38
Table 14	Calculated SI for WDS 46 and 47.....	40

Summary

This report presents a literature review of soil and sediment inundation methodologies and describes a pilot scale laboratory inundation study.

Changing weather conditions, subsequent flooding events, and the increased frequency of such events both in the UK and worldwide is highlighting the need to research the area of contaminant mobility from soils and sediments under inundated conditions. The findings of such investigations impact on a wide variety of sectors, including human and ecological health, agriculture, building, transport, world economy and climate change.

Standardised methodologies for the investigation of contaminant mobility resulting from soil/sediment inundation episodes are not available. Most research has been conducted in the agricultural sector for nutrient transport, as part of soil fertility and plant nutrition studies. Only recently has work been undertaken for studying potentially harmful element transport in inundated sediments/soils.

A pilot scale laboratory study was undertaken using contaminated bank sediment samples collected from the Rookhope Burn catchment, Northern England, UK, with the aim to examine the extent of contaminant mobilisation from flooded sediments. The catchment has been affected by historical mining and processing of lead and zinc ore and is representative of several catchments affected by the environmental legacy related to mining in the Northern Pennine Orefield.

Bank sediment Pb and Zn concentrations were found significantly above both the TEL and PEL sediment quality criteria, posing potentially a significant hazard to aquatic organisms. The source of the Pb and Zn in the sediments is related to the underlying mineralisation, mining activities and mine water discharges in the catchment. Abundances of original sulphide ore and authigenic metal-bearing phases were expected to vary through the catchment.

The study design simulated rising flood water, a slow saturation of the sediment in order to induce a slow change in physico-chemical properties, followed by a 3 month (88 day) stagnation period. Natural day-night cycles were simulated by undertaking the study on the bench top during the winter of 2009/2010 (November to February). The chemical changes in the inundation water during the experiment were monitored and the sediment pore water at the end of the inundation period analysed. The inundation water pH remained alkaline to neutral, while redox measurements indicated oxic conditions in the water column throughout the inundation period.

The pilot study showed that inundation of river bank sediments from the Rookhope Burn may be a significant pathway for contaminants in the catchment and that mobilisation from the sediments may pose a hazard to environmental receptors in the area, particularly with respect to Pb and Zn contamination. The different degrees and different rates of metal losses to the overlying water column observed during the flooding of the Rookhope Burn bank sediments demonstrated that the significance of metal mobilisation was dictated by the sediment composition.

The inundation water composition monitored during the sediment flooding was used to indirectly infer possible processes that control contaminant fluxes from the sediments to the overlying water. Dissolved Pb concentration in the inundation water reflected the original concentration in the solid material and in sediments that had XRD-detectable galena and cerussite the dissolved Pb concentration reached a maximum value of $395 \mu\text{g l}^{-1}$. Cerussite, which is commonly formed as coatings on galena during the sulphide weathering, was close or supersaturated in those solutions, suggesting that the lead carbonate mineral phase provided a continuous source of Pb to these solutions.

The initial dissolved Zn in the inundation waters was independent of the original concentration in the sediments. Sediments downstream a mine water discharge showed a greater availability of easily mobilised Zn, producing high initial Zn concentration in the inundation water, despite the relatively low Zn concentration in the inundated sediment. The Zn/SO₄ and Cd/Zn molar ratios were both consistent with sphalerite mineral oxidation. The final inundation water solutions had the highest Zn concentrations for those sediment samples where sphalerite was detected by XRD.

Redox sensitive elements such as Fe and Mn could not unequivocally indicate the presence of reducing conditions within the flooded sediments and the redox measurements were carried out only in the overlying water column (ORP above 200-350 mV). Low organic matter content and sandy texture would not have favoured the rapid formation of an anoxic layer. Yet, only extending the ORP measurements to the submerged sediment would determine the presence of flooding-induced reducing conditions. Reductive dissolution of Mn oxyhydroxides would result in release of Mn into solution, along with other trace metals, such as Pb and Zn. Mn increased in the inundation water throughout most or all the inundation period for some of the studied sediments. Their final pore water composition was significantly enriched in Mn (1300-6500 µg l⁻¹). Saturation indices indicated both rhodocrosite (MnCO₃) and Mn oxides reached saturation. Therefore, it was not possible to preclude either the role of rhodocrosite as solubility controlling solid phase or the reductive dissolution of Mn oxides for accounting the enhanced Mn concentrations in the pore water and overlying water column without a better characterisation of the solid phase and monitoring of the sediment redox conditions.

Amendments to the inundation test design have been recommended, which comprise:

- set-up to allow for the continuous monitoring of pore water dynamics and allow for the collection of pore water at the different times and measurement of pore water pH and Eh;
- inclusion of a blank test cell, to test the influence of the properties and the volume of the inundation water;
- inclusion of flow-cell tests to assess the influence of moving or stagnant inundation water;
- the inclusion of abiotic blanks to identify the role microbes play in the solubilisation of contaminants.
- complementary characterisation of the solid phase material and metal distribution in the sediment before and after the inundation experiment.

1 Introduction

1.1 CONTAMINATED LAND AND INUNDATION EVENTS

Phenomena such as increased incidences of flooding are expected to become more common with continuing climate change effects (Howe and White, 2002; Macklin and Rumsby, 2007; Smit *et al.*, 2008). The floods in October and November 2000 and in 2007 affected large areas of the UK and caused chaos, affecting many urban and rural communities (Dennis *et al.*, 2003; BBC, 2007). In 2000 the widespread disruption and damage to property was estimated at £1 billion (Dennis *et al.*, 2003). In light of the changing weather conditions, subsequent flooding events, and the increased frequency of such events in the UK, it is considered that the size of land mass which is potentially 'at risk' will be substantially increased in size by 2050 (BBC, 2007). There is now an increasing awareness of flood and inundation hazard in many sectors at local, national and international level, likely because of the frequency of such events in many regions. The sectors affected include health, insurance, building, food and transport.

There is a growing body of peer reviewed papers discussing the physical effects of extreme weather events (Kennedy *et al.*, 2011; Romanescu *et al.*, 2011). A large proportion of these studies have concentrated on issues such as the physical destruction of the surrounding area, *e.g.* the widespread inundation of land, which has resulted in the physical destruction of embankments and buildings and the loss of human and animal life (Robins *et al.*, 2011; Romanescu *et al.*, 2011). Key papers are available that discuss flood management plans from 'notice to alert and alarm' with respect to better risk management and protection from inundation and improvement of public perception of said risk management (Hernandez *et al.*, 2011; Pagneux *et al.*, 2011; Pappenberger *et al.*, 2011; Yin *et al.*, 2011). In light of the inundation caused by the Japanese earthquake, tsunami and subsequent damage to the Fukushima Nuclear plant, consideration in the literature is also now being given to the impacts of extreme weather events on existing nuclear power plants and the siting of future facilities (Wilby *et al.*, 2011). This is particularly important in terms of the potential mobilisation of radionuclides through the geosphere.

In response to flood disturbance, contaminant transport may be affected by both the physical movement and chemical effects of flooding, such as soil/sediment erosion or re-deposition (Rotkin-Ellman *et al.*, 2010; Bert *et al.*, 2009; Boardman *et al.*, 2009), and remobilisation, as a result of changes in the physico-chemical characteristic of the solid matrix (Zhao *et al.*, 2009). International research has shown soil Potentially Harmful Element (PHE) mobility to be affected by flooding events (Charlatchka and Cambier, 2000; Codling and Dao, 2007; Erber and Felix-Henningsen, 2001; Golden *et al.*, 1997; Lacal *et al.*, 2003; Ma and Dong, 2004; Moalla and Pulford, 1995; McGeechan, 1996; Naftz *et al.*, 2005; Neumeister *et al.*, 1997; Newman and Pietro, 2001; Pant *et al.*, 2002; Reynolds *et al.*, 1999; Schreiber *et al.*, 2005; Van den Berg *et al.*, 1998). The mobility of PHEs in sediments as a result of flooding has been studied by Batson *et al.*, 1996; Johnston *et al.*, 2011. In a review by Bert *et al.* (2009) it was noted that PHE mobility is significantly influenced by changes in oxygenation and the redox status of sediments and the bacterial colonies living within the sediment; depending on the PHEs present, these changes may further mobilise or immobilise contaminants which will in turn impact on the (eco)toxicity of the sediment to the surrounding 'at risk' environmental receptors. Such conditions had been previously investigated by Van der Geest and Leon Pauman (2008), whose study of a polluted floodplain found that changing environmental conditions resulted in a stable chemical environment with no detrimental effect to ecological receptors. However, this finding appears to be site specific or potentially related to the source/composition of the inundation water. Du Laing *et al.*, (2008) found that cadmium (Cd) mobilisation in oxidised sediment layers was influenced by the salt content of the flood water.

Geochemical mapping of soils and sediments (Billett *et al.*, 1997; Fordyce *et al.*, 2005; Johnson *et al.*, 2005; Jorgensen *et al.*, 2005; Simpson *et al.*, 1996; Simpson *et al.*, 1993) has shown that

there are large areas of the UK where there are potentially hazardous concentrations of a number of PHEs, *e.g.* arsenic (As), Cd, chromium (Cr), nickel (Ni), lead (Pb) and zinc (Zn). In addition to the naturally occurring sources of PHEs in the environment, current and historical metal mining, both internationally, but more specifically in the UK in the context of this study, has contributed to large areas of contaminated land, river channels and floodplains (Macklin *et al.*, 2006; Zhao *et al.*, 2009). Whether their presence in soils/sediments poses a risk to human or ecological receptors depends upon a number of factors, one being the presence of an exposure pathway, in the commonly used pollutant linkage paradigm of source-pathway-receptor (Holdgate, 1979). Inevitably, whichever pathway is considered, the mechanism which allows the pathway to exist involves the solubilisation of the PHE. For example, in the case of plant uptake the PHE has to be dissolved in the soil pore-water, while for human uptake by soil or plant ingestion the PHE requires dissolution in the digestive fluids of the receptor before its toxicity can take effect. The key to measurement of risk is therefore the mobility of the PHE into different environments. Groundwater and stream water vulnerability is a concern as these are primary environments that are at potential risk from PHE contamination resulting from increased incidences of flooding in the UK.

1.2 IMPACT OF MINING CONTAMINATED SEDIMENTS IN RESPONSE TO FLOOD DISTURBANCE

The UK has a legacy of mining-related contamination from its industrial past, which has resulted in contaminated areas with associated discrete pockets of specific contaminants; these mining areas may be particularly vulnerable to contaminant mobilisation from flooding. Historically contaminated alluvium is indeed recognised as a very important source of sediment-borne metals in all mining-affected river systems in England and Wales through remobilisation of the sediment by organisms or through river erosion processes or flood events (Hudson-Edwards *et al.*, 2008). As such, these sediments may be causing damage to aquatic ecosystems in rivers and contributing to failure of Water Framework Directive (WFD) good ecological status, even after remedial treatment of ongoing mine water discharges. Better evidence is needed to understand the potential impact of contaminated sediments on riverine ecology and their significance in terms of representing a significant barrier to the target of good ecological status, as defined in the European Water Framework Directive, in mining-impacted catchments.

This report considers the effects of flooding on contaminated sediments from the Rookhope Burn, a tributary of the River Wear in the North Pennines of the UK, an area that has a history related to the lead-zinc ore mineralization and associated mining (Banks and Palumbo-Roe, 2010). This can contribute to inform the assessment of the role of mining contaminated sediments on the river system ecology.

Objectives of the study are:

- to review existing laboratory scale methodologies of sediment inundation;
- to design and carried out a pilot laboratory-based inundation test to simulate the effects of flooding events on the potential mobility of PHEs from contaminated bank sediments and identify possible improvements/modifications in the experimental design;
- to describe the results of inundation test undertaken on the contaminated bank sediments from the Rookhope Burn catchment, a mining-impacted catchment in the Northern Pennines, UK.

2 Inundation Methodology Literature Search

An ongoing literature review of the current research highlights that there are no standardised methodologies currently available to investigate inundation. Workers from a number of different science areas (agriculture, climate change and contaminated land) are interested in both the physical (Dennis *et al.*, 2003) and chemical (Batson *et al.*, 1996; Emmerson *et al.*, 2000; Weber *et al.*, 2009 and 2010) effects of flooding, and in changes in nutrient flow to support different plant communities at sites of interest (Courtwright and Findlay, 2011). Some workers have studied the effects of inundation in-situ, in 'field' locations where tidal or floodplain inundation occurs (Camici *et al.*, 2011; Kobayashi, *et al.*, 2011; Courtwright and Findlay, 2011 and Johnston *et al.*, 2011), whilst others have simulated inundation under 'controlled' conditions (Webster *et al.*, 2002; Chatain *et al.*, 2005; Loeb *et al.*, 2006; Tack *et al.*, 2006; Begum *et al.*, 2006; Simpson *et al.*, 2008; Striker, 2008 and Nagasaka *et al.*, 2009).

The majority of available methodologies, at the time of the review, were centred on the agricultural sector and focussed on the mobility or availability of nutrients. Therefore, in order to find suitable laboratory methodologies to apply to PHE mobility, research from the agricultural sector has been used as a primary source of information with the aim of transferring methods to the Rookhope Burn Catchment in a pilot study.

In a review of the methodological aspects of flooding in relation to plant responses, Striker (2008) noted that from a database of 132 articles, crop and non-crop studies were conducted differently, with significant distinctions being the duration of the inundation. When investigating inundation of crop species, a shorter exposure time of 16 days was chosen, ranging from 8 to 28 days for the 25th and 75th percentiles. For non-crop species flooding lasted considerably longer, *circa.* 45 days, ranging from 28 to 61.5 days. This review indicates that, although there is more research in the agricultural area for inundation, there is little information regarding standard methodologies available.

Olde Venterink *et al.*, (2002) measured the effects of soil drying and re-wetting on the nitrogen mineralization and de-nitrification on soil cores from southern Sweden. When compared to keeping the soil under continuously wet conditions, the soil drying process impacted on both processes, by stimulating nitrogen mineralization by a factor of 5 and reducing de-nitrification by a factor of 3.

Inundation tests using column experiments were carried out by Nagasaka *et al.*, (2009), in order to see if the agricultural use of acid sulphate soils could be improved. In a simple column set-up, drinking water was pumped from the bottom of the column until inundation (saturation) was reached and the column was left to inundate for a total of 4 days. The outflow of the column was sampled from the bottom, until all flow had ceased, and the sulphate concentration was determined as a *pseudo* measure of soil quality improvement.

The effects of short term inundation of acid sulphate soils on the potential mobilisation of contaminants of concern was assessed in the lower River Murray and associated lakes (Simpson *et al.*, 2008). Samples were air dried at 40°C and the re-mobilisation of metals and nutrients was assessed by a simple re-suspension of the material in oxygenated unfiltered Murray River water for 24 h, using a solid to liquid ratio of 1:10 and agitation on a roller shaker at 60 rpm. Previous research indicated suitable solid:liquid ratios and extraction times. In the case of the solid:liquid ratio, substance release during shaking is expected to be partially dependent on the suspended solid concentration. However, at suspended solid concentrations greater than 10-50 g l⁻¹, substance release reaches a plateau and is independent of the suspended solid concentration. Accordingly, the authors chose the ratio of 100 g l⁻¹, i.e. 1:10. A 24 h extraction time was chosen based on kinetics experiments showing that initial contaminant release was rapid, occurring during the first 6 h of inundation and with >50% release after 24 h.

In order to determine the changes in metal biogeochemistry under different hydrological conditions Tack *et al.*, (2006) carried out two lab and field scale experiments over a two year period and investigated different physico-chemical parameters, such as metal mobility, redox status, organic matter, clay content, *etc.* For the lab experiments, 42 barrels were filled with three different soils and flooded by water of differing salinity. In contrast, the field based experiments consisted of 4 soil filled tanks (2 soil types), placed on a platform in the river Scheldt and flooded daily by river water. The mobile metal content of the soils was shown not to be related to the total metal content, but influenced by soil pH, cation exchange capacity (CEC), redox status, organic matter (OM), carbonate and clay content.

Webster *et al.*, (2002) considered the impact of contaminants at Vanda Station, New Zealand's only mainland Antarctic base, and its removal from the shores of Lake Vanda. Although the site was subject to potential inundation, soils collected from the area were only subjected to a toxicity characteristic leaching procedure (TCLP) test to look for contaminants leached with respect to their mobility.

Chatain *et al.*, (2005) investigated the effects of experimentally induced reducing conditions, by periodic inundation from fluctuating groundwater levels, on the mobility of As from a mining soil. This research used chemical reductants, sodium ascorbate ($C_6H_7NaO_6$) and sodium borohydride ($NaBH_4$), and oxidants, nitric acid (HNO_3) or potassium hydroxide (KOH), to influence the mobility of As. A solid: liquid ratio of 1:10 was applied for both the reducing and oxidising conditions; extraction was carried out at 20°C with end-over-end shaking at a rotation speed of 28 rpm. For the oxidised conditions, a pH range of 2-12 was applied to investigate As release as a function of pH. It was found that a 48 h shaking time was sufficient to reach equilibrium conditions. However, under reducing conditions, where ascorbate and borohydride were used, it was found that, because of slow reaction kinetics, a 10 day extraction was required.

The switch of soil respiration to anaerobic conditions by soil flooding was investigated by Loeb *et al.*, (2007). Mesocosm experiments were undertaken at two temperatures to test the effects of flooding with and without sulphate, as sulphate-rich river waters may induce higher phosphate mobility from soil as a result of sulphur-iron interactions. Inundated and control soils were both placed in pots with perforations at the bottom, held in containers that contained a total volume of 10L and fed fluid at a rate of 10L week⁻¹. For the inundated test soils, the containers contained an outflow 5 cm above the soil surface and for the control soils the outflow was situated 10 cm below the soil surface. All soils were stored at 5°C with an 8 h light/16 h dark regime for 4 weeks. After acclimatisation, summer flooding temperatures were simulated (20°C daytime/15°C night-time) for a total of 7 weeks. This method simulates flooding water movement, by the use of 10L week⁻¹, and not standing water, therefore it is similar in its action to 'soil washing'. Each week, a soil sample was collected and the pore water analysed for major and trace anions and cations, pH and alkalinity. On completion of the simulated flooding, all soils were allowed to dry and analysed for OM by loss on ignition (LOI), total element concentrations by acid digest and ICP, redox potential, CEC and the amorphous iron oxide content. Samples were also subjected to sequential extraction to determine the phosphorus fractionation within the material. The results of the inundation experiments show that redox potential dropped during inundation, leading to higher soil pore water manganese, iron, phosphate, ammonium, calcium and alkalinity concentrations. On drying, the redox potential increased immediately, leading to the oxidation of manganese, ammonium and iron and immobilising phosphate. An effect of temperature was seen in terms of rate of release of contaminants, *i.e.* at higher temperatures (20°C) manganese, iron, phosphate and calcium were released more quickly.

In order to determine the effects of sowing depth and the time, duration and depth of flooding glasshouse experiments were carried out on the emergence, survival and growth of a widespread weed, the *Fimbristylis milicea* (L.) Vahl (Cyperaceae family) (Begum *et al.*, 2006). When considering parameters for flooding, three flooding depths (saturated soil with no standing water,

5 cm and 10 cm above the soil surface) and three flooding durations (7, 14 and 21 days) were investigated. Unger *et al.*, (2009) investigated the flooding effects on soil microbial communities under greenhouse and field conditions. Different flood treatments (stagnant, flowing and intermittent) were compared with no treatment (control). Treatments were carried out in clear plastic trays (22 x 35 cm) lined with white bags (to reduce the amount of light entering the tray and reduce the amount of algal and moss growth) with opaque lids. Different soil treatments were applied to a soil layer of 10 cm, *circa*. 9.2 kg of material. Four replicates of each treatment were carried out, with each treatment lasting 56 days. A day was considered to be 9 h daylight and 16 h night-time, the air temperatures ranged between 17 and 20°C and the soil temperatures ranged between 16 and 18°C. The control treatment was 2.5L of de-ionised water, with further additions in order that a constant tray weight and soil water content of 30% was maintained. For the inundation treatments, flood water was added to a level 5cm above the soil surface, after Cirtain *et al.*, (2004). In the case of the stagnant water treatment, no further work was undertaken; for the flowing water scenario, water was pumped through the tray at 2.73 L min⁻¹, and for the intermittent scenario a two week flooding-drying cycle was applied, whereby the surface water was removed by bailing and draining. On completion of the inundation simulation, two 3.8 cm diameter soil cores were collected from the centre of each tray, placed in plastic bags, frozen and later freeze dried prior to analysis. The results indicated that stagnant conditions affected (decreased) the microbial biomass and markers for aerobic bacteria.

Weber *et al.* (2009) investigated the release of metals from temporarily flooded freshwater floodplain soils using microcosm experiments. This study used well drained and aerated topsoil (200 - 2000µm), collected from within 15 m of the river Mulde, near Muldenstein, Germany, an area typically flooded for periods of days to weeks within a year. A series of independent microcosm experiments were setup, whereby soil (450 g) was submerged in synthetic river water resembling the composition of river Mulde water during high flow in Spring 1998 (1500 mL 0.6 mM CaSO₄, 0.6 mM NaCl, 0.3 mM Mg (NO₃)₂ solution), suspended end-over-end for 2 h, centrifuged and the resulting soil paste directly transferred to a microcosm. The independent microcosms were setup to cover a range of parameters including height of water saturated layer, pore-water to soil ratio and total porosity under *circa* 6 cm of supernatant water. Pore water from the microcosms were sampled from below the soil-supernatant interface directly into an anoxic glovebox and filtered for elemental analysis. The results showed that initial mobilization of contaminants was driven by the reductive dissolution of Fe (III) and Mn (IV, III) hydr(oxides) and microbial activity accounted for other contaminant transformations. More recently, this group of researchers has carried out laboratory-based microcosm experiments at different temperatures to study the effects of temperature on As mobilization as a result of flooding over a 52 day period (Weber *et al.*, 2010). The study monitored Fe (II) and As (III) formation in the soil solid-phase, when a contaminated floodplain soil was flooded at 23, 14 and 5°C. Anoxic conditions were induced at all temperatures resulting in increased concentrations of dissolved Fe (II) and As (III). However, the decrease in temperature from 23 to 5°C slowed the soil reduction and, as a result, slowed also Fe and As release. The rate of microbial Fe (III) (hydr)oxide reduction was considered as the controlling mechanism of As (V) reduction and solubilisation.

3 Sampling of Rookhope Burn River Bank Sediments and Stream Water

Five river bank sediment samples were collected along the Rookhope Burn during the week of May 11th – 15th 2009, during low river flow conditions. The Rookhope catchment has been affected by historical mining and processing of Pb ore and fluorspar and is representative of several catchments affected by the environmental legacy related to mining in the Northern Pennine Orefield, Northern England, UK. Sample localities are shown in Figure 1. Evidence of former mining (mine waste heaps, tailings lagoons, mine adits) are distributed widely throughout the catchment and all sampling sites are downstream main mining features. Specific features associated with the locations are summarised in Table 1 and illustrated through Figure 2 to Figure 10.

At individual sites, a composite sample of the sediment was obtained using a stainless steel scoop, along 3-5 m on both sides of the river banks of Rookhope Burn. Cobbles and boulders were avoided. The sediments were collected in uniquely labelled sealable plastic bags and stored under refrigeration at 0-8 °C prior to further preparation and characterisation. In addition, a stream water sample was collected from the Rookhope Burn at the footbridge in the Rookhope village (co-ordinates 393750 542840) and stored in a 20 L High Density Poly Ethylene (HDPE) carboy under refrigeration at 0-8 °C prior to undertaking the inundation studies at the BGS Mine Waste Characterisation Laboratory, located within the Environmental Materials Facility (EMF). Three separate aliquots of the stream water were sampled from the original 20L carboy and preserved for analysis of its anion and cation compositions: filtration at 0.45µm for anions; filtration at 0.45µm and acidification to 1% with HNO₃ for cations.

Preparation of the sediment samples was undertaken by drying at 35°C and sieving to <150µm. The prepared material was then characterised to determine the total element composition, by mixed acid digestion (HF/HClO₄/HNO₃) and Inductively Coupled Plasma Atomic Emission Spectrometry (ICP-AES), the pH and organic matter content by a CaCl₂/slurry method and loss on ignition (LOI) at 450°C, and mineralogical analysis by X-ray Diffraction (XRD) analysis. The major and trace anion and cation composition of the Rookhope Burn stream water was characterised by Ion Chromatography (IC) and (ICP-MS). Non-Purgeable Organic Carbon analysis (NPOC) was also carried out. The pH and alkalinity of the stream water was determined in the field. The methodologies used to analyse the sediments and stream water sample collected from the Rookhope Burn catchment are described in section 5 and the data obtained from the characterisation are summarised in section 6 and appendices 1 to 10.

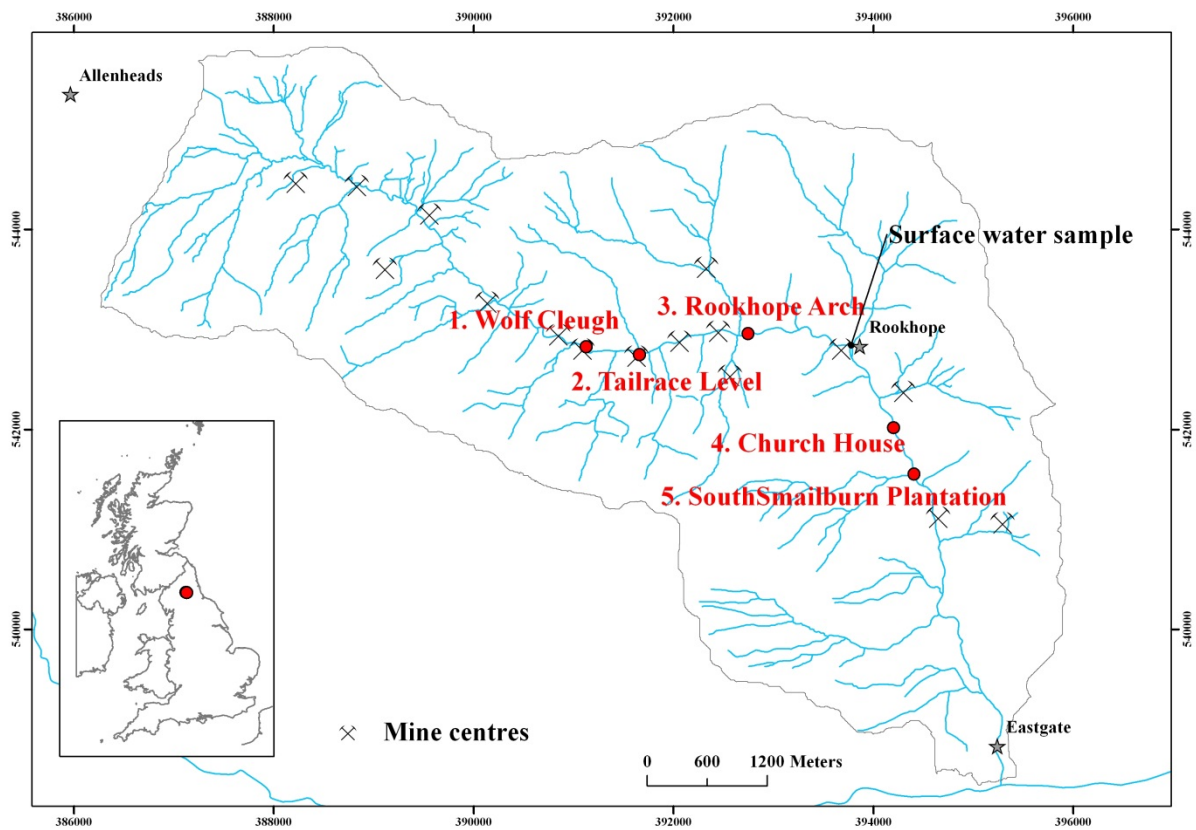


Figure 1 Sampling locations.

Table 1 Rookhope Burn Sediment Samples (upstream to downstream sequence)

Sample Name	Coordinates	General Location	Associated Mining Features	Geology
WDS 46	391127-542825	1. Rookhope Burn at Wolf Cleugh	Sampling point downstream the immediately downstream a mine water outburst. Evidence of ochre deposits on the bed sediments of the Rookhope Burn receiving the mine water discharge.	Alluvium/Stainmore formation
WDS 45	391661-542747	2. Rookhope Burn at Tailrace Level	Sampling point corresponds with the position of Tailrace water level	Alluvium/Stainmore formation
WDS 16	392747-542957	3. Rookhope Burn at Rookhope Arch	Sampling point corresponds with the position of the Rookhope Arch, the remaining section of a series of arches supporting flues taking fumes from the smelt mill up to the hillside.	Alluvium over till/Stainmore formation
WDS 23	394203-542016	4. Rookhope Burn at Church House	Sampling point downstream the washing plant of Boltsburn mine, the remnants can still be seen along the river.	Alluvium over till/ Alston formation
WDS 47	394410-541554	5. Rookhope Burn at South Smailburn Plantation	Sampling point 500 m downstream previous sampling point.	Alluvium over till/ Alston formation



Figure 2 Sampling location 1: Wolf Cleugh (sample WDS 46).



Figure 3 Detail of river banks at Wolf Cleugh (sample WDS 46).



Figure 4 Sampling location 2: Tailrace Level (sample WDS 45).



Figure 5 Details of river banks at Tailrace Level (sample WDS 45).



Figure 6 General view of Rookhope Burn near the Rookhope Arch (Sampling location 3).



Figure 7 Sampling Location 3: Rookhope Burn near Rookhope Arch (sample WDS 16).



Figure 8 Sampling location 4: Rookhope burn near Church House (sample WDS 23).

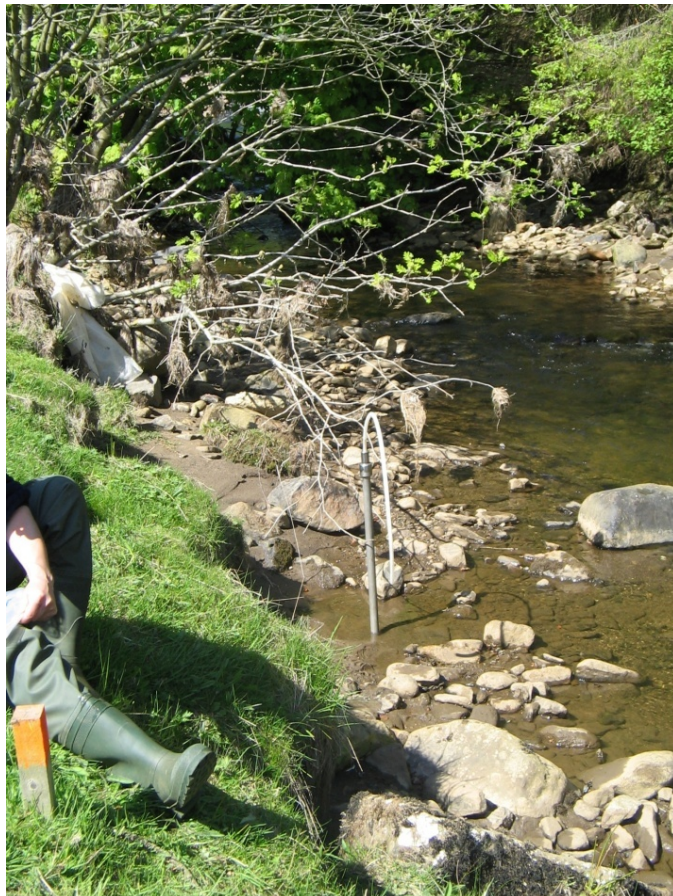


Figure 9 Detail of sampling location 4 of Rookhope burn riverbank sediments near Church House (sample WDS 23).



Figure 10 Sampling location 5: Rookhope Burn at South Smailburn plantation (sample WDS 47).

4 Inundation Pilot Experiment

Five sediments collected from the river banks of the Rookhope Burn were subjected to a laboratory scale inundation by river water collected from the area (co-ordinates 393750 542840), under controlled conditions, for prolonged residence times in order to determine whether there is potential mobility of PHEs following flooding.

4.1 EXPERIMENTAL SET-UP

As no standard methodologies are available from the literature for carrying out inundation studies the experimental set-up was based on a combination of methodologies from the literature and chosen in terms of being practicable for the amount of sediment material to use, the suitability of equipment, the timescales and the availability of laboratory space.

The inundation pilot study was designed to simulate rising flood water, so a saturated experimental design was put into place, where a slow saturation of the sediment was imitated in order to induce a slow change in physico-chemical properties, such as redox potential and pH, leaving the flood water sitting stagnant over the sediment for a 3 month (88 days) period, at a sediment to inundation water ratio of 1:10 (Simpson *et al*, 2008). Duplicate samples of each sediment sample were inundated to obtain an estimate of the repeatability of the PHE mobility data. The pilot study was carried out during the winter of 2009/2010, November to February, and although the temperature in the laboratory was not maintained at a constant, both the laboratory temperature and the inundation water temperature were monitored at each sampling date. The study was carried out on the bench top in order that the study was exposed to the natural day/night cycle for the length of the study.

About 50 g of air-dried sediment was accurately weighed into each uniquely labelled 1000 ml wide-mouth HDPE bottle (product code 2104-0032) and the sediment was tapped across the bottom of the bottle to ensure an even distribution. 500 ml of Rookhope stream water was slowly added so that the sediment was not disturbed, each sample bottle was then capped and left on the bench top in order that the stream water could slowly percolate through the sediment material and displace any air present. The resulting microcosm geometry consisted of a ~2.5 cm high soil layer under ~ 12.5 cm of supernatant water.

After 1, 7, 28, 60 and 88 days of inundation the temperature in the laboratory and the temperature, the pH and Eh of the inundation water were measured, after stirring the inundation water without disturbing the sediment at the bottom of the bottle. The ambient laboratory temperature and the inundation water temperature and pH/Eh were measured using handheld Hannah combination HI 9125 meters with associated probes. Laboratory measurements made throughout the inundation period are summarised in Appendices 3-9. Inundation water samples were collected for analysis of alkalinity, NPOC and the major and trace anion and cation composition. Each inundation water sample was collected using a 10 ml disposable syringe and filtered through a 0.45 µm nylon Gellman Acrodisc™. All samples for analysis were collected in Sarstedt polypropylene tubes with screw top lids (catalogue number 60.541.545, 101 x 16.5 mm, with a capacity of 13 ml). Samples for the analysis of alkalinity, NPOC and major and trace anions (13 ml in total) were refrigerated (at 0 – 8 °C) with no further preservation and samples for the analysis of major and trace cations were acidified to 1% with respect to concentrated HNO₃ for species preservation purposes prior to refrigeration.

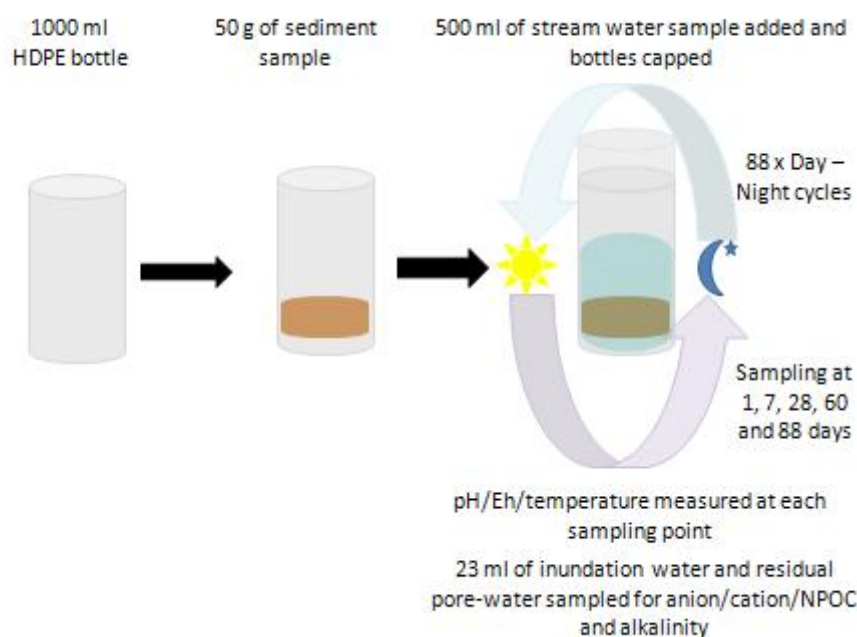


Figure 11 Schematic of the laboratory based inundation experiment.

In order to get an estimation of the composition of the bulk pore-water from the inundated sediment, the pore-water was collected at the conclusion of the 88 day inundation period. After collection of the final inundation water sample, the remaining flood water was carefully decanted from the reaction vessels, so that no obvious standing water was observed. The reaction vessels were then centrifuged for 5 minutes at 3000 G in order for any pore-water left within the sediment material to be released. This was collected for analysis of the same suite of analytes as the inundation water samples. The volume of each pore water sample and its colour before and after filtration and preservation was noted in Table 2. The colour change in the samples from yellow in the unfiltered solutions to colourless in the filtered solutions is indicative of the presence of iron species/particulates in solution.

Table 2 Volume and colour of bulk pore water (pre and post filtering)

Sample Name	Volume (ml)	Colour (pre filtering)	Colour (post filtering)
Rookhope Arch (WDS 16)	9.0	Clear, pale yellow	Clear, colourless
Rookhope Arch (WDS 16 Duplicate)	8.5	Clear, pale yellow	Clear, colourless
Church House (WDS 23)	6.0	Clear, colourless	Clear, colourless
Church House (WDS 23 Duplicate)	4.5	Clear, colourless	Clear, colourless
Tailrace level (WDS 45)	6.0	Clear, yellow	Clear, colourless
Tailrace level(WDS 45 Duplicate)	7.5	Clear, yellow	Clear, colourless
Wolf Cleugh (WDS 46)	7.5	Clear, pale yellow	Clear, colourless
Wolf Cleugh (WDS 46 Duplicate)	6.0	Clear, pale yellow	Clear, colourless
South Smailburn Plantation (WDS 47)	6.0	Clear, colourless	Clear, colourless
South Smailburn Plantation (WDS 47 Duplicate)	4.5	Clear, colourless	Clear, colourless

5 Analytical Techniques

The analyses carried out, described in sections 3.1 to 3.5 and 3.7, have been completed in accordance with the relevant UKAS procedures. All analytical techniques are subjected to rigorous quality control (QC). Quality control standards are analysed at the beginning and end of each run and after not more than a set number of unknown solutions, as described in each procedure.

5.1 CHARACTERISATION OF SEDIMENTS BY X-RAY DIFFRACTION ANALYSIS (XRD)

5.1.1 Instrumentation

XRD analysis was carried out on the original sediment samples using a PANalytical X'Pert Pro series diffractometer equipped with a cobalt-target tube, X'Celerator detector and operated at 45kV and 40mA.

5.1.2 Analytical Method

In order to provide a finer and uniform particle-size for whole-rock XRD analysis, a *circa*. 3 g portion of the milled material was wet-micronised under water for 10 minutes, dried, disaggregated and back-loaded into standard stainless steel sample holders for analysis.

The samples were scanned from 4.5-85°2 θ at 2.76°2 θ /minute. Diffraction data were initially analysed using PANalytical X'Pert Highscore Plus Version 2.2a software coupled to the latest version of the International Centre for Diffraction Data (ICDD) database.

Following identification of the mineral species present in the samples, mineral quantification was achieved using the Rietveld refinement technique (*e.g.* Snyder and Bish, 1989) using PANalytical Highscore Plus software. This method avoids the need to produce synthetic mixtures and involves the least squares fitting of measured to calculated XRD profiles using a crystal structure databank. Errors for the quoted mineral concentrations are typically $\pm 2.5\%$ for concentrations >60 wt%, $\pm 5\%$ for concentrations between 60 and 30 wt%, $\pm 10\%$ for concentrations between 30 and 10 wt%, $\pm 20\%$ for concentrations between 10 and 3 wt% and $\pm 40\%$ for concentrations <3 wt% (Hillier *et al.*, 2001). Where a phase was detected but its concentration was indicated to be below 0.5%, it is assigned a value of $<0.5\%$, since the error associated with quantification at such low levels becomes too large.

5.2 MIXED ACID DIGESTION OF SEDIMENTS

5.2.1 Theory

Total digestion of samples using mixed acids (HF, HNO₃ and HClO₄⁻) is often the preferred method in geological laboratories as it dissolves silicate minerals. However Si is volatilised in the digestion process and as a result cannot be determined by this method (Hill *et al.*, 2004).

5.2.2 Analytical Method

The digestion is based on a method by Thompson and Walsh (1983). In this method 0.25 g of sediment sample was weighed accurately into a PFA beaker. At least one sample blank, one certified reference material (NIST, Butte Montana 2711) and one sample of the BGS 102 ironstone derived guidance soil (Wragg, 2009) were digested per analytical run. For every ten samples at least one was digested in duplicate. 2.0 ml of concentrated nitric acid (69%, HNO₃) was added to each sample beaker, followed by, after the subsidence of any effervescence, 2.50 ml of concentrated hydrofluoric acid (48%, HF) and 1.0 ml of perchloric acid (70%, HClO₄). After swirling of the sample, each beaker was placed into the hot block and the heating

programme set for the specified digestion programme: 8 hours at 80°C, 2 hours at 100°C, 1 hour at 120°C, 3 hours at 140°C and 4 hours at 160°C. On completion of the heating cycle, the hot block was allowed to cool to 50°C, where 2.5 ml of 50% HNO₃ was added and the samples were allowed to further digest for 30 minutes, followed by 15 minutes at 30°C on the addition of 2.5 ml of concentrated hydrogen peroxide (30%, H₂O₂). On removal from the hot block the volume of the digestion solution was made up to 25.0ml with freshly prepared deionised water. The digestion solutions were stored at 0-8.0°C prior to analysis of a range of major and trace elements by ICP-AES.

5.2.3 Determination of Major and Trace cations by Inductively Coupled Plasma Atomic Emission Spectrometry (ICP-AES)

INSTRUMENTATION

The determination of major and trace metals, S, P and B in the original sediments and the residual sediments after the inundation experiments, was carried out on a Varian/Vista AX CCD simultaneous instrument with dedicated Varian SPS-5 Autosampler. The instrument views the plasma along its axis and is equipped with a high resolution Echelle polychromator with a Vista Chip™ image mapped Charge Coupled Device (CCD) solid-state detector covering a wavelength range of 167 to 785 nm. The sample is introduced via a peristaltic pump into a glass concentric nebuliser connected to a cyclonic action spray chamber. The system is controlled by a dedicated PC running software supplied by the instrument manufacturer.

ANALYTICAL METHOD

Major cations (Ca, Mg, Na, K), trace cations (Ba, Sr, Mn, Fe, Al, Zn, Li), total S, total P and B are determined directly by ICP-AES. Analysis was carried out on c. 5.0 ml of each pre or post inundation digested stream sediment. The instrument was calibrated at the beginning of the analytical run and re-calibrated after not more than every 120 samples. Two QC standards, high and low (at *circa* 10% and 80% of the calibration range for each individual analyte), were analysed after each calibration, during the run after no more than twenty unknown solutions and at the end of each run to check for drift. Blanks, calibration standards and quality control standards were matrix matched to the samples to be analysed. All reported measurements are based on the average of three replicate analyses.

DATA QUALITY

Measurable concentrations of Al and Fe were determined in procedural blanks, but were negligible when compared with the reported data, less than 0.1% in both cases. Data for Mo have been reported with an increased limit of detection in the digestion solution at 0.125 mg l⁻¹, which calculates as c.12.5 mg kg⁻¹ in the sediment. As a result all Mo concentrations in the sediment samples under investigation have been reported below the detection limits of detection.

Recovery data for the CRM NIST 2711 and the guidance material BGS 102 were in the range of 75 to 104% for all elements analysed, with the higher recoveries for NIST 2711, which are considered acceptable. Recovery data for Mo could not be calculated for either NIST 2711 or BGS 102, as the limit of detection reported was above the values quoted for these two reference/guidance materials. The recovery of Cd for BGS 102 was erroneously high (>200%), this was deemed to be a result of the closeness of the analytical result to the method detection limit for the sample.

The calculated repeatability, from the duplicate digestion of the Wolf Cleugh sample (WDS 46), was <5% for all elements under investigation.

All species in a digestion matrix are considered to be stable over an appreciable length of time and certainly within the period between sampling and analysis. Wavelengths and conditions of

analysis are optimised to ensure that interference effects are minimised for all elements; samples with complex matrices, such as digests, are diluted prior to analysis.

5.2.4 Determination of Sediment pH

The pH was measured using a glass electrode and Orion 720A meter. The pH of each sediment was analysed by a recognised standard protocol, (Rowell, 1994). The pH meter was calibrated to 4 and 7 or 7 and 9 depending on the pH of the slurry to be measured. A 25 ml aliquot of 0.01M CaCl₂ was added to 10.0 g of the sediment. The 0.01M CaCl₂ was prepared as 1.1098 g AnalaR[®] CaCl₂ made up to 1 l with freshly prepared deionised water. The samples were magnetically stirred for one minute and then left to settle for 15 minutes. Prior to analysis the samples were stirred to reform the suspension. Buffer check solutions were analysed before and after every ten soil suspensions and at least one unknown sample was measured in duplicate per ten.

5.2.5 Determination of Loss on Ignition (LOI) at 450°C

Loss on ignition (LOI) at 450°C has been determined in the Rookhope sediment samples as a surrogate for the organic carbon content. The LOI was determined as the proportion of the decrease in sample mass after heating. A QC soil was measured within each batch of unknown samples.

5.3 ANALYSIS OF THE ROOKHOPE STREAM WATER, OF THE INUNDATION WATER AND BULK PORE WATER

5.3.1 Determination of Major and Trace Anions by Ion Chromatography (IC)

INSTRUMENTATION

The analysis of major and trace anions in the Rookhope stream water, the inundation water samples and the bulk pore water sample was carried out on a Dionex DX-600 Ion Chromatograph consisting of the following modules: GP50 gradient pump, ED50A electrochemical detector, AD20 absorbance detector, AS50 autosampler and AS50 thermal compartment. The whole system is controlled and data captured by a dedicated computer, installed with the Chromeleon Software version 6.40, which is connected to the instrument via a Netgear[®] Ethernet hub. Separation is performed using an AG14 guard column and an AS14 analytical column using an injection volume of 100 µl.

ANALYTICAL METHOD

Major and trace anions (Cl⁻, SO₄²⁻, NO₃⁻, NO₂⁻, Br⁻, HPO₄²⁻, S₂O₃²⁻ and F⁻) were determined by ion chromatography as described by Charlton *et al.* (2003). The instrument was calibrated at the beginning of every analytical run using twelve standards, two of which are prepared manually, the other ten being prepared on line by the instrument. QC and blank samples are analysed at the start and end of each run and after not less than every 20 samples. A calibration drift check standard was run at the end of each run and after not less than every 50 samples. The analysis followed a pre-programmed schedule and the data were collected by the software with peaks identified by retention time. The method is limited by the number of exchange sites available within the column. With the injection loop and column used in this study, solutions with total anion concentrations of up to 1000 mg l⁻¹ can be analysed; above this the column becomes overloaded, causing poor peak shapes, variable retention times and thus unreliable results. To overcome this problem, more concentrated solutions were diluted. Dilution was also used to bring the analyte concentration within the concentration range covered by the standards.

DATA QUALITY

No F- data for sample WDS 23, collected 1 day after inundation was determined because of an ion chromatographic interference which could not be corrected for.

Most anions are stable in solution for an appreciable length of time and certainly within the period between sampling and analysis.

5.3.2 Determination of Major and Trace Cations by Inductively Coupled Plasma – Mass Spectroscopy (ICP-MS)

INSTRUMENTATION

Major and trace cations in the Rookhope stream water, the inundation water samples and the bulk pore water sample was carried out on an Agilent 7500cx series, quadrupole inductively coupled plasma mass spectrometer (ICP-MS). The system had an octopole reaction system (ORS) with a CETAC autosampler and a dedicated PC with Agilent 7500 ICP-MS Chemstation B.03.06 (U300-0132) software.

ANALYTICAL METHOD

Major and trace cations (Ag, Al, As, B, Ba, Be, Ca, Cd, Ce, Co, Cr, Cs, Cu, Dy, Er, Eu, Fe, Ga, Gd, Hf, Ho, K, La, Li, Lu, Mg, Mo, Mn, Na, Nb, Nd, Ni, P, Pb, Pr, Rb, S, Sb, Se, Si, Sm, Sn, Sr, Ta, Tb, Th, Ti, Tl, Tm, U, V, W, Y, Yb, Zn, Zr) were determined by ICP-MS as described by Breward *et al.* (2009). The instrument was calibrated at the beginning of every analytical run using at least three standards and a blank for each trace element and two standards and a blank for major elements. The calibration ranges for the suite of elements listed in Table 1 are summarised in Table 6, the calibration ranges for the full suite of elements available can be found in Breward *et al.*, (2009). Internal standards were added to all solutions to correct for any signal suppression and a suitable QC check standard, within the analytical range and of similar composition to the samples under investigation was analysed at the beginning and end of every analytical run and after a maximum of 20 unknown samples.

DATA QUALITY

All aqueous data reported here for this method are outside the scope of UKAS accreditation. All species preserved by acidification are considered to be stable over an appreciable length of time and certainly within the period between sampling and analysis. Wavelengths and conditions of analysis are optimised to ensure that interference effects are minimised for all elements; samples with complex matrices, such as digests, are diluted prior to analysis.

5.3.3 Determination of Non Purgeable Organic Carbon (NPOC)

INSTRUMENTATION

The NPOC content of the Rookhope stream water, the inundation water samples and the bulk pore water sample was determined using a Shimadzu TOC-V CPH analyser (Serial No.41546360) with associated ASI-V auto-sampler (Serial No. 41D78299). The system is controlled and data captured by a PC, installed with TOC Control V Software. The carrier gas is high purity air supplied by a Parker Balston 78-40-220 TOC gas generator connected to a Jun Air OF301-4S oil-free compressor.

ANALYTICAL METHOD

The instrument is calibrated in two ranges: a low range (0-10 mg l⁻¹) and a high range (0-100 mg l⁻¹) at the start of each analytical run. Two working standards at 10 and 100 mg l⁻¹ are prepared and each is diluted automatically by the instrument to give three further calibration standards in each of the two calibration ranges. Calibration standards, quality control standards,

blanks and samples were poured into the standard/sample vials and covered with laboratory film prior to analysis to prevent absorption of CO₂ from the atmosphere, and loaded into the appropriate positions in the dedicated autosampler. Working QC standards were prepared from the stock QC standard on the day of analysis at 50 mg l⁻¹, 10 mg l⁻¹ and 5 mg l⁻¹ and analysed at the beginning and end of every run and after no more than every 20 samples.

DATA QUALITY

All data for this method are outside the scope of UKAS accreditation.

Table 3 ICP-MS calibration ranges for elements listed in Table 1, after Breward *et al.* (2009)

Element	Isotope	Units	Top Calibration Std
Cr	52	µg l ⁻¹	100
Cr	53	µg l ⁻¹	100
Ni	60	µg l ⁻¹	100
Cu	63	µg l ⁻¹	100
Zn	66	µg l ⁻¹	1000
As	75	µg l ⁻¹	100
Cd	111	µg l ⁻¹	100
Cd	114	µg l ⁻¹	100
Pb	208	µg l ⁻¹	100

5.3.4 Determination of Alkalinity

INSTRUMENTATION

The determination of the alkalinity of the Rookhope stream water used to inundate the sediment samples, the post inundation water samples and the bulk pore water sample was carried out on a Radiometer auto titrator consisting of a VIT 90 video controller module with an ABU 93 autoburette and a SAM 90 sample section. The VIT 90 is connected to a printer and results for each sample are printed upon completion of analysis.

ANALYTICAL METHOD

The instrument is calibrated for pH using pH 4 and pH 10 buffers after entering the laboratory temperature. This calibration is then checked with a pH 7 buffer for which the result must be within 0.02 pH units. The alkalinity titration is checked at the beginning and end of every run and not less than every 10 unknown samples using a 200 mg l⁻¹ HCO₃⁻ QC solution. A known quantity of sample is placed in the titration vessel and the electrodes lowered in to the solution. The sample is allowed to stabilise before the pH reading is taken and the titration started. Once the titration has begun, the instrument adds small amounts of acid to the solution until the end point is reached at approximately pH 2.8. The instrument then calculates the concentration of HCO₃⁻, this information is then printed and the electrodes and vessel rinsed and wiped before the next sample.

DATA QUALITY

All data for this method are within the scope of UKAS accreditation.

6 Results

6.1 ROOKHOPE SEDIMENTS CHARACTERISATION

6.1.1 Texture

The texture of the 5 sediment samples differed only slightly (Table 4), with prevalent sand (87 to 95 %) except for sample at location 1, Wolf Cleugh, WDS 46, containing 29 % gravel, 68% sand and 3 % among silt and clay.

Table 4 Particle size distribution in Rookhope river bank sediment samples

Sample code	Location Area	>2 mm	2-1 mm	1 mm-500 um	500-250 um	250-125 um	125-63 um	<63 um	loss
		gravel	very coarse sand	coarse sand	medium sand	fine sand	very fine sand	silt and clay	
		Mass retained as % of original sample							
WDS 46	1. Wolf Cleugh	29.0	11.5	19.5	19.0	13.4	4.9	2.7	0.1
WDS 45	2. Tailrace Level	1.5	6.1	26.9	37.7	21.2	4.8	2.0	0.0
WDS 16	3. Rookhope Arch	7.0	10.7	17.8	22.2	25.5	11.2	5.5	0.1
WDS 23	4. Church House	5.6	4.4	9.9	32.2	35.8	9.4	2.6	0.1
WDS 47	5. South Smailburn Plantation	2.0	2.7	13.1	40.7	32.6	6.8	2.0	0.2

6.1.2 Mineralogy

The XRD mineral data, summarised in Appendix 2, indicate that all five sediment samples were dominated by the presence of quartz (*circa.* 58 – 76 %), with additional contributions from mica (*circa.* 8.6 – 14 %), fluorite (*circa.* 2 – 12 %), kaolin (*circa.* 2 – 5 %) and chlorite (*circa.* 2 – 3 %). The sample from Rookhope Arch (WDS 16) also had an additional, but minor albite (*circa.* 2%) and <0.5 % K-feldspar. Both of the samples from Church House and South Smailburn Plantation were noticeably different because of the presence of a small percentage (<3) of calcite, cerussite, dolomite, galena, and sphalerite compared to the other samples under investigation. The presence of carbonates in these two most downstream samples reflects the influence of the underlying geology (the Alston formation) characterised by thick limestones.

6.1.3 Geochemistry

The pH of the sediments ranged between 5.4 and 6.9 (Appendix 3). The organic matter content, as measured by LOI, of the sediment samples was low, with concentrations ranging between 3 and 4.2%.

Table 5 summarises the pre-inundation sediment chemical data for the suite of elements considered in the EA sediment quality criteria (Appendix 1) and reports the Rookhope Burn stream water chemical data for elements listed in the EC Dangerous Substances Directive (76/464/EEC). Appendix 3 and Appendix 4 provide details of the full suite of analytes determined for the sediment samples and the stream water, respectively.

For Cd, Pb and Zn, all of the sediments tested have concentrations above the PEL. Two samples were identified as having much higher concentrations of PHEs than the others under investigation; these were the most downstream samples collected from Church House and South Smailburn Plantation (WDS 23 and WDS 47). The high Zn and Pb concentrations in these samples correspond to a mineral assemblage containing Zn and Pb sulphides and Pb carbonates, identifiable in the XRD patterns due to their abundance. WDS 23 and WDS 47 contain,

respectively, 1.2% and 0.6% cerussite (PbCO_3). XRD analysis identified trace amounts of galena (PbS), an additional source of Pb, sphalerite (ZnS), a source of Zn and potential source of Cd, as Cd is known to substitute Zn (Wakita and Schmitt, 1970), and pyrite (FeS_2), a potential source of As in both samples. The observed enrichment is to be related to the close proximity of these two sediment samples to the Boltsburn Mine washing plant, its remnants still visible along the river (Table 1). The Pb concentration decreases from 29500 to 14400 mg kg^{-1} going from the upstream Church House sample (WDS 23) to the downstream South Smailburn Plantation sample (WDS 47). This decrease in sediment contamination is commonly observed downstream of discrete point sources, due to the effect of hydraulic sorting and dilution by uncontaminated sediment from tributaries. The relatively lower concentrations of PHEs, but still above the PEL quality thresholds, in the remaining sediment samples (WDS 46, WDS 45 and WDS 16) upstream of the Boltsburn Mine washing plant, suggest that relict ore minerals might still be present, although not identifiable by XRD due to their low abundance. Moreover, authigenic phases formed by precipitation from metal-rich mine waters discharging into the Rookhope Burn may be particularly significant metal-bearing mineral phases in this part of the catchment affected by two major mine water discharges (Banks and Palumbo-Roe, 2010). This aspect could be investigated by carrying out selective chemical extractions on all sediment samples in order to determine the metal solid speciation among different fractions (*e.g.* exchangeable, carbonates, Fe-Mn oxides, sulphides, *etc.*) of the sediment and to highlight possible differences in the samples collected along the catchment. Significant changes in the solid metal speciation in sediments of mining impacted catchments has been observed in Hudson-Edwards (2003); Pulford *et al.*, (2009); Byrne *et al.*, (2010).

Table 5 Summary of concentrations of selected environmentally sensitive elements in Rookhope Burn stream sediments, mg kg^{-1} , ordered from upstream to downstream (PHEs that are above the TEL are highlighted in *italics* and those PHEs above both the TEL and the PEL are denoted by *bold italics*)

Sample	Mn	Fe	As	<i>Cd</i>	Cr	<i>Cu</i>	<i>Ni</i>	<i>Pb</i>	V	<i>Zn</i>
Wolf Cleugh (WDS 46)	1165	31783	9.38	<i>1.02</i>	46.1	14.8	24	<i>976</i>	37.7	<i>336</i>
Tailrace level (WDS 45)	1562	35972	9.61	<i>1.25</i>	48.2	18.6	26.5	<i>1351</i>	38.9	<i>346</i>
Rookhope Arch (WDS 16)	1689	35768	9.25	<i>1.36</i>	49.6	16.8	35.1	<i>975</i>	41.7	<i>637</i>
Church House (WDS 23)	4580	87351	23.5	<i>5.13</i>	29.7	<i>474</i>	24	<i>29514</i>	18.1	<i>1691</i>
South Smailburn Plantation (WDS 47)	4589	85303	20.6	<i>4.85</i>	29.1	<i>375</i>	25.4	<i>14421</i>	20.4	<i>1620</i>

6.2 INUNDATION EXPERIMENTS

6.2.1 Stream water

The Rookhope Burn stream water collected at the footbridge in Rookhope village (co-ordinates 393750 542840) was used to flood the sediments for this laboratory study. The NPOC concentration of the stream water sample was 2.57 mg l^{-1} and the pH 7.82, as measured in the laboratory using a hand held pH meter with associated glass probe. As, Cd, Fe and Pb concentrations for the Rookhope Burn stream water data are all below their respective EQS. The average concentration of HCO_3^- in the stream water was 92.6 mg l^{-1} , which equates to c.

76 mg l⁻¹ CaCO₃. The Cr, Cu, Ni and V concentrations in the stream water at this carbonate concentration are below the EQS at the respective equivalent CaCO₃ concentration of 50-100 mg l⁻¹ in Table A 3 in Appendix 1. However, at this equivalent CaCO₃ concentration, the EQS for Zn is slightly exceeded, with an average Rookhope Burn stream water Zn concentration of 59 µg l⁻¹ compared to an EQS of 50 µg l⁻¹, indicating a potential hazard. At present there are no EQS for Mn, B and F, but these elements are considered to be environmentally active and thus have been included within the suite of analytes investigated.

Table 6 Summary of concentrations of selected environmentally sensitive elements in Rookhope Burn stream water sample

Sample Name	Mn	Fe	As	Cd	Cr	Cu	Ni	Pb	V	Zn	B	F ⁻
	µg l ⁻¹											mg l ⁻¹
Replicate 1	0.500	48.0	0.420	0.040	<0.10	4.20	2.80	0.700	<0.10	58	20.0	1.57
Replicate 2	0.400	44.0	0.250	0.040	<0.10	3.50	2.70	0.700	<0.10	59.0	<20.0	1.58
Replicate 3	0.400	51.0	0.280	0.030	<0.10	3.50	2.70	0.600	<0.10	60.0	<20.0	1.57

6.2.2 Effect of Sediment on inundation water pH

The pH of the Rookhope stream water was measured immediately prior to inundation in the laboratory at 7.82. Figure 12 shows that the pH of the stream water was immediately reduced, by *circa*. 0.1 to 0.6 pH units by the introduction of the Rookhope stream sediments over the first 24 hours of the study. Over the first 28 days of the inundation test the pH of the flood water became more acidic, in general reaching equilibrium after a 28 day inundation period. Two distinct groupings in the sediments were observed; Figure 12 shows that two of the samples, WDS 45 and 46, had the greatest impact on the pH of the Rookhope stream water, reducing the pH by the largest amount, *circa*. 1 pH unit in total, and maintaining a solution pH below 7 after the 28 day inundation period. The characterisation data for the sediments (Appendix 3) shows that these two samples had the lowest measured pH, 5.38 and 5.83, respectively. Samples WDS 16, WDS 23 and WDS 47 maintained a pH above 7 throughout the inundation period.

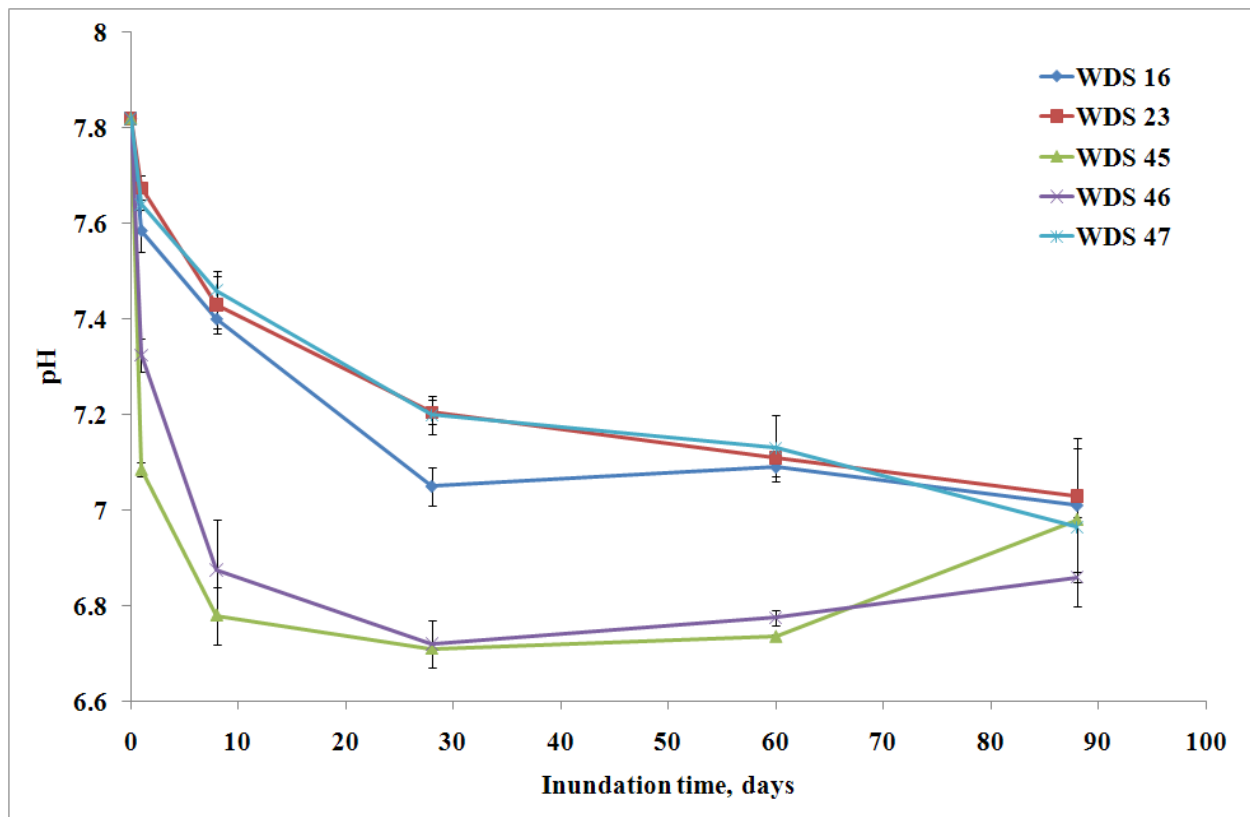


Figure 12 pH changes during the flooding of the Rookhope sediments, the errors are calculated as the difference between the two replicates divided by two.

6.2.3 Redox (ORP) measurements

The ORP measurements made on the inundation waters ranged from 200 to 350 mV, increasing through the course of the inundation and in all samples indicating oxic conditions (Appendix 5). These measurements were made when the inundation cells were temporarily exposed to the aerated conditions in the laboratory during sampling. During flooding conditions in the natural environment, the rising groundwater table may cause soils and sediments to become temporarily anoxic. The flood induced redox conditions within the sediment and the pore water were, however, not monitored.

6.2.4 Mobilisation of PHEs

The information from the inundation experiment, with respect to the elements released from the inundated sediment, has been plotted in the form of rate release curves for each element. Two different rate release curves per element have been produced; one that shows the release of the individual elements as an absolute value in mg or μg per litre, with the concentration of the element of interest in the inundation water at time 0 as the starting point. A second curve represents the element release relative to the amount of each given element in the sediment, as a %. The rate release curves for Mn, Fe, SO_4 , Cu, Pb and Zn are described below. All other rate release curves produced during the pilot study are presented in Appendix 12. The error bars displayed on each figure are calculated as the difference between the two replicate values divided by 2, where the data point is the mean replicate value.

IRON

Figure 13 shows the Fe rate release curves as $\mu\text{g l}^{-1}$ in each sediment sample, indicating the differences between the individual sediments. Table 7 summarises the dissolved Fe concentrations in the overlying water column at each individual sampling time for each inundated sediment sample.

The range of Fe concentrations in the inundation water over time across the sample locations was *circa.* 2 to 37 $\mu\text{g l}^{-1}$ (Table 7). The Rookhope Burn streamwater, the initial inundation water used in the study, had an average Fe concentration of 48 $\mu\text{g l}^{-1}$. Inundation of the sediment samples depleted Fe from the inundation water. Figure 13 shows that depletion of Fe occurred during the initial 28 days of the study for all sampling locations and then slowed. No relationship between the degree of depletion and the total amount of Fe present in the original sediment sample was observed.

Table 7 Average iron concentrations in the inundation water during flooding. Concentrations in bold are above the EQS.

Sample	Time (d)	Fe ($\mu\text{g l}^{-1}$)
Inundation Water	0	48.0
WDS 16	1	45.0
WDS 16	8	18.5
WDS 16	28	5.50
WDS 16	60	4.50
WDS 16	88	6.00
WDS 23	1	28.0
WDS 23	8	19.0
WDS 23	28	4.50
WDS 23	60	2.00
WDS 23	88	3.50
WDS 45	1	28.5
WDS 45	8	29.0
WDS 45	28	10.0
WDS 45	60	4.50
WDS 45	88	5.00
WDS 46	1	36.5
WDS 46	8	30.0
WDS 46	28	10.5
WDS 46	60	8.00
WDS 46	88	6.50
WDS 47	1	32.0
WDS 47	8	10.5
WDS 47	28	3.50
WDS 47	60	2.50
WDS 47	88	2.50

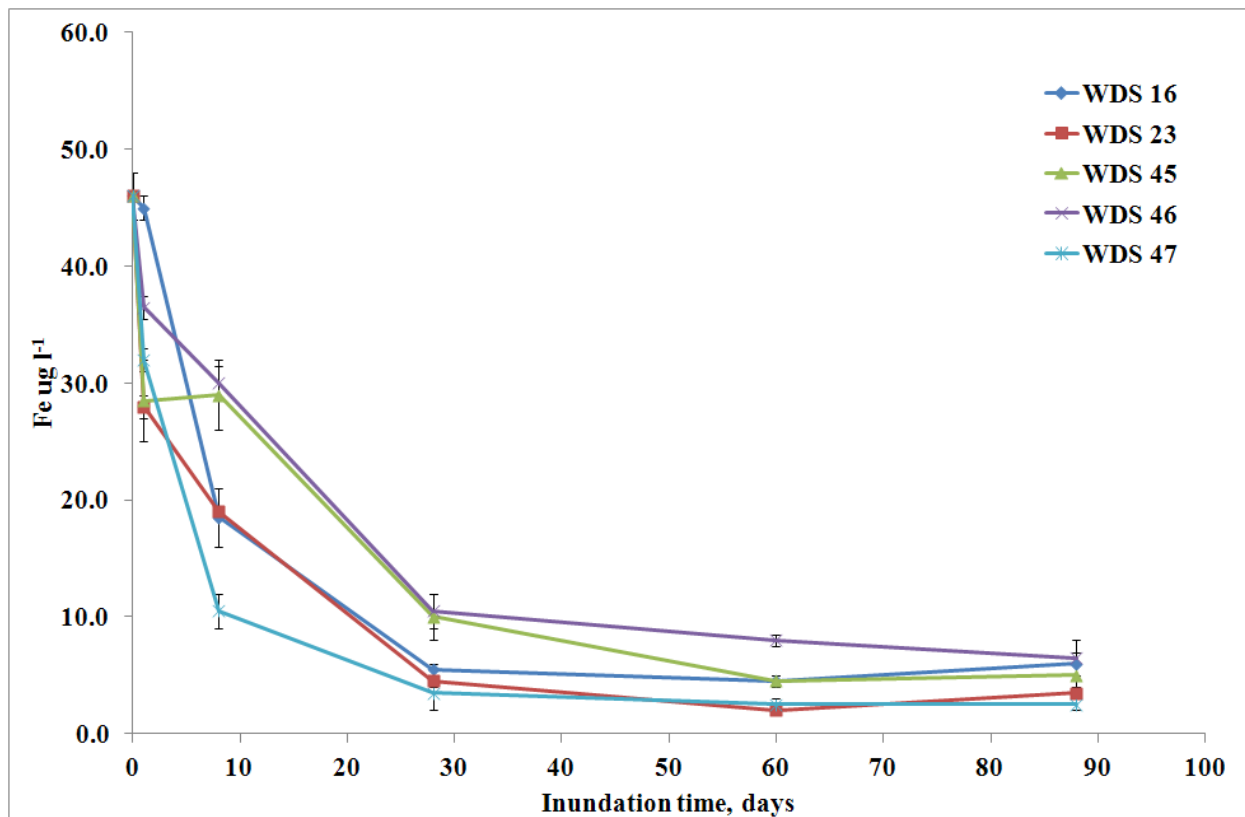


Figure 13 Iron release rate curve, $\mu\text{g l}^{-1}$.

LEAD

Table 8 shows that during the inundation period, the Rookhope Burn stream water became enriched in soluble Pb. Comparison with the EQS for Pb ($7.2 \mu\text{g l}^{-1}$) indicates that inundation of samples from Church House and South Smailburn Plantation (WDS 23 and WDS 47) would result in higher values than the EQS for Pb. For both sediment samples, the release of Pb to reach concentrations higher than the EQS is likely to occur within 1 day of inundation (Figures 14 - 16). In the case of WDS 23 this would be a 5-6 fold increase with respect to the EQS for Pb and for WDS 47 a twofold increase, with a % increase in the inundation water Pb concentration of between 65 and >100%.

Table 8 shows that initial release of Pb occurred during the first day of inundation, and that for the sediment from Church House (WDS 23) a continual increase was observed. For all the other sediment samples similar trends in Pb solubilisation were observed: after an initial solubilisation a distinct dip in the release rate of dissolved Pb was observed until around 28 to 60 days, after which point a further solubilisation of Pb was noted. The relative mobility of Pb in the sediment samples follows the same pattern as the total Pb concentrations shown in Table 5, Church House>South Smailburn Plantation>Wolf Cleugh>Tailrace level>Rookhope Arch (WDS 23>WDS 47>WDS 45>WDS 46>WDS 16).

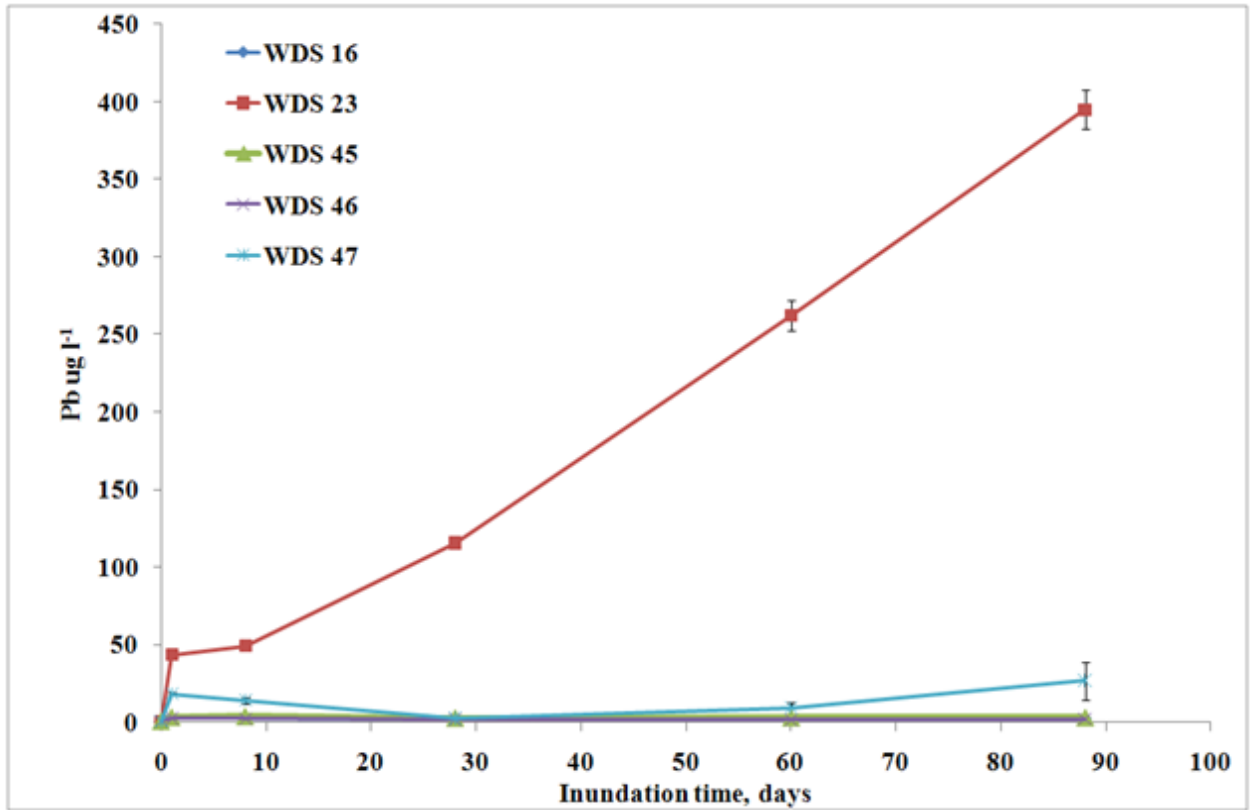


Figure 14 Lead release rate curve, µg l⁻¹.

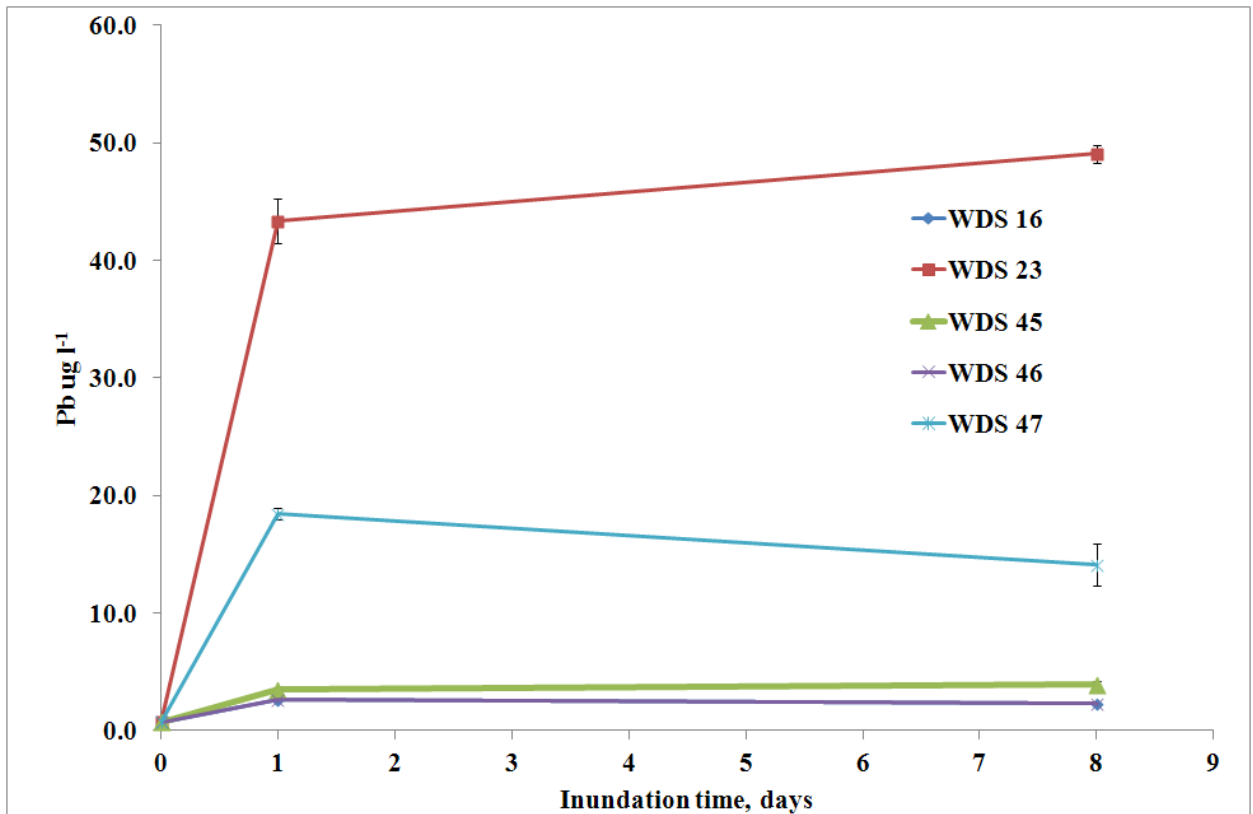


Figure 15 Expanded lead release rate curve, µg l⁻¹ for the 0-10 day time period.

Table 8 Average lead concentrations in the inundation water during flooding. Concentrations in bold are above the EQS.

Sample	Time (d)	Pb ($\mu\text{g l}^{-1}$)
Inundation Water	0	0.670
WDS 16	1	2.10
WDS 16	8	1.15
WDS 16	28	0.450
WDS 16	60	0.650
WDS 16	88	1.10
WDS 23	1	43.4
WDS 23	8	49.1
WDS 23	28	116
WDS 23	60	261
WDS 23	88	395
WDS 45	1	3.45
WDS 45	8	3.90
WDS 45	28	2.80
WDS 45	60	3.00
WDS 45	88	3.15
WDS 46	1	2.60
WDS 46	8	2.25
WDS 46	28	1.65
WDS 46	60	1.60
WDS 46	88	2.05
WDS 47	1	18.4
WDS 47	8	14.1
WDS 47	28	2.50
WDS 47	60	9.25
WDS 47	88	26.9

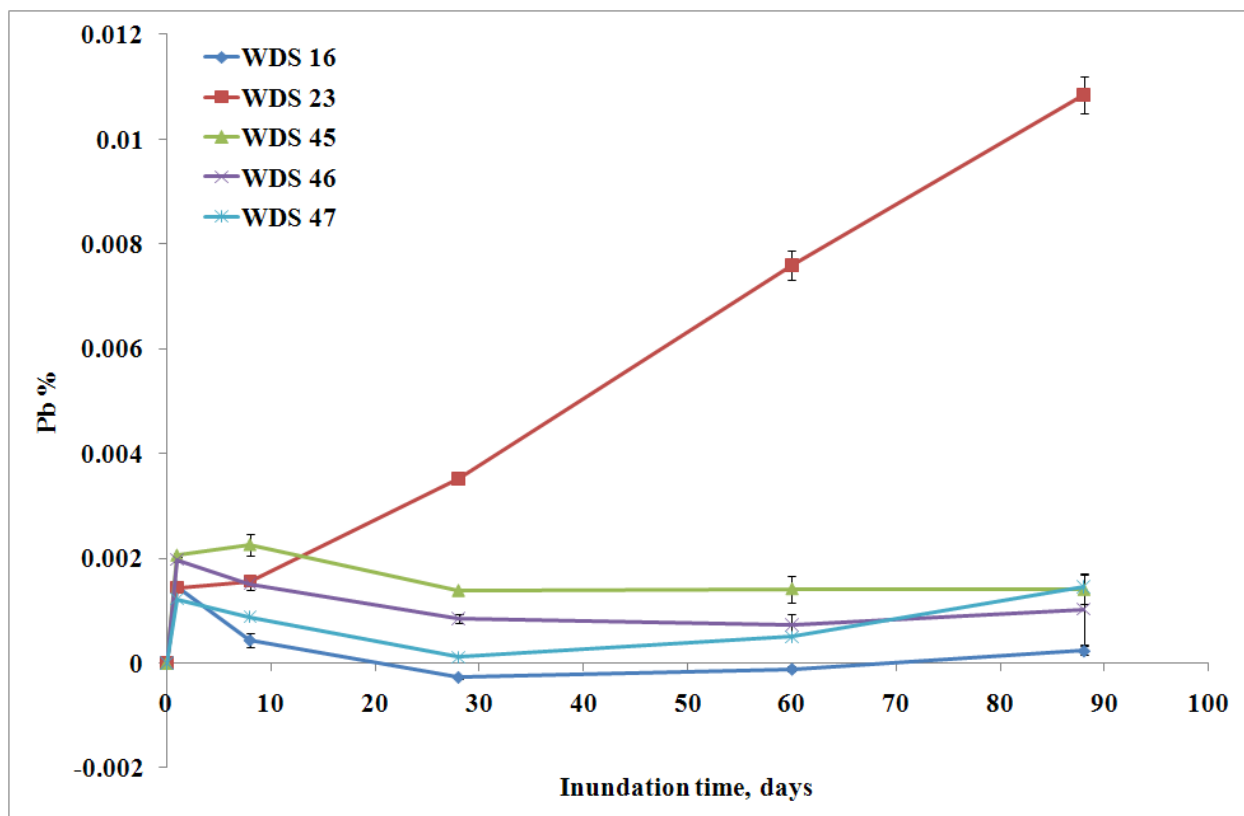


Figure 16 Lead release rate curve, % of the original sediment concentration.

COPPER

Figure 17 and Figure 18 summarise the Cu rate release curves as $\mu\text{g l}^{-1}$ and as a function of the total amount of Cu present in each sediment sample, indicating the differences between the individual sediments. Table 9 summarises the dissolved Cu concentrations in the inundation water at each individual sampling point for each inundated sediment sample.

Figure 17 and Table 9 indicate that during the initial inundation period (up to 8 days) the Rookhope stream water was generally enriched with Cu, with the exception of an initial depletion prior to the enrichment for the sediments from the Tailrace level (WDS 45) and Wolf Cleugh (WDS 46). This feature is shown more clearly by Figure 18. For all samples, the amount of Cu solubilised during inundation appears to plateau or tail off at around 8 days. Figure 18 shows the % Cu released from the sediment over the inundation period. For the samples collected from Rookhope Arch, Church House and South Smailburn Plantation (WDS 16, 23 and 47) a net Cu gain to the inundation water was observed, indicating overall enrichment of the stream water equating to <0.5 to 42% of the total Cu present in the original inundation water, compared to a net depletion of 5 to 12% for samples collected from the Tailrace level and Wolf Cleugh (WDS 45 and 46). The highest inundated Cu concentrations were observed for those samples where sediment concentrations above the PEL for Cu were observed, i.e. in sediment samples from Church House and South Smailburn Plantation (WDS 23 and 47). The equivalent CaCO_3 , calculated from the measured HCO_3^- ranged between 36.1 and 171 mg l^{-1} corresponding to highest Cu EQS of 10 $\mu\text{g l}^{-1}$ for 150-250 mg l^{-1} CaCO_3 . After inundation, the Rookhope Burn stream water did not exceed the hardness related EQS for Cu for three of the five sampling locations. However, for sediment samples collected from Church House and South Smailburn Plantation, the Cu EQS was exceeded during the initial 28 days of the inundation period, where the Cu EQS was 6 $\mu\text{g l}^{-1}$ at a corresponding CaCO_3 equivalent of 50-100 mg l^{-1} .

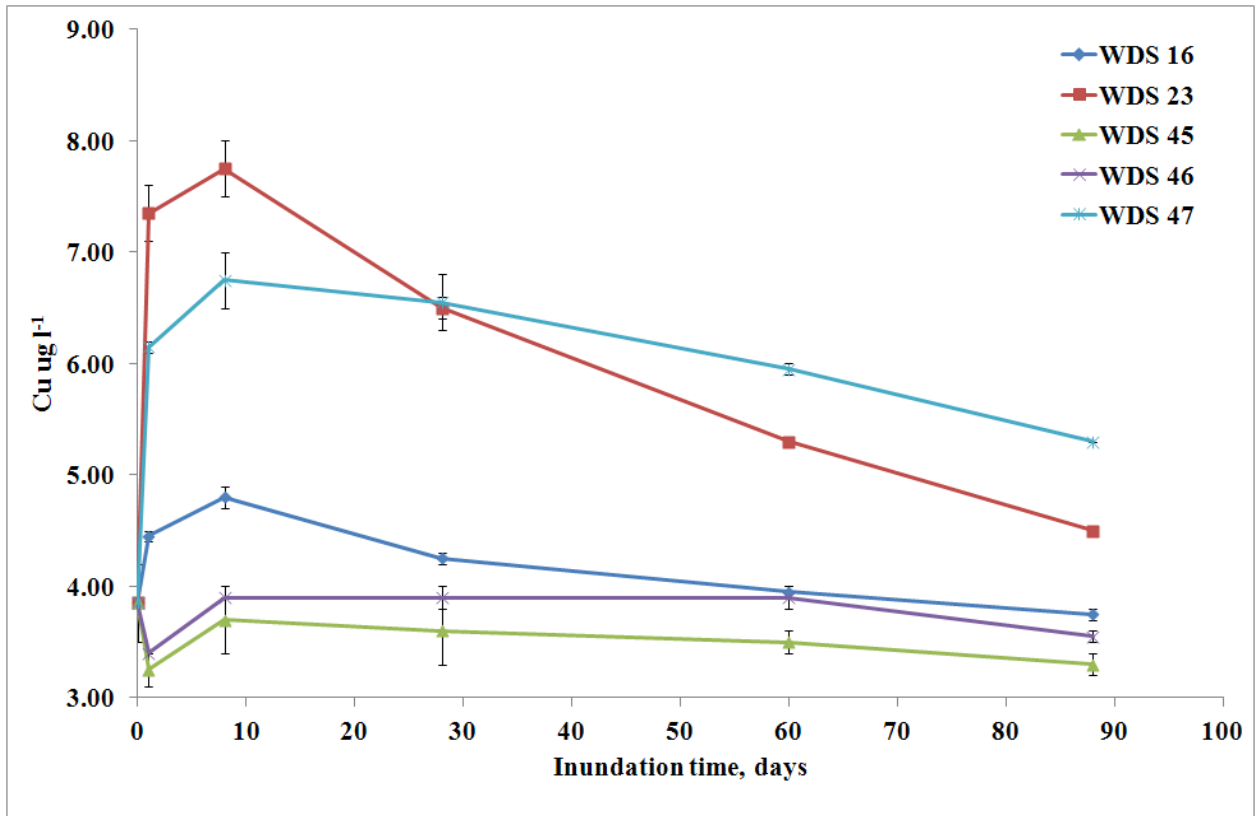


Figure 17 Copper release rate curve, $\mu\text{g l}^{-1}$.

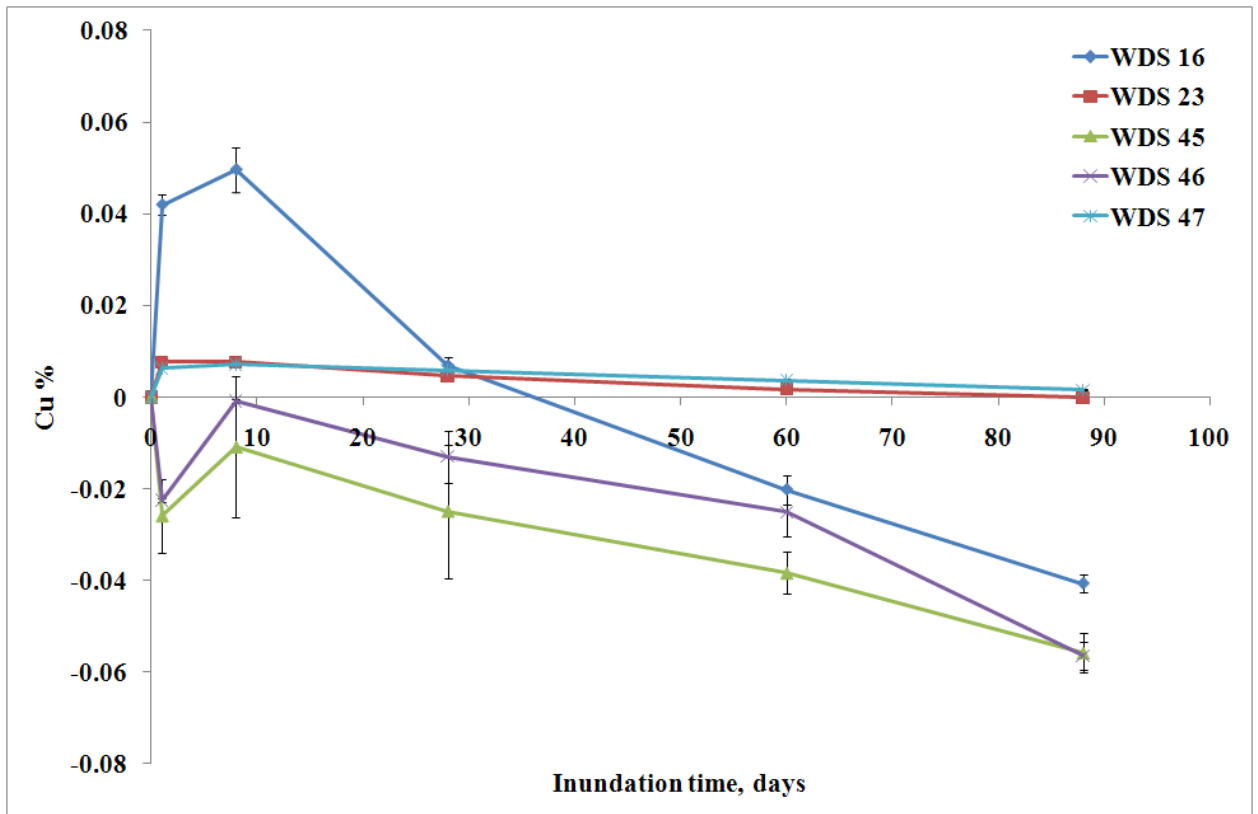


Figure 18 Copper release rate curve, % of the original sediment concentration.

Table 9 Average copper concentrations in the inundation water during flooding. Concentrations in bold are above the EQS

Sample	Time (d)	Cu ($\mu\text{g l}^{-1}$)
Inundation Water	0	3.73
WDS 16	1	4.45
WDS 16	8	4.80
WDS 16	28	4.25
WDS 16	60	3.95
WDS 16	88	3.75
WDS 23	1	7.35
WDS 23	8	7.75
WDS 23	28	6.50
WDS 23	60	5.30
WDS 23	88	4.50
WDS 45	1	3.25
WDS 45	8	3.70
WDS 45	28	3.60
WDS 45	60	3.50
WDS 45	88	3.30
WDS 46	1	3.40
WDS 46	8	3.90
WDS 46	28	3.90
WDS 46	60	3.90
WDS 46	88	3.55
WDS 47	1	6.15
WDS 47	8	6.75
WDS 47	28	6.55
WDS 47	60	5.95
WDS 47	88	5.30

MANGANESE

Figure 19 and Figure 20 summarise the release rates of dissolved Mn from the Rookhope Burn sediment samples over the inundation period, as $\mu\text{g l}^{-1}$ and as a % of the total Mn content of each sediment sample. Table 10 provides the average Mn concentrations ($\mu\text{g l}^{-1}$) in the inundation water for each individual sampling point of the pilot study.

Figure 19 and Table 10 shows that Mn behaved differently under the inundation conditions in the five sediments under investigation, depending on the individual samples and the inundation time at each location. Mn was continually solubilised from the Church House sediment (WDS 23) over the inundation period, whereas for sediments from the Tailrace Level and Wolf Cleugh (WDS 45 and WDS 46), after an enrichment of the dissolved Mn concentration at day 1, a decrease was observed for the remaining inundation period. Sediment samples WDS 16 (Rookhope Arch) and WDS 47 (South Smailburn Plantation) behaved similarly in that Mn was solubilised over the initial 28 day period of inundation. This period is followed by a depletion stage for the remaining inundation period, where the amount of dissolved Mn in the inundation water decreased. Comparison of the initial and final Mn concentrations in the inundation water indicates a Mn increase of c. 330-440% for samples from Church House and South Smailburn Plantation (WDS 23 and WDS 47). Figure 20 shows that over the initial day of inundation the

greatest % of Mn released was from the sediments from Rookhope Arch, the Tailrace Level and Wolf Cleugh (WDS 16, WDS 45 and WDS 46), the three sediments with the lower total Mn concentrations (Table 5).

Table 10 Average manganese concentrations in the inundation water during flooding

Sample	Time (d)	Mn ($\mu\text{g l}^{-1}$)
Inundation Water	0	0.430
WDS 16	1	394
WDS 16	8	694
WDS 16	28	2.35
WDS 16	60	1.55
WDS 16	88	1.85
WDS 23	1	70.2
WDS 23	8	307
WDS 23	28	1772
WDS 23	60	3637
WDS 23	88	4773
WDS 45	1	302
WDS 45	8	138
WDS 45	28	3.00
WDS 45	60	2.75
WDS 45	88	2.10
WDS 46	1	199
WDS 46	8	66.6
WDS 46	28	2.25
WDS 46	60	1.60
WDS 46	88	2.80
WDS 47	1	45.3
WDS 47	8	175
WDS 47	28	394
WDS 47	60	1.90
WDS 47	88	2.35

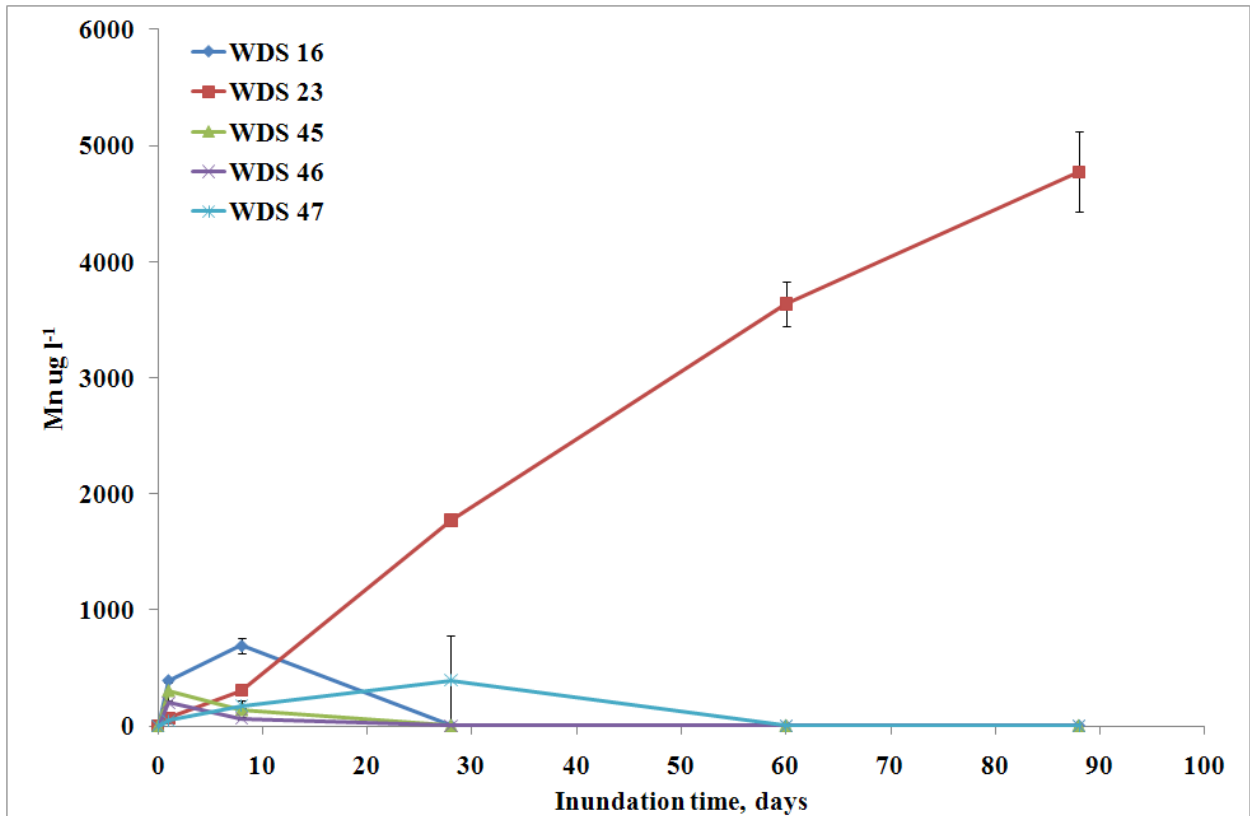


Figure 19 Manganese release rate curve, $\mu\text{g l}^{-1}$.

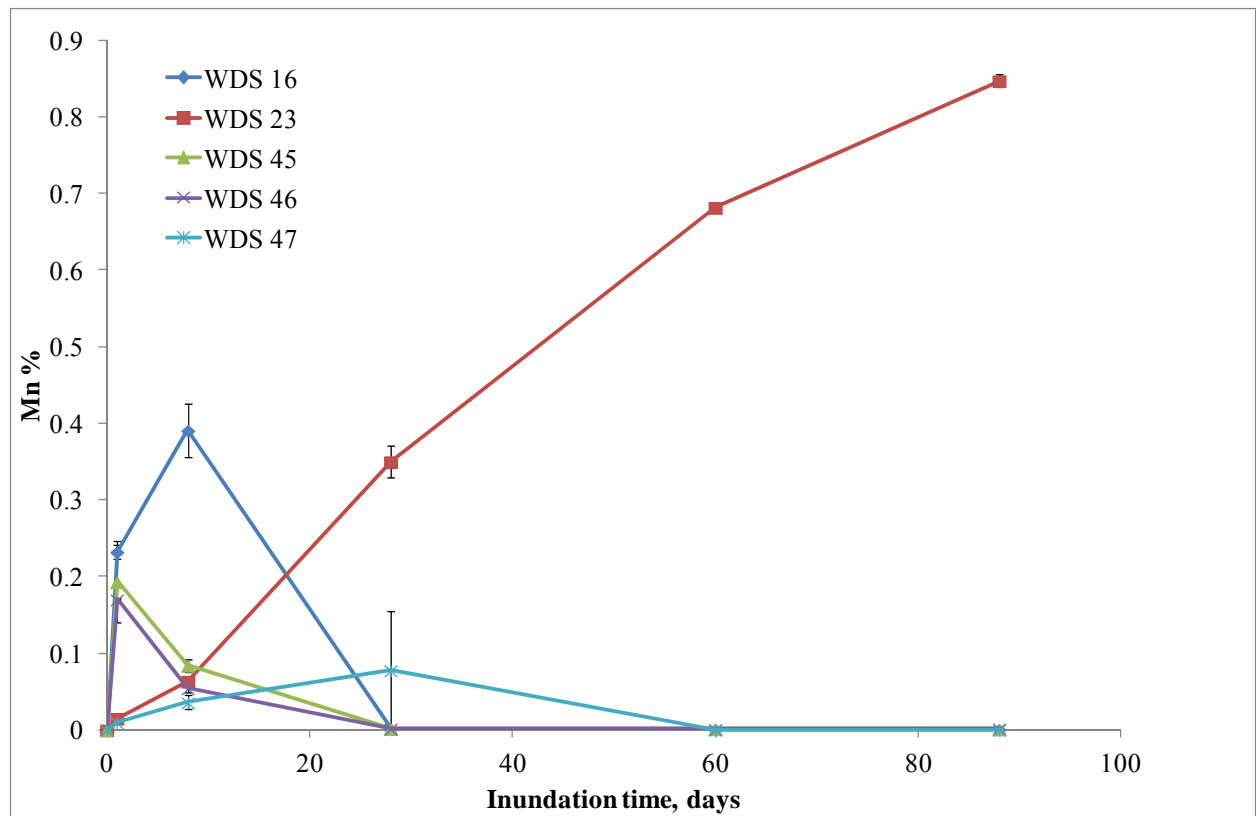


Figure 20 Manganese release rate curve, % of the original sediment concentration.

ZINC

Figure 21 and Figure 22 summarise the release rate curves for Zn over the inundation period as $\mu\text{g l}^{-1}$ and as a % of the total amount of Zn present in each sediment sample. Table 11 summarises the average Zn concentration ($\mu\text{g l}^{-1}$) in the inundation water measured at each sampling stage of the inundation pilot study.

The results show that the initial Rookhope stream inundation water became slightly depleted in Zn on contact with the sediment samples from Rookhope Arch (WDS 16) over the initial 24 hour period and Wolf Cleugh (WDS 46) and South Smailburn Plantation (WDS 47) over the first 8 days of the trial. In all cases, after the initial depletion of Zn from the stream water, a period of enrichment followed. For the two downstream samples, Church House and South Smailburn Plantation (WDS 23 and WDS 47) enrichment was for the duration of the study, for WDS 16 (Rookhope Arch) enrichment ceased at 28 days and for WDS 46 (Wolf Cleugh) cessation was observed at 60 days, whereupon slight depletion was again observed. In the case of the sample collected from the Tailrace level sampling point (WDS 45) enrichment of the stream water with Zn was immediately observed and continued throughout the inundation period.

At all sampling locations the concentrations of Zn in the stream sediments was above the PEL; Table A 3 shows that the hardness related EQS for Zn was exceeded during the inundation study at all locations at the Rookhope Burn test site during different periods of inundations. For two locations, Church House and Tailrace level (WDS 23 and 45), the EQS was exceeded for the whole of the inundation time, whereas for Rookhope Arch (WDS 16) exceedance occurred at 8 days only. For the Wolf Cleugh sample (WDS 46) the EQS was exceeded from 8 days until the completion of the experiment and for the South Smailburn Plantation sample (WDS 47) at 28 days until the end of the experiment.

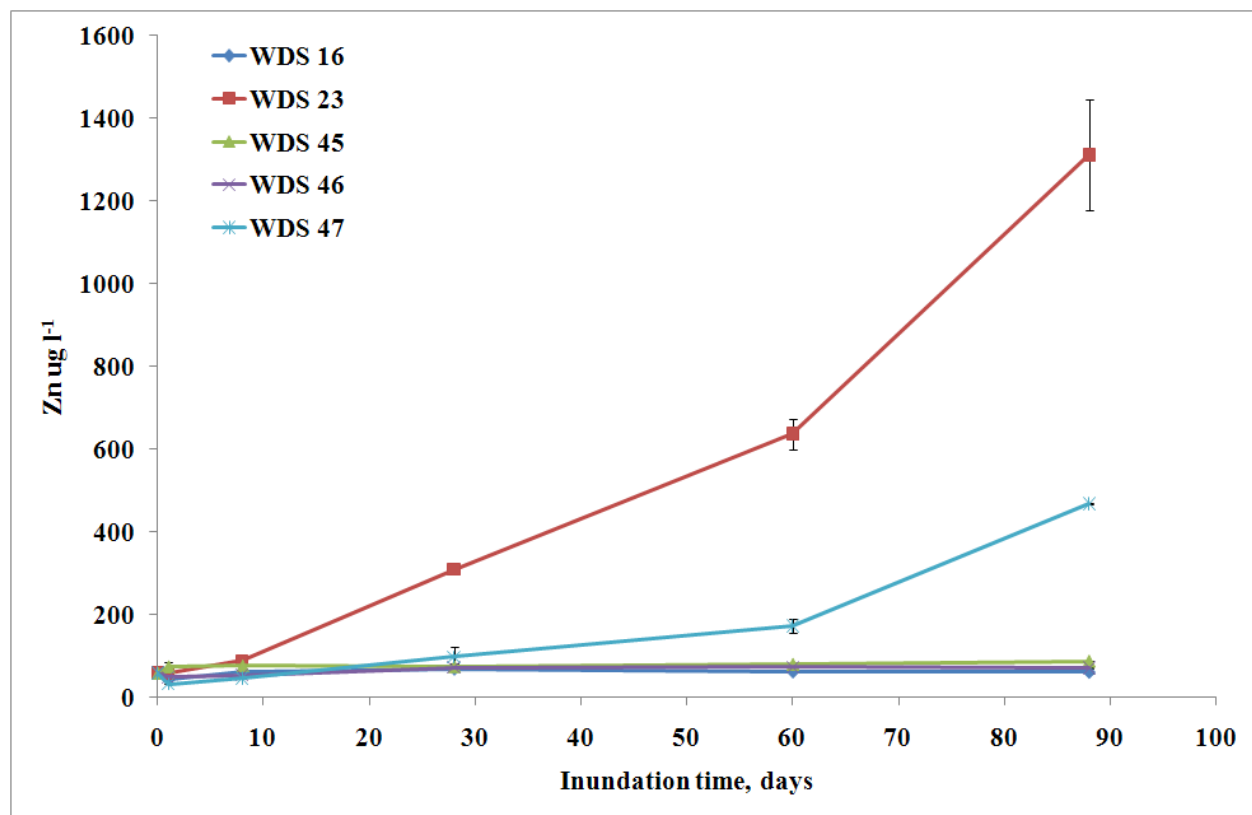


Figure 21 Zinc release rate curve, $\mu\text{g l}^{-1}$.

Table 11 Average zinc concentrations in the inundation water during flooding. Concentrations in bold are above the EQS.

Sample	Time (d)	Zn ($\mu\text{g l}^{-1}$)
Inundation Water	0	59.0
WDS 16	1	43.5
WDS 16	8	63.0
WDS 16	28	68.0
WDS 16	60	61.5
WDS 16	88	60.5
WDS 23	1	58.0
WDS 23	8	89.0
WDS 23	28	309
WDS 23	60	637
WDS 23	88	1312
WDS 45	1	74.5
WDS 45	8	77.0
WDS 45	28	75.0
WDS 45	60	80.5
WDS 45	88	88.0
WDS 46	1	49.0
WDS 46	8	54.0
WDS 46	28	72.0
WDS 46	60	73.5
WDS 46	88	71.0
WDS 47	1	32.0
WDS 47	8	46.0
WDS 47	28	98.0
WDS 47	60	173
WDS 47	88	469

SULPHATE

Figure 23 summarises the release rate curve for SO_4^{2-} over the inundation period as mg l^{-1} in each sediment sample. Table 12 summarises the average SO_4^{2-} concentration (mg l^{-1}) measured at each sampling stage of the inundation pilot study.

Sulphate concentrations in the inundation water increased throughout the duration of the inundation experiment for all samples.

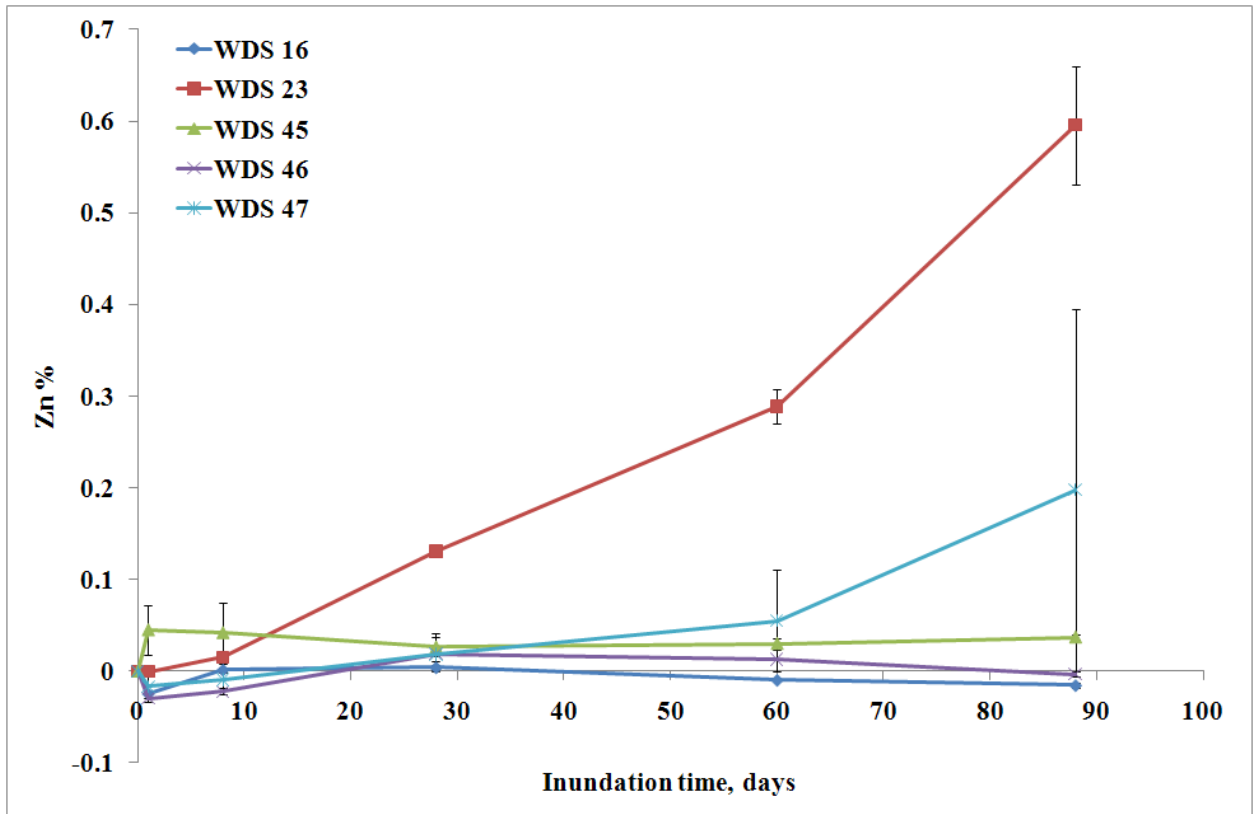


Figure 22 Zinc release rate curve, % of the original sediment concentration.

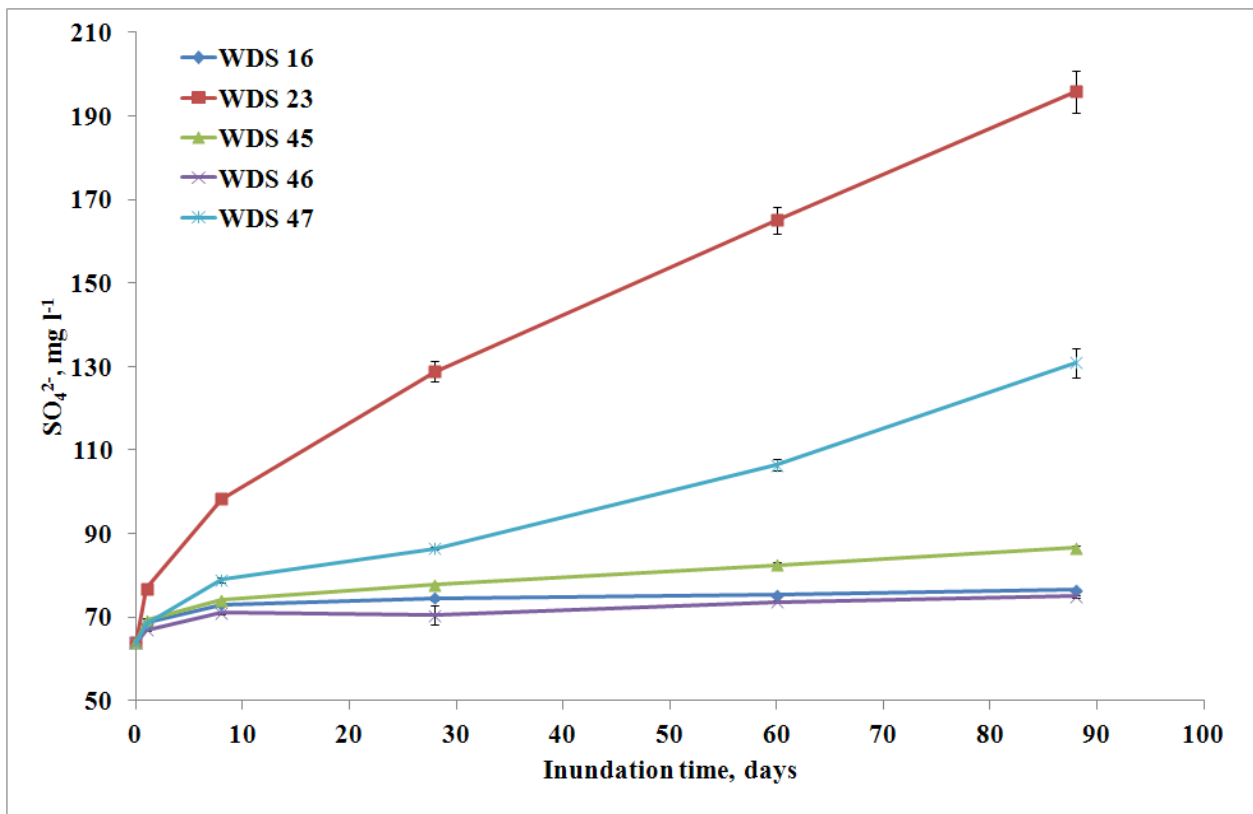


Figure 23 SO₄²⁻ release rate curve, mg l⁻¹.

Table 12 Average sulphate concentrations in the inundation water during flooding.

Sample	Time (d)	SO ₄ ²⁻ (mg l ⁻¹)
Inundation Water	0	64.0
WDS 16	1	68.7
WDS 16	8	73.1
WDS 16	28	74.6
WDS 16	60	75.4
WDS 16	88	76.6
WDS 23	1	76.8
WDS 23	8	98.4
WDS 23	28	129
WDS 23	60	165
WDS 23	88	196
WDS 45	1	69.2
WDS 45	8	74.1
WDS 45	28	77.8
WDS 45	60	82.5
WDS 45	88	86.6
WDS 46	1	67.0
WDS 46	8	71.0
WDS 46	28	70.5
WDS 46	60	73.6
WDS 46	88	75.0
WDS 47	1	68.5
WDS 47	8	78.9
WDS 47	28	86.5
WDS 47	60	106
WDS 47	88	131

6.3 PORE WATER COMPOSITION

Composition of the pore water is shown in Appendix 11. Figure 24 summarises the range of bulk pore water (PW) concentrations for the Rookhope Burn sediments for selected elements as a Box & Whisker plot. The range of element concentrations in the associated inundation waters (IW) at the end of the inundation period (88 days) is also represented. Each box represents the 25th and 75th percentile of the data, with the median value represented by the bold black line running horizontally across each box. The upper and lower whiskers represent the maximum and minimum values. Outliers are shown as black circles and the element concentration in the Rookhope stream water used to inundate the samples is represented by a dotted horizontal line.

Median dissolved SO₄, Mn, Fe, Zn and Pb data (Figure 24) indicates a general trend for enrichment of bulk pore water across the Rookhope Burn sampling locations. For Mn, Fe and Pb, this enrichment is up to 6500, 350 and 500 µg l⁻¹, respectively, and is greater than any increase in the inundation water data. The range of Cu concentrations in the pore water was 3 times that measured in the inundation water samples. Figure 24 shows that, although enriched compared to the original Rookhope stream water sample, the range of SO₄ and Zn concentrations in the bulk pore waters at the end of the study were similar to those observed in the final sample of inundation water.

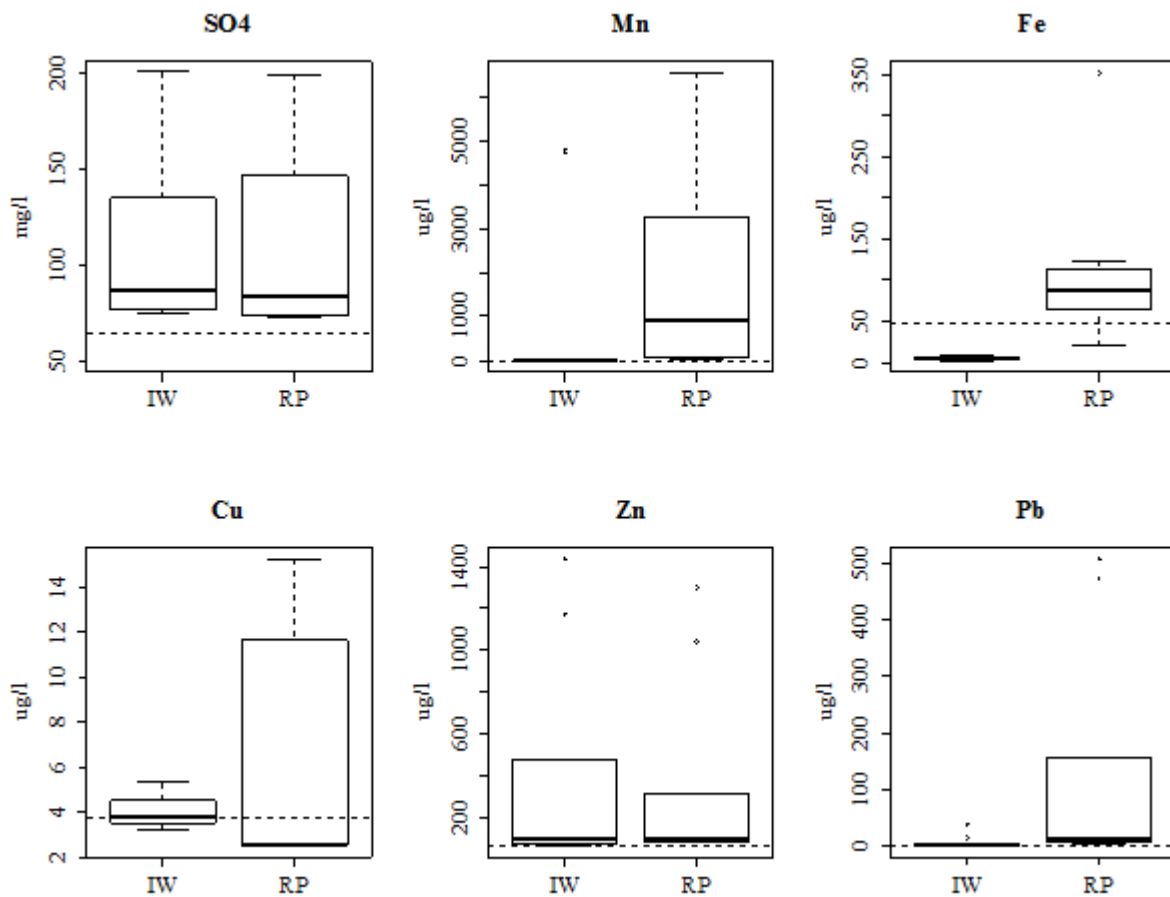


Figure 24 Box and Whisker plots showing the range of selected analyte concentrations in the inundation waters collected at 88 days (IW) and the sediment bulk pore waters (PW) for the sites under investigation.

6.4 SATURATION INDICES

In order to assess how close to saturation the inundation water solutions were with respect to phases which were likely to be present in the sediment or possibly formed during the experiment, saturation indices (SI) were calculated using PHREEQC (Parkhurst and Appelo, 1999) and the WATEQ4F.dat database (Ball and Nordstrom, 1991). The calculation of the SI may also provide means to estimate whether further dissolution of the PHE of interest may be possible, as this will be affected by saturation of the inundation water.

The SI is calculated from the equation: $SI = \text{Log} (IAP/K_{ss})$, where IAP is the ionic activity product of the specific reaction and K_{ss} the equilibrium constant. A SI of zero indicates that the solution is in equilibrium with a particular mineral. A $SI < 0$ indicates that the solution is undersaturated with respect to a particular mineral and a $SI > 0$ indicates oversaturation.

Measured pH, Eh and total element concentrations in the inundation waters were used as input parameters and the calculated SI are summarised in Tables 13 and 14. The precipitation of all solids was suppressed.

The solubility control of Fe concentrations in the inundation waters is evident by the $SI > 1$ of goethite and of poorly crystalline ferric hydroxide.

Gypsum was always undersaturated.

SI values of calcite were within 0 ± 0.5 for samples WDS 16, WDS 23 and WDS 47. Equilibrium of the solutions with calcite for these samples is reasonably inferred considering the XRD evidence of the presence of calcite in these sediments.

The SIs for the carbonates and oxides of Zn (smithonite $ZnCO_3$; zincite ZnO) were generally closer to equilibrium, however, without reaching saturation. Bianchite ($ZnSO_4$) was always undersaturated.

Anglesite ($PbSO_4$) was undersaturated in all samples. Cerussite ($PbCO_3$) was near saturation in most samples. Inundation waters of WDS 23 reached saturation with respect to cerussite after 28 days.

All or most of WDS 16, WDS 23, WDS 47 inundation waters were supersaturated with Mn minerals rhodochrosite ($MnCO_3$), manganite $MnO(OH)$ and pyrolusite (MnO_2). Although we lack direct XRD-based evidence, Mn-rich coatings, consisting of hydrous Fe-Mn oxides and carbonates, have been observed in many mining contaminated streams (Bargar *et al.*, 2009).

Table 13 Calculated SI for WDS 16, 23 and 45

Sample	Time (days)	SI Anglesite	SI Cerrussite	SI Calcite	SI Dolomite	SI Fe(OH)3(a)	SI Goethite
WDS 16	1	-5.2	-2.1	-0.2	-0.9	1.7	7.4
	8	-5.4	-2.4	-0.3	-1.1	1.3	7.0
	28	-5.6	-2.8	-0.4	-1.4	1.0	6.5
	60	-5.4	-2.5	-0.3	-1.2	0.9	6.4
	88	-5.0	-2.3	-0.5	-1.7	1.2	6.6
Pore water		-5.1	-1.6	0.4	0.3	1.7	7.6
WDS 16 Dup.	1	-5.2	-2.1	-0.2	-0.8	1.7	7.5
	8	-5.4	-2.3	-0.2	-0.9	1.5	7.1
	28	-5.5	-2.7	-0.5	-1.6	0.9	6.4
	60	-5.6	-2.6	-0.3	-1.1	0.8	6.4
	88	-5.3	-2.3	-0.2	-1.1	1.1	6.5
Pore water		-5.8	-1.9	0.7	1.0	1.2	7.1
WDS 23	1	-3.9	-0.8	-0.2	-0.9	1.5	7.3
	8	-3.6	-0.7	-0.3	-1.1	1.4	7.1
	28	-2.8	-0.3	-0.6	-1.9	1.0	6.5
	60	-2.2	0.0	-0.7	-2.2	0.5	6.0
	88	-1.7	0.1	-1.0	-2.8	0.9	6.3
Pore water		-1.9	0.2	-0.7	-1.9	2.3	8.2
WDS 23 Dup.	1	-4.0	-0.8	-0.1	-0.7	1.5	7.3
	8	-3.5	-0.7	-0.4	-1.4	1.4	7.1
	28	-2.8	-0.3	-0.5	-1.8	0.9	6.4
	60	-2.2	0.0	-0.7	-2.0	0.5	6.1
	88	-1.8	0.2	-0.9	-2.7	1.0	6.4
Pore water		-2.1	0.2	-0.5	-1.5	1.6	7.5
WDS 45	1	-4.6	-1.9	-0.7	-1.8	1.5	7.2
	8	-4.3	-1.9	-1.0	-2.5	1.5	7.1
	28	-4.1	-2.1	-1.5	-3.4	1.1	6.6
	60	-3.9	-2.0	-1.5	-3.4	0.7	6.2
	88	-3.8	-2.0	-1.6	-3.7	0.9	6.3
Pore water		-3.8	-1.3	-0.9	-2.1	1.9	7.8
WDS 45 Dup.	1	-4.6	-1.9	-0.7	-1.9	1.4	7.1
	8	-4.1	-1.9	-1.2	-2.8	1.3	7.0
	28	-4.1	-2.1	-1.5	-3.4	0.9	6.4
	60	-4.1	-2.2	-1.5	-3.4	0.6	6.1
	88	-4.0	-2.1	-1.6	-3.6	1.0	6.3
Pore water		-3.7	-1.3	-0.9	-2.1	1.9	7.7

Table 13 (continued) Calculated SI for WDS 16, 23 and 45

Sample	time (days)	SI Gypsum	SI Bianchite	SI Smithsonite	SI Zincite(c)	SI Rhodochrosite	SI Manganite	SI Pyrolusite
WDS 16	1	-1.9	-8.1	-2.2	-2.8	0.1	-1.1	-3.3
	8	-1.8	-7.9	-2.1	-3.1	0.2	0.2	-0.9
	28	-1.7	-7.9	-2.3	-3.9	-2.5	-2.0	-2.9
	60	-1.7	-8.0	-2.3	-3.9	-2.5	-2.5	-3.6
	88	-1.6	-8.0	-2.6	-4.6	-2.8	-3.5	-6.0
Pore water		-1.7	-7.9	-1.5	-2.2	1.0	1.7	2.3
WDS 16 Dup.	1	-1.9	-8.1	-2.1	-2.7	0.2	-0.7	-2.7
	8	-1.8	-7.9	-2.1	-3.0	0.4	0.5	-0.4
	28	-1.7	-7.9	-2.4	-4.0	-2.5	-2.2	-3.2
	60	-1.7	-8.0	-2.3	-3.9	-2.6	-2.4	-3.3
	88	-1.6	-8.0	-2.3	-4.0	-2.4	-2.3	-4.3
Pore water		-1.7	-8.4	-1.6	-1.8	0.8	2.6	3.9
WDS 23	1	-1.8	-7.9	-2.0	-2.5	-0.6	-1.3	-3.2
	8	-1.6	-7.6	-2.0	-2.7	0.0	0.3	-0.5
	28	-1.5	-6.9	-1.8	-3.0	0.3	0.8	-0.5
	60	-1.3	-6.5	-1.6	-2.8	0.4	0.9	-0.2
	88	-1.2	-6.1	-1.6	-2.8	0.3	0.7	-1.4
Pore water		-1.3	-6.2	-1.2	-1.3	0.6	1.9	2.6
WDS 23 Dup.	1	-1.8	-8.0	-2.0	-2.4	-0.5	-1.0	-2.6
	8	-1.6	-7.6	-2.1	-2.9	-0.2	-0.4	-1.6
	28	-1.5	-7.0	-1.8	-2.9	0.3	0.8	-0.6
	60	-1.4	-6.6	-1.6	-2.8	0.5	0.9	-0.3
	88	-1.3	-6.2	-1.6	-2.9	0.3	0.8	-1.3
Pore water		-1.3	-6.3	-1.1	-1.2	0.9	2.4	3.2
WDS 45	1	-1.9	-7.8	-2.3	-3.2	-0.5	-1.3	-2.8
	8	-1.9	-7.8	-2.6	-3.8	-1.0	-1.4	-2.7
	28	-1.9	-7.7	-3.0	-4.5	-3.0	-3.3	-4.9
	60	-1.8	-7.6	-3.0	-4.4	-3.2	-3.1	-4.4
	88	-1.8	-7.6	-3.1	-4.5	-3.2	-3.5	-6.0
Pore water		-1.9	-7.6	-2.3	-2.6	-2.0	-1.2	-0.8
WDS 45 Dup.	1	-1.9	-7.7	-2.2	-3.2	-0.3	-1.1	-2.7
	8	-1.9	-7.6	-2.6	-3.8	-1.1	-1.6	-2.9
	28	-1.9	-7.6	-3.0	-4.4	-3.1	-3.4	-5.2
	60	-1.8	-7.6	-3.0	-4.4	-3.1	-3.0	-4.3
	88	-1.8	-7.5	-3.0	-4.5	-3.4	-4.0	-6.8
Pore water		-1.9	-7.6	-2.3	-2.4	-2.0	-1.3	-1.1

Table 14 Calculated SI for WDS 46 and 47

Samples	time (days)	SI Anglesite	SI Cerrusite	SI Calcite	SI Dolomite	SI Fe(OH)3(a)	SI Goethite
WDS 46	1	-4.8	-2.0	-0.6	-1.6	1.6	7.3
	8	-4.4	-2.2	-1.2	-2.8	1.3	7.0
	28	-4.5	-2.3	-1.2	-2.9	1.1	6.6
	60	-4.5	-2.3	-1.1	-2.7	0.9	6.5
	88	-4.4	-2.1	-1.2	-2.9	1.1	6.5
Pore water		-4.2	-1.4	-0.6	-1.5	1.7	7.6
WDS 46 Dup.	1	-4.9	-2.0	-0.5	-1.5	1.6	7.3
	8	-4.6	-2.1	-0.9	-2.3	1.4	7.1
	28	-4.4	-2.3	-1.3	-3.1	1.0	6.5
	60	-4.5	-2.3	-1.2	-2.8	0.9	6.5
	88	-4.4	-2.1	-1.2	-2.9	1.1	6.5
Pore water		-4.4	-1.6	-0.5	-1.4	1.5	7.4
WDS 47	1	-4.3	-1.1	-0.2	-0.9	1.6	7.3
	8	-4.2	-1.2	-0.2	-1.1	1.2	6.9
	28	-4.6	-1.8	-0.4	-1.6	1.0	6.5
	60	-4.3	-1.6	-0.5	-1.6	0.6	6.2
	88	-3.5	-1.3	-0.8	-2.3	0.7	6.1
Pore water		-3.7	-0.3	0.6	0.6	1.9	7.8
WDS 47 Dup.	1	-4.4	-1.2	-0.1	-0.8	1.6	7.3
	8	-4.4	-1.3	-0.2	-1.0	1.1	6.8
	28	-5.1	-2.3	-0.3	-1.4	0.6	6.1
	60	-4.1	-1.3	-0.3	-1.3	0.5	6.1
	88	-3.3	-0.7	-0.4	-1.6	0.8	6.1
Pore water		-3.9	-0.4	0.7	0.7	1.8	7.7

Table 14 (continued) Calculated SI for WDS 46 and 47

Samples	time (days)	SI Gypsum	SI Bianchite	SI Smithsonite	SI Zincite(c)	SI Rhodochrosite	SI Manganite	SI Pyrolusite
WDS 46	1	-1.9	-8.0	-2.4	-3.2	-0.5	-1.0	-2.4
	8	-1.9	-7.9	-2.9	-4.3	-1.5	-2.3	-3.8
	28	-1.8	-7.8	-2.8	-4.4	-3.0	-3.3	-5.0
	60	-1.8	-7.7	-2.8	-4.3	-3.2	-3.5	-4.9
	88	-1.8	-7.7	-2.8	-4.4	-3.1	-3.7	-6.4
Pore water		-1.9	-7.8	-2.1	-2.4	-0.6	0.0	0.2
WDS 46 Dup.	1	-1.9	-8.0	-2.3	-3.1	-0.4	-1.3	-3.1
	8	-1.9	-7.9	-2.6	-3.8	-1.3	-1.8	-3.0
	28	-1.9	-7.8	-2.9	-4.6	-3.1	-3.8	-5.8
	60	-1.8	-7.7	-2.8	-4.3	-3.1	-3.2	-4.5
	88	-1.8	-7.7	-2.8	-4.4	-2.7	-3.5	-6.5
Pore water		-1.9	-7.8	-2.1	-2.3	-0.7	-0.1	0.0
WDS 47	1	-1.8	-8.3	-2.3	-2.9	-0.8	-1.3	-2.8
	8	-1.7	-8.0	-2.2	-3.1	-0.2	-0.5	-1.9
	28	-1.6	-7.6	-2.1	-3.4	0.1	0.0	-1.5
	60	-1.5	-7.4	-2.0	-3.5	-2.7	-2.8	-4.1
	88	-1.4	-6.8	-1.9	-3.8	-2.8	-4.0	-7.1
Pore water		-1.4	-7.3	-1.0	-1.0	1.5	2.7	3.2
WDS 47 Dup.	1	-1.8	-8.3	-2.2	-2.6	-0.8	-1.0	-2.4
	8	-1.7	-8.1	-2.2	-3.0	-0.4	-0.4	-1.6
	28	-1.6	-7.8	-2.2	-3.5	-2.3	-2.3	-3.8
	60	-1.5	-7.3	-1.8	-3.1	-2.4	-2.2	-3.4
	88	-1.4	-6.8	-1.6	-3.2	-2.6	-3.1	-5.9
Pore water		-1.4	-7.5	-1.1	-1.1	1.4	2.7	3.2

6.5 ZN/SO₄ AND CD/ZN MOLAR RATIOS

The Zn/SO₄ and Cd/Zn molar ratios can be useful to infer the solid phase/process responsible for the metals in solution (Nordstrom, 2011) during water/rock interaction and are summarised in Figure 25. The Zn/SO₄ molar ratio derived from sphalerite dissolution according to $ZnS = Zn^{2+} + SO_4^{2-}$ is 1:1. Sphalerite is also characterised by a specific range of Cd (0.1-0.5%) (Fuge *et al.*, 1993; Wakita and Schmitt, 1970).

The Zn/SO₄ molar ratios in the inundation water ranged between 1:1 and 1.4:1 for sample WDS16, 1.5:1 and 1.6:1 for WDS45, 1.1:1 and 1.5:1 for WDS46, close enough to the 1:1 ratio of a sphalerite (ZnS) oxidation product to suggest its influence on the overlying water Zn composition. On the contrary, the Zn/SO₄ molar ratio varied considerably, from 1.1:1 to 10:1 for WDS 23 and from 0.7:1 to 5.4:1 for WDS47 over the course of the inundation, indicating potential dissolution of another Zn-bearing solid phase.

The Cd/Zn molar ratio is also in the range of sphalerite composition (0.0007- 0.0037), and, within this range, it is noticeably higher in WDS 23 and WDS 47.

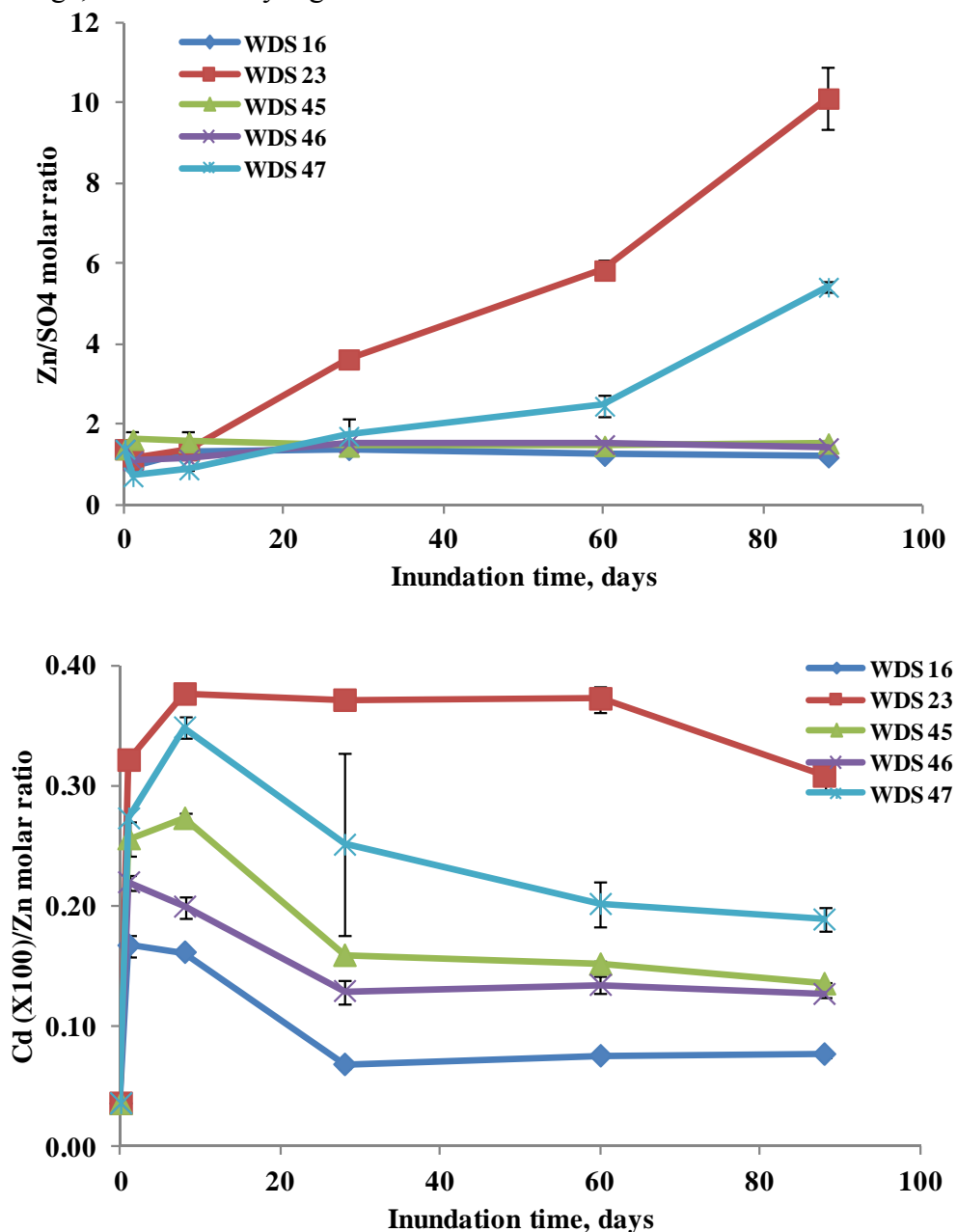


Figure 25 Plots of Zn/SO₄ and Cd (x100)/Zn molar ratios across the inundation period.

7 Discussion

Chemical analysis of bank sediments collected from the Rookhope Burn catchment identified Pb and Zn concentrations highly above both the TEL and PEL sediment quality criteria, posing a potentially significant hazard to aquatic organisms. The source of the Pb and Zn in the sediments under study is related to the underlying mineralisation and mining activities in the area. Above all, the most downstream sediment samples from Church House (WDS 23) and South Smailburn Plantation (WDS 47) are highly enriched in Pb (29514 and 14421 mg kg⁻¹, respectively) and Zn (1691 and 1620 mg kg⁻¹, respectively) and contain cerussite, galena and sphalerite. The observed enrichment of ore mineral phases in these sediments is to be related to the close proximity to the Boltsburn Mine (1903-1970) washing plant (its remnants still visible along the river), where the Pb ore was crushed and fine particles of galena separated from waste with water flowing across an inclined table (Bowes and Wall, 1995). Due to the inefficiency of the processing operations, the spoil heaps contained large residual quantities of metal ore. Also, in the other sediments (WDS 46, WDS 45 and WDS 16), upstream of the Boltsburn Mine washing plant, authigenic phases formed by sorption or precipitation from metal-rich mine waters discharging into the Rookhope Burn in the upper part of the catchment (Banks and Palumbo-Roe, 2010) may be particularly significant metal-bearing mineral phases. Significant variations throughout the catchment in sediment composition and in solid phase metal speciation of the Rookhope sediments can be expected.

The inundation pilot study carried out over an 88 day (3 month period) period showed that Cu, Mn, Pb, Zn and SO₄ were all mobilised from the sediment samples of the Rookhope Burn catchment, while dissolved Fe in the overlying inundation water decreased.

Metal release from contaminated sediments to the overlying water is controlled by matrix diffusion driven by the metal concentration gradient between the water column and the sediment pore water, across the sediment-water interface.

The initial high values of metal concentrations in the overlying inundation water observed for all the studied sediment samples are due to equilibration of the overlying water with the sediment pore water. As time elapse during the sediment flooding, metal fluxes to the overlying water will change depending on a number of factors among which the sediment physico-chemical conditions (e.g. Eh, T, pH, dissolved O) and composition (e.g. mineralogy, organic matter content) and the geochemical affinity and solubility of each element. These account for the fact that the Rookhope bank sediments showed different degrees and different rates of metal losses to the overlying water column during flooding.

A model of sediment metal fluxes needs to take into account multiple processes: i) solid-phase dissolution through solid phase solubility control or kinetic controls; ii) metal sequestrations in newly formed salts (carbonates, hydroxides, sulphates) or sparingly soluble sulphide precipitates depending on the solution composition, metal supply and redox conditions; iii) redox changes affecting contaminant redox speciation and causing reductive dissolution of sorbent phases (e.g. Fe and Mn oxy-hydroxides) with release into solution of sorbed elements.

The microbial catalysis of many of these processes is also important because many indigenous or contaminant organisms use PHE as either electron donors or acceptors, as part of their metabolic processes. Examples include the use of As (V) as a terminal electron acceptor for respiration by many bacteria, resulting in the reduction of As (V) to As (III), which is less strongly sorbed and preferentially released into solution at acidic and near neutral pH and the dissolution of poorly crystalline Fe (III) (hydr)oxides by dissimilatory Fe (III) reducing bacteria (Weber *et al.*, 2010).

Di Toro *et al.*, (1996) described the sediment exposed to molecular oxygen through contact with the overlying water as a sequence of an aerobic zone and an anaerobic zone. Whether or not inundation lowered redox potentials in pore water in the simulated flooding regime is, however, uncertain. The water column maintained oxic conditions with an ORP above 200-350 mV, as the

experiments were carried out in conditions that were exposed to the open environment at periodic times of sampling. The studied bank sediments were relatively poor in clays and organic matter, which are both known to favour the establishment of reducing conditions in saturated soil and sediment systems, respectively limiting the oxygen diffusion and consuming the dissolved oxygen by organic matter decomposition. This suggests that an extensive reduced redox zone might have not been formed and reductive dissolution processes might not be the main controlling processes affecting the contaminant dynamics in the studied sediment under the simulated flooding regime. Yet, only extending the Eh measurements to the submerged sediment would allow distinguishing the presence of flooding-induced reducing conditions.

The inundation water composition monitored during the sediment flooding could be used to indirectly infer possible processes among the ones above described that control contaminant fluxes from the studied flooded sediments to the overlying water.

Dissolved Fe concentrations decreased greatly in the first stage of the inundation period in the overlying water column of all sediments, due to the Fe (III) tendency to form colloidal oxyhydroxide precipitates already at low pH (~ 3.5) (Smith, 1999). The bulk pore water at the end of the experiment was significantly enriched in Fe than the overlying inundation water, indicating the potential for continuous diffusion flux of Fe through the sediment-water interface as a result of the concentration gradient. However, once at the sediment-water boundary the Fe would quickly precipitate as Fe (III) oxyhydroxides. These can provide additional sorption sites for metals.

For Mn, all initial inundation waters immediately after the flooding became enriched in dissolved Mn resulting from the overlying water equilibration with the sediment pore water, regardless of the initial concentration in the solid sediment material. However, for two of the sediments, from the Tailrace Level and Wolf Cleugh sites (WDS 45 and WDS 46), a decrease of dissolved Mn was observed already after a week of inundation, suggesting favourable conditions for its sequestration in the sediments. This could be further investigated by secondary electron microscopy (SEM) analysis of the water-sediment boundary layer. For the sediment samples WDS 16 (Rookhope Arch) and WDS 47 (South Smailburn Plantation) Mn continued to enrich in the inundation water, until the 28 day period of inundation, after which the amount of dissolved Mn in the inundation water decreased. Mn was continually solubilised from the Church House sediment (WDS 23) over the inundation period. Increasing concentrations of Mn in solution following the development of reducing conditions inducing reductive dissolution of Mn oxyhydroxides is a well known phenomenon and the release of trace metals, such as e.g. Pb and Zn, previously sorbed on the oxyhydroxides often observed. The final pore water composition of WDS 16, WDS 23 and WDS 47 was significantly enriched in Mn (1300- 6500 $\mu\text{g l}^{-1}$). Saturation indices indicated both rhodocrosite (MnCO_3) and Mn oxides as reaching saturation. Therefore, it is not possible to preclude either the role of rhodocrosite as solubility controlling solid phase or the reductive dissolution of Mn oxides for accounting the enhanced Mn concentrations in the pore water and overlying water column without a better characterisation of the solid phase and monitoring of the sediment redox conditions.

Dissolved Pb concentration in the inundation water reflected the original concentration in the solid material and in samples that had XRD-detectable galena and cerussite the dissolved Pb concentration reached a maximum value of 395 $\mu\text{g l}^{-1}$. Cerussite, which is commonly formed as coatings on galena during the sulphide weathering, was close or supersaturated in those solutions, suggesting that the lead carbonate mineral phase provided a continuous source of Pb to these solutions.

The initial Zn in the inundation water was independent of the original concentration in the solid material, similarly to Mn. It is especially noticeable for the greater Zn concentration at the initial flooding stage for WDS 16 at Tailrace Level, a sediment with relatively low Zn concentration. At this location, the Tailrace Level has continuously discharged mine water with high Zn concentrations since the closure of Frazer's Grove mine. Johnson and Younger (2002) reported

peak Zn concentrations as high as 35.6 mg l^{-1} via the Tailrace Level during the mine rebound. Downstream mine water discharges, streams tend to attenuate their metal content through various chemical and physical processes, including dilution, precipitation-sedimentation-concretion, and adsorption-ion exchange on bed sediments and settling of suspended particles (Chapman *et al.*, 1983). The resulting contaminated sediments are often only a temporary store of metals, as these particle-bound metals (*e.g.* secondary metal-bearing Fe and Mn hydroxides, soluble sulphates, *etc.*) can be more easily remobilised than those present in the original sulphide ore minerals. This could be the case for WDS 16 showing a greater availability of easily mobilised Zn, producing high initial leachate concentration, despite the lower Zn concentration in the sediment. This easily mobilised metal fraction was, though, quickly depleted and the Zn release rate rapidly decreased during the inundation period. The final inundation water solutions had the highest Zn concentrations for those samples where sphalerite was detected by XRD, such as in WDS 23 (Church House) and WDS 47 (South Smailburn Plantation). Although the Zn/SO₄ molar ratios was initially close to the 1:1 ratio of a sphalerite (ZnS) oxidation product, as flooding time elapsed it became closer to 10:1, suggesting potential dissolution of another Zn-bearing solid phase or incongruent dissolution.

8 Conclusions

A literature review has found that although inundation studies are not a new idea, the majority of work in this area has previously been carried out as part of soil fertility and plant nutrition studies. The study of contaminants, and specifically metal mobility, is now coming to the fore, as a growth area in the literature. However, there has been little, if any, work to standardise inundation methodologies/protocols. As there was no suitable, single documented protocol available, this study combined practical methodologies from other studies. However, the following amendments to the study design are recommended for future studies:

1. Further investigation into the optimum parameters for the geometry of the microcosm set-up to allow for the continuous monitoring of pore water dynamics within the system and allow for the collection of pore water at the different time points and measurement of pore water pH and Eh, *etc.*;
2. Inclusion of a sediment washing stage prior to the start of the main inundation experiment, to remove the soluble/easily leachable fraction;
3. A blank inundation of all test materials with de-ionised water, to test the influence of the properties and the volume of the inundation water;
4. Comparison of water movement with stagnant flooding, this study only considered stagnant flooding;
5. A longer inundation time to investigate whether those PHE that were observed to be increasing in solubility at 88 days would continue to increase; and,
6. A different ambient temperature to investigate the effect of temperature on the system.
7. This pilot study was a purely chemical analysis of the test system and did not assess the presence or effect of microbes on the solubility of PHE after inundation. The inclusion of microbes as a test parameter would be recommended for future studies, as microbes are known to influence the redox conditions in soils and sediment systems creating reducing conditions and thereby increasing the mobility of and potential risk to aquatic organisms and other receptors from contaminants (Cummings *et al.*, 2000; Lloyd and Oremland, 2006; Rowland *et al.*, 2007).

The pilot study has shown that inundation of river bank sediments from the Rookhope Burn is a significant pathway for PHE in the catchment and mobilisation of PHE from the sediments may pose a hazard to environmental receptors in the area, particularly with respect to Pb and Zn contamination.

The mechanisms of release and potential sorption/precipitation of the PHE have only partially been addressed in this report. The different degrees and different rates of metal losses to the overlying water column observed during the flooding of the Rookhope Burn bank sediments demonstrated that the significance of metal mobilisation was dictated by the sediment composition. Further work, in the form of solid phase characterisation and possible further experimental work aimed at monitoring the pore water changes is required to fully understand the processes taking place in the test system. Although the XRD analysis alludes to the differences in the solid phase distribution of the PHE at the different sampling locations, further selective chemical extractions aimed at characterising the element distribution in the solid phases would help to confirm these differences. Inclusion of scanning electron microscopy observations of the sediment samples may also identify PHE solid phase transformations and redistributions from one host substrate (*e.g.* carbonates, oxides, sulphides) to another from processes such as desorption, re-adsorption, precipitation, oxidation, *etc.*

Appendix 1 Water and Sediment Quality Standards

Environment Agency (EA) have published soil guideline values (SGVs) for a number of PHEs with respect to human health risk assessment (Environment Agency, 2009), which incorporate the ingestion, inhalation and dermal contact exposure pathways. SGVs are scientifically-based generic assessment criteria used to help evaluate long term human health risks associated with a contaminant in a soil at a given site. The SGVs are trigger values that may pose a significant risk to human health; however, this is generally determined by carrying out a detailed quantitative risk assessment and not by exceedance of the SGV alone. Currently, in the UK there are no statutory Environmental Quality Standards (EQS) for sediments, however, sediment guideline values are being developed that could be used to trigger further investigation (Environment Agency, 2008). The guidelines are based on the approach of Environment Canada, which considers a Toxic Effect Level (TEL, the concentration below which sediment associated contaminants are not considered to represent significant hazards to aquatic organisms) and a Predicted Effect Level (PEL, the concentration representing the lower limit of the range of concentrations associated with adverse biological effects) (Table A1). Freshwater EQS from the European Community (EC) Dangerous Substances Directive (76/464/EEC), lists 1 and 2 are shown in Table A2 and A3. Such EQS are an integral part of the European Water Framework Directive (WFD), which aims to deliver an integrated approach to river basin management (Comber *et al.*, 2008) across Europe.

Table A 1 Draft sediment quality criteria (TEL, PEL) for England and Wales, mg kg⁻¹ (after Environment Agency, 2008)

PHE	TEL (mg kg ⁻¹)	PEL (mg kg ⁻¹)
As	5.9	17
Cd	0.596	3.53
Cr	37.3	90
Cu	36.7	197
Pb	35	91.3
Ni	18	35.9
Zn	123	315

Table A 2 Freshwater EQS for selected list 1 and 2 dangerous substances, after EC Dangerous Substances Directive (76/464/EEC), µg l⁻¹

PHE	EQS (µg l ⁻¹)
As	50
Cd	5
Fe	1000
Pb	7.2

Table A 3 - Annual average EQS at different CaCO₃ content for selected list 2 dangerous substances, after EC Dangerous Substances Directive (76/464/EEC), µg l⁻¹

PHE	Cr (µg l⁻¹)	Cu (µg l⁻¹)	Ni (µg l⁻¹)	V (µg l⁻¹)	Zn (µg l⁻¹)
0-50 mg l ⁻¹ CaCO ₃	5	1	50	20	8
50-100 mg l ⁻¹ CaCO ₃	10	6	100	20	50
100-150 mg l ⁻¹ CaCO ₃	20	10	150	20	75
150-200 mg l ⁻¹ CaCO ₃	20	10	150	20	75
200-250 mg l ⁻¹ CaCO ₃	50	10	200	60	75
>250 mg l ⁻¹ CaCO ₃	50	28	200	60	125

Appendix 2 XRD Sediment Characterisation data

Sample	Mineralogy (%)													
	albite	calcite	cerrussite	chlorite	dolomite	fluorite	galena	'kaolin'	K-feldspar	'mica'	pyrite	quartz	siderite	sphalerite
WDS 16	1.8	<0.5	nd	1.8	nd	2.4	nd	5.3	<0.5	13.6	<0.5	74.3	nd	nd
WDS 23	nd	0.8	1.2	1.7	2.6	12.2	0.8	2.3	nd	9.2	<0.5	58.5	10.3	<0.5
WDS 45	nd	nd	nd	3.0	nd	3.4	nd	4.8	nd	13.8	<0.5	74.7	nd	nd
WDS 46	nd	nd	nd	2.0	nd	3.6	nd	4.9	nd	13.4	<0.5	75.9	nd	nd
WDS 47	nd	0.6	0.6	1.8	2.3	11.3	<0.5	1.9	nd	8.6	0.2	62.8	9.1	<0.5

Appendix 3 Sediment Characterisation data, Organic Matter (OM, %), pH and total elemental concentrations (mg kg⁻¹)

Sample Code	OM	pH	Al	As	B	Ba	Ca	Cd	Co	Cr	Cu	Fe	K	Li	Mg	Mn	Mo	Na	Ni	P	Pb	S	Se	Sr	V	Zn
WDS 16	3.81	6.65	48278	9.25	43.0	173	14069	1.36	28.8	49.6	16.8	35768	12951	112	2647	1689	<12.4	418	35.1	487	975	640	<12.4	45.8	41.7	637
WDS 23	4.24	6.84	22014	23.5	107	155	66134	5.13	10.3	29.7	474	87351	6258	55.2	4396	4580	<12.5	292	24.0	278	29514	6571	<12.5	33.8	18.1	1691
WDS 45	2.97	5.38	47983	9.61	45.0	162	16603	1.25	27.0	48.2	18.6	35972	12955	115	2442	1562	<12.5	242	26.5	479	1351	757	<12.5	32.9	38.9	346
WDS 46	3.21	5.83	45589	9.38	39.0	160	16805	1.02	22.0	46.1	14.8	31783	12407	110	2297	1165	<12.5	359	24.0	426	976	496	<12.5	29.2	37.7	336
WDS 47	4.12	6.90	24629	20.6	101	148	62377	4.85	12.6	29.1	375	85303	6746	58.2	4165	4589	<12.5	317	25.4	343	14421	4409	<12.5	36.7	20.4	1620

Appendix 4 Inundation water characterisation data

Sample Name	Ca	Mg	Na	K	HCO ₃ ⁻	Cl ⁻	SO ₄ ²⁻	NO ₃ ⁻	Br ⁻	NO ₂ ⁻	HPO ₄ ²⁻	F ⁻	NPOC	Total P
	mg l ⁻¹	mg l ⁻¹	mg l ⁻¹	mg l ⁻¹	mg l ⁻¹	mg l ⁻¹	mg l ⁻¹	mg l ⁻¹	mg l ⁻¹	mg l ⁻¹				
Replicate 1	44.4	7.23	8.30	3.60	92.5	11.8	63.9	0.433	0.033	<0.010	<0.100	1.57	2.39	0.010
Replicate 2	44.6	7.16	8.30	3.60	91.2	11.8	64.0	0.443	0.022	<0.010	<0.100	1.58	2.64	<0.010
Replicate 3	45.4	7.30	8.40	3.70	94.2	11.8	63.9	0.425	0.021	<0.010	<0.100	1.57	2.67	<0.010
	Total S	Si	SiO ₂	Ba	Sr	Mn	Total Fe	Li	Be	B	Al	Ti	V	Cr
	mg l ⁻¹	mg l ⁻¹	mg l ⁻¹	µg l ⁻¹	µg l ⁻¹	µg l ⁻¹	µg l ⁻¹	µg l ⁻¹	µg l ⁻¹	µg l ⁻¹	µg l ⁻¹	µg l ⁻¹	µg l ⁻¹	µg l ⁻¹
Replicate 1	20.0	2.18	4.66	11.1	169	0.500	48.0	12.0	0.255	20.0	20.0	3.60	<0.100	<0.100
Replicate 2	21.0	2.21	4.73	11.2	167	0.400	44.0	12.0	0.236	<20.0	13.0	0.100	<0.100	<0.100
Replicate 3	21.0	2.21	4.73	11.4	164	0.400	51.0	12.0	0.247	<20.0	12.0	<0.100	<0.100	<0.100
	Co	Ni	Cu	Zn	Ga	As	Se	Rb	Y	Zr	Nb	Mo	Ag	Cd
	µg l ⁻¹	µg l ⁻¹	µg l ⁻¹	µg l ⁻¹	µg l ⁻¹	µg l ⁻¹	µg l ⁻¹	µg l ⁻¹	µg l ⁻¹	µg l ⁻¹				
Replicate 1	0.030	2.80	4.20	58.0	0.060	0.420	0.030	13.5	0.017	0.070	<0.050	<0.200	<0.005	0.040
Replicate 2	0.030	2.70	3.50	59.0	<0.050	0.250	0.030	13.8	0.017	0.050	<0.050	<0.200	<0.005	0.040
Replicate 3	0.030	2.70	3.50	60.0	<0.050	0.280	0.030	14.1	0.017	0.040	<0.050	<0.200	<0.005	0.030
	Sn	Sb	Cs	La	Ce	Pr	Nd	Sm	Eu	Tb	Gd	Dy	Ho	Er
	µg l ⁻¹	µg l ⁻¹	µg l ⁻¹	µg l ⁻¹	µg l ⁻¹	µg l ⁻¹	µg l ⁻¹	µg l ⁻¹	µg l ⁻¹	µg l ⁻¹				
Replicate 1	0.200	0.554	0.300	0.005	<0.010	<0.005	0.008	<0.005	<0.005	<0.005	<0.005	<0.005	<0.005	<0.005
Replicate 2	<0.100	0.551	0.300	<0.005	<0.010	<0.005	0.009	<0.005	<0.005	<0.005	<0.005	<0.005	<0.005	<0.005
Replicate 3	<0.100	0.547	0.300	<0.005	<0.010	<0.005	0.007	<0.005	<0.005	<0.005	<0.005	<0.005	<0.005	<0.005
	Tm	Yb	Lu	Hf	Ta	W	Tl	Pb	Th	U				
	µg l ⁻¹	µg l ⁻¹	µg l ⁻¹	µg l ⁻¹	µg l ⁻¹	µg l ⁻¹								
Replicate 1	<0.005	<0.005	<0.005	<0.050	<0.100	<0.500	<0.100	0.700	<0.050	0.185				
Replicate 2	<0.005	<0.005	<0.005	<0.050	<0.100	<0.500	<0.100	0.700	<0.050	0.159				
Replicate 3	<0.005	<0.005	<0.005	<0.050	<0.100	<0.500	<0.100	0.600	<0.050	0.159				

Appendix 5 Inundation Experiment Information and Laboratory Measurement Data

Sample Name	Inundation Time	Weight	Volume of Inundation Water	Laboratory Temperature	Sample Temperature	pH	Eh*
	Days	g	ml	C	C		mV
WDS 16	1	50	500	18.5	21	7.54	203
WDS 16	8	50	500	16.3	18.9	7.38	294
WDS 16	28	50	500	11.7	14.6	7.09	352
WDS 16	60	50	500	12.9	15.5	7.07	332
WDS 16	88	50	500	8.4	10.8	6.87	302
WDS 16 Duplicate	1	50.3	500	18.5	20.9	7.63	212
WDS 16 Duplicate	8	50.3	500	16.3	18.9	7.42	296
WDS 16 Duplicate	28	50.3	500	11.7	14.5	7.01	345
WDS 16 Duplicate	60	50.3	500	12.9	15.4	7.11	338
WDS 16 Duplicate	88	50.3	500	8.4	10.8	7.15	312
WDS 23	1	50.2	500	18.5	20.8	7.65	216
WDS 23	8	50.2	500	16.3	18.9	7.49	301
WDS 23	28	50.2	500	11.7	14.7	7.18	322
WDS 23	60	50.2	500	12.9	15.6	7.09	329
WDS 23	88	50.2	500	8.4	10.9	7.02	311
WDS 23 Duplicate	1	50.2	500	18.5	20.9	7.7	226
WDS 23 Duplicate	8	50.2	500	16.3	18.9	7.37	283
WDS 23 Duplicate	28	50.2	500	11.7	14.6	7.23	313
WDS 23 Duplicate	60	50.2	500	12.9	15.4	7.13	322
WDS 23 Duplicate	88	50.2	500	8.4	10.7	7.04	309
WDS 45	1	50.1	500	18.5	20.8	7.22	262
WDS 45	8	50.1	500	16.3	18.9	6.98	304
WDS 45	28	50.1	500	11.7	14.8	6.7	326
WDS 45	60	50.1	500	12.9	15.6	6.72	343
WDS 45	88	50.1	500	8.4	10.9	6.76	300
WDS 45 Duplicate	1	50.1	500	18.5	20.7	7.19	264

Eh*= Pt electrode measured value, uncorrected to the Standard Hydrogen Electrode

Sample Name	Inundation Time	Weight	Volume of Inundation Water	Laboratory Temperature	Sample Temperature	pH	Eh*
WDS 45 Duplicate	8	50.1	500	16.3	19	6.86	310
WDS 45 Duplicate	28	50.1	500	11.7	14.7	6.7	323
WDS 45 Duplicate	60	50.1	500	12.9	15.5	6.71	343
WDS 45 Duplicate	88	50.1	500	8.4	10.8	6.77	284
WDS 46	1	50.3	500	18.5	20.8	7.29	267
WDS 46	8	50.3	500	16.3	19	6.77	304
WDS 46	28	50.3	500	11.7	14.8	6.77	323
WDS 46	60	50.3	500	12.9	15.7	6.76	332
WDS 46	88	50.3	500	8.4	11	6.85	282
WDS 46 Duplicate	1	50.1	500	18.5	20.9	7.36	239
WDS 46 Duplicate	8	50.1	500	16.3	19.1	6.98	306
WDS 46 Duplicate	28	50.1	500	11.7	14.8	6.67	313
WDS 46 Duplicate	60	50.1	500	12.9	15.6	6.79	335
WDS 46 Duplicate	88	50.1	500	8.4	10.8	6.87	272
WDS 47	1	50.1	500	18.5	21	7.58	240
WDS 47	8	50.1	500	16.3	19.1	7.42	270
WDS 47	28	50.1	500	11.7	14.9	7.16	307
WDS 47	60	50.1	500	12.9	15.9	7.06	320
WDS 47	88	50.1	500	8.4	11.1	6.8	269
WDS 47 Duplicate	1	50.8	500	18.5	21.1	7.7	242
WDS 47 Duplicate	8	50.8	500	16.3	19	7.5	275
WDS 47 Duplicate	28	50.8	500	11.7	14.9	7.24	299
WDS 47 Duplicate	60	50.8	500	12.9	15.7	7.2	318
WDS 47 Duplicate	88	50.8	500	8.4	10.9	7.13	266

Eh*= Pt electrode measured value, uncorrected to the Standard Hydrogen Electrode

Appendix 6 WDS 16, Inundated water data

Sample Name	Ca	Mg	Na	K	HCO ₃ ⁻	Cl ⁻	SO ₄ ²⁻	NO ₃ ⁻	Br ⁻	NO ₂ ⁻	HPO ₄ ²⁻	F ⁻	NPOC	Total P
	mg l ⁻¹	mg l ⁻¹	mg l ⁻¹	mg l ⁻¹	mg l ⁻¹	mg l ⁻¹	mg l ⁻¹	mg l ⁻¹	mg l ⁻¹	mg l ⁻¹				
WDS 16-1	46.0	7.72	9.50	4.00	95.956	13.4	67.6	0.417	0.075	<0.010	<0.100	2.04	22.1	0.020
WDS 16-8	53.2	8.86	10.1	4.60	121.49	14.1	73.2	0.561	0.057	0.034	<0.100	1.69	9.29	0.010
WDS 16-28	67.8	10.6	10.2	4.10	158.56	13.8	75.0	11.0	0.047	1.03	<0.100	1.40	9.16	<0.010
WDS 16-60	77.8	11.5	10.1	4.40	181.25	14.7	75.5	10.5	0.071	0.015	<0.100	1.26	10.6	<0.010
WDS 16-88	82.8	12.0	10.0	3.90	206.71	15.1	76.7	10.1	0.074	0.013	<0.100	1.16	12.8	<0.010
WDS 16 -1 Duplicate	46.3	8.01	9.70	4.10	90.101	13.7	69.7	1.34	0.038	<0.010	<0.100	1.65	8.91	0.020
WDS 16-8 Duplicate	54.5	8.98	10.1	4.80	123.61	14.8	72.9	0.474	0.050	0.012	<0.100	1.70	13.9	0.010
WDS 16-28 Duplicate	66.8	10.6	10.0	4.20	152.96	13.6	74.2	10.1	<0.020	1.57	<0.100	1.32	9.78	<0.010
WDS 16-60 Duplicate	77.2	11.3	9.90	4.10	195.26	14.6	75.2	11.5	0.054	<0.010	<0.100	1.18	11.3	<0.010
WDS 16-88 Duplicate	85.7	11.9	10.3	4.10	209.26	14.7	76.5	11.5	0.054	<0.010	<0.100	1.09	12.1	<0.010
	Total S	Si	SiO ₂	Ba	Sr	Mn	Total Fe	Li	Be	B	Al	Ti	V	Cr
	mg l ⁻¹	mg l ⁻¹	mg l ⁻¹	µg l ⁻¹	µg l ⁻¹	µg l ⁻¹	µg l ⁻¹	µg l ⁻¹	µg l ⁻¹	µg l ⁻¹	µg l ⁻¹	µg l ⁻¹	µg l ⁻¹	µg l ⁻¹
WDS 16-1	25.0	2.12	4.54	20.5	174	376	44.0	8.00	0.186	<20.0	15.0	0.200	<0.100	0.100
WDS 16-8	23.0	2.00	4.28	23.5	204	630	16.0	6.00	0.205	<20.0	12.0	0.200	<0.100	0.100
WDS 16-28	21.0	2.21	4.73	22.8	275	1.90	6.00	5.00	0.209	<20.0	14.0	0.300	<0.100	0.300
WDS 16-60	21.0	2.23	4.77	24.4	319	1.90	5.00	4.00	0.164	<20.0	17.0	0.200	<0.100	0.400
WDS 16-88	23.0	2.40	5.13	23.6	337	1.40	8.00	4.00	0.139	<20.0	14.0	0.200	<0.100	0.400
WDS 16-1 Duplicate	23.0	2.12	4.54	21.1	176	411	46.0	8.00	0.196	<20.0	19.0	0.400	0.100	0.200
WDS 16-8 Duplicate	21.0	1.98	4.24	23.1	212	758	21.0	6.00	0.198	<20.0	15.0	0.200	0.100	0.200
WDS 16-28 Duplicate	22.0	2.26	4.83	24.4	274	2.80	5.00	5.00	0.213	<20.0	14.0	0.200	<0.100	0.300
WDS 16-60 Duplicate	22.0	2.27	4.86	25.2	309	1.20	4.00	4.00	0.177	<20.0	16.0	0.200	<0.100	0.400
WDS 16-88 Duplicate	23.0	2.48	5.31	24.3	341	2.30	4.00	4.00	0.125	<20.0	17.0	0.300	<0.100	0.400

	Co	Ni	Cu	Zn	Ga	As	Se	Rb	Y	Zr	Nb	Mo	Ag	Cd
	$\mu\text{g l}^{-1}$													
WDS 16-1	0.560	3.50	4.40	43.0	<0.050	0.590	0.170	14.3	0.071	0.070	<0.050	<0.200	0.011	0.130
WDS 16-8	0.460	5.90	4.70	61.0	<0.050	1.06	0.290	27.9	0.080	0.050	<0.050	<0.200	0.013	0.170
WDS 16-28	0.160	5.20	4.20	66.0	<0.050	0.970	0.260	8.21	0.081	0.050	<0.050	<0.200	<0.005	0.080
WDS 16-60	0.140	3.80	4.00	61.0	<0.050	0.660	0.210	7.54	0.077	0.050	<0.050	<0.200	0.011	0.080
WDS 16-88	0.120	3.30	3.70	58.0	<0.050	0.550	0.260	6.47	0.066	0.070	<0.050	<0.200	<0.005	0.080
WDS 16-1 Duplicate	0.600	3.60	4.50	44.0	<0.050	0.690	0.190	15.0	0.081	0.230	<0.050	<0.200	0.015	0.120
WDS 16-8 Duplicate	0.570	6.00	4.90	65.0	<0.050	1.06	0.250	28.0	0.088	0.050	<0.050	0.200	0.011	0.180
WDS 16-28 Duplicate	0.160	5.10	4.30	70.0	<0.050	0.950	0.250	8.53	0.087	0.050	<0.050	<0.200	0.009	0.080
WDS 16-60 Duplicate	0.150	3.60	3.90	62.0	<0.050	0.600	0.220	7.57	0.077	0.050	<0.050	<0.200	0.010	0.080
WDS 16-88 Duplicate	0.110	3.10	3.80	63.0	<0.050	0.570	0.220	6.30	0.064	0.060	<0.050	<0.200	<0.005	0.080
	Sn	Sb	Cs	La	Ce	Pr	Nd	Sm	Eu	Tb	Gd	Dy	Ho	Er
	$\mu\text{g l}^{-1}$													
WDS 16-1	<0.100	0.641	0.250	0.016	0.030	0.006	0.028	0.010	0.006	<0.005	0.015	0.012	<0.005	0.007
WDS 16-8	<0.100	0.845	0.670	0.016	0.020	<0.005	0.026	0.009	0.006	<0.005	0.015	0.013	<0.005	0.007
WDS 16-28	<0.100	0.501	0.110	0.013	0.010	<0.005	0.026	0.010	0.006	<0.005	0.014	0.013	<0.005	0.007
WDS 16-60	<0.100	0.575	0.120	0.015	0.010	<0.005	0.026	0.010	0.006	<0.005	0.014	0.011	<0.005	0.006
WDS 16-88	<0.100	0.613	0.100	0.014	0.010	<0.005	0.019	0.006	0.005	<0.005	0.011	0.010	<0.005	<0.005
WDS 16-1 Duplicate	<0.100	0.665	0.270	0.017	0.030	0.006	0.029	0.012	0.007	<0.005	0.016	0.014	<0.005	0.006
WDS 16-8 Duplicate	<0.100	0.865	0.660	0.017	0.030	0.006	0.029	0.011	0.007	<0.005	0.015	0.015	<0.005	0.008
WDS 16-28 Duplicate	<0.100	0.531	0.120	0.015	0.010	<0.005	0.027	0.012	0.007	<0.005	0.015	0.014	<0.005	0.007
WDS 16-60 Duplicate	<0.100	0.601	0.110	0.016	0.010	<0.005	0.025	0.009	0.006	<0.005	0.012	0.011	<0.005	<0.005
WDS 16-88 Duplicate	<0.100	0.630	0.090	0.014	0.010	<0.005	0.019	0.008	0.005	<0.005	0.010	0.008	<0.005	0.005

	Tm	Yb	Lu	Hf	Ta	W	Tl	Pb	Th	U	pH			
	$\mu\text{g l}^{-1}$													
WDS 16-1	<0.005	<0.005	<0.005	<0.050	0.100	<0.500	<0.100	2.00	<0.050	0.270	7.21			
WDS 16-8	<0.005	0.006	<0.005	<0.050	<0.100	<0.500	<0.100	1.00	<0.050	0.336	7.97			
WDS 16-28	<0.005	0.005	<0.005	<0.050	<0.100	<0.500	<0.100	0.400	<0.050	0.323	7.84			
WDS 16-60	<0.005	<0.005	<0.005	<0.050	<0.100	<0.500	<0.100	0.700	<0.050	0.549	7.75			
WDS 16-88	<0.005	<0.005	<0.005	<0.050	<0.100	<0.500	<0.100	1.20	<0.050	0.686	7.84			
WDS 16-1 Duplicate	<0.005	<0.005	<0.005	<0.050	<0.100	<0.500	<0.100	2.20	<0.050	0.293	7.87			
WDS 16-8 Duplicate	<0.005	0.006	<0.005	<0.050	<0.100	<0.500	<0.100	1.30	<0.050	0.368	7.64			
WDS 16-28 Duplicate	<0.005	<0.005	<0.005	<0.050	<0.100	<0.500	<0.100	0.500	<0.050	0.305	7.82			
WDS 16-60 Duplicate	<0.005	<0.005	<0.005	<0.050	<0.100	<0.500	<0.100	0.600	<0.050	0.538	7.68			
WDS 16-88 Duplicate	<0.005	<0.005	<0.005	<0.050	<0.100	<0.500	<0.100	1.00	<0.050	0.661	7.60			

Appendix 7 WDS 23, Inundated water data

Sample Name	Ca	Mg	Na	K	HCO ₃ ⁻	Cl ⁻	SO ₄ ²⁻	NO ₃ ⁻	Br ⁻	NO ₂ ⁻	HPO ₄ ²⁻	F ⁻	NPOC	Total P
	mg l ⁻¹	mg l ⁻¹	mg l ⁻¹	mg l ⁻¹	mg l ⁻¹	mg l ⁻¹	mg l ⁻¹	mg l ⁻¹	mg l ⁻¹	mg l ⁻¹				
WDS 23-1	49.7	7.28	9.10	3.80	82.4	12.9	77.6	<0.020	0.061	<0.010	<0.100	nd	17.3	<0.010
WDS 23-8	57.8	7.68	9.10	4.10	93.0	13.4	99.2	1.03	0.038	0.060	<0.100	2.13	6.10	<0.010
WDS 23-28	69.7	8.71	9.20	4.10	87.8	13.4	131	4.19	0.057	<0.010	<0.100	2.08	3.80	<0.010
WDS 23-60	79.0	9.26	9.40	4.50	69.2	13.4	168	4.52	0.034	<0.010	<0.100	1.90	4.39	<0.010
WDS 23-88	84.6	9.96	9.40	4.50	51.4	13.4	201	4.23	0.035	<0.010	<0.100	1.74	7.88	<0.010
WDS 23-1 Duplicate	48.1	7.33	9.10	3.80	90.5	13.0	76.1	1.07	<0.020	<0.010	<0.100	1.91	3.33	0.030
WDS 23-8 Duplicate	57.5	7.56	9.20	4.10	93.8	13.3	97.6	0.843	0.069	0.072	<0.100	2.06	5.72	<0.010
WDS 23-28 Duplicate	65.7	8.31	9.00	4.00	92.1	13.5	127	3.71	0.039	<0.010	<0.100	2.10	4.02	<0.010
WDS 23-60 Duplicate	76.9	9.08	9.40	4.30	75.1	13.4	162	3.40	0.036	<0.010	<0.100	1.95	6.13	<0.010
WDS 23-88 Duplicate	81.0	9.36	9.10	4.30	57.6	13.2	191	3.00	0.033	<0.010	<0.100	1.78	7.34	<0.010
	Total S	Si	SiO ₂	Ba	Sr	Mn	Total Fe	Li	Be	B	Al	Ti	V	Cr
	mg l ⁻¹	mg l ⁻¹	mg l ⁻¹	µg l ⁻¹	µg l ⁻¹	µg l ⁻¹	µg l ⁻¹	µg l ⁻¹	µg l ⁻¹	µg l ⁻¹	µg l ⁻¹	µg l ⁻¹	µg l ⁻¹	µg l ⁻¹
WDS 23-1	22.0	2.01	4.30	28.9	185	74.5	29.0	8.00	0.117	<20.0	14.0	0.200	<0.100	<0.100
WDS 23-8	30.0	1.91	4.09	38.2	222	330	19.0	7.00	0.119	<20.0	11.0	<0.100	<0.100	<0.100
WDS 23-28	41.0	1.90	4.06	72.6	269	1874	5.00	7.00	0.123	<20.0	15.0	0.200	<0.100	<0.100
WDS 23-60	52.0	1.98	4.24	117	315	3650	2.00	7.00	0.131	<20.0	19.0	0.200	0.100	<0.100
WDS 23-88	62.0	2.00	4.28	152	342	4729	3.00	8.00	0.157	<20.0	21.0	0.300	0.100	0.200

	Total S	Si	SiO ₂	Ba	Sr	Mn	Total Fe	Li	Be	B	Al	Ti	V	Cr
	mg l ⁻¹	mg l ⁻¹	mg l ⁻¹	μg l ⁻¹										
WDS 23-1 Duplicate	23.0	2.10	4.49	27.1	189	65.8	27.0	8.00	0.111	<20.0	13.0	0.100	<0.100	0.100
WDS 23-8 Duplicate	29.0	1.90	4.06	37.1	215	284	19.0	7.00	0.106	<20.0	11.0	0.200	<0.100	<0.100
WDS 23-28 Duplicate	38.0	1.84	3.94	68.3	266	1671	4.00	7.00	0.102	<20.0	8.00	0.100	<0.100	<0.100
WDS 23-60 Duplicate	50.0	1.89	4.04	113	300	3623	2.00	7.00	0.126	<20.0	13.0	0.200	<0.100	<0.100
WDS 23-88 Duplicate	60.0	1.95	4.17	143	327	4817	4.00	7.00	0.142	<20.0	16.0	0.2	<0.1	0.1
	Co	Ni	Cu	Zn	Ga	As	Se	Rb	Y	Zr	Nb	Mo	Ag	Cd
	μg l ⁻¹													
WDS 23-1	0.300	2.60	7.60	59.0	<0.050	0.400	0.150	11.4	0.054	0.020	<0.050	<0.200	0.008	0.320
WDS 23-8	0.690	3.60	8.00	90.0	<0.050	0.570	0.170	16.6	0.057	0.030	<0.050	<0.200	<0.005	0.580
WDS 23-28	3.73	7.40	6.60	320	0.120	0.670	0.110	8.06	0.054	0.390	<0.050	<0.200	0.046	2.05
WDS 23-60	9.16	11.9	5.30	674	0.140	0.620	0.110	8.32	0.047	0.040	<0.050	<0.200	0.029	4.18
WDS 23-88	15.9	17.8	4.50	1445	0.170	0.420	0.080	8.09	0.049	0.090	<0.050	<0.200	0.033	7.39
WDS 23-1 Duplicate	0.270	2.50	7.10	57.0	<0.050	0.410	0.130	11.2	0.049	0.030	<0.050	<0.200	0.005	0.320
WDS 23-8 Duplicate	0.650	3.40	7.50	88.0	<0.050	0.590	0.170	16.1	0.056	0.040	<0.050	<0.200	<0.005	0.570
WDS 23-28 Duplicate	3.21	7.10	6.40	298	<0.050	0.560	0.130	8.05	0.051	0.020	<0.050	<0.200	0.005	1.89
WDS 23-60 Duplicate	8.18	10.9	5.30	600	0.080	0.500	0.110	8.46	0.048	0.030	<0.050	<0.200	<0.005	3.95
WDS 23-88 Duplicate	13.8	15.1	4.50	1178	0.110	0.440	0.090	8.03	0.050	0.030	<0.050	<0.200	0.012	6.44

	Sn	Sb	Cs	La	Ce	Pr	Nd	Sm	Eu	Tb	Gd	Dy	Ho	Er
	$\mu\text{g l}^{-1}$													
WDS 23-1	<0.100	1.66	0.180	0.016	0.030	<0.005	0.025	0.007	0.007	<0.005	0.009	0.007	<0.005	<0.005
WDS 23-8	<0.100	3.37	0.320	0.019	0.030	<0.005	0.025	0.007	0.007	<0.005	0.012	0.009	<0.005	<0.005
WDS 23-28	<0.100	5.39	0.110	0.019	0.030	<0.005	0.020	0.008	0.010	<0.005	0.009	0.006	<0.005	<0.005
WDS 23-60	<0.100	5.87	0.130	0.021	0.030	<0.005	0.019	<0.005	0.013	<0.005	0.007	0.006	<0.005	<0.005
WDS 23-88	<0.100	4.57	0.110	0.028	0.030	<0.005	0.020	0.005	0.016	<0.005	0.008	0.005	<0.005	<0.005
WDS 23-1 Duplicate	<0.100	1.60	0.180	0.017	0.020	<0.005	0.016	0.006	0.006	<0.005	0.010	0.007	<0.005	<0.005
WDS 23-8 Duplicate	<0.100	3.38	0.300	0.019	0.030	<0.005	0.021	0.007	0.007	<0.005	0.010	0.008	<0.005	<0.005
WDS 23-28 Duplicate	<0.100	5.37	0.110	0.018	0.020	<0.005	0.020	0.006	0.009	<0.005	0.009	0.006	<0.005	<0.005
WDS 23-60 Duplicate	<0.100	6.24	0.130	0.022	0.020	<0.005	0.019	0.007	0.012	<0.005	0.008	0.006	<0.005	<0.005
WDS 23-88 Duplicate	<0.100	4.99	0.110	0.028	0.030	<0.005	0.020	0.006	0.015	<0.005	0.007	<0.005	<0.005	<0.005
	Tm	Yb	Lu	Hf	Ta	W	Tl	Pb	Th	U	pH			
	$\mu\text{g l}^{-1}$													
WDS 23-1	<0.005	<0.005	<0.005	<0.050	<0.100	<0.500	<0.100	45.2	<0.050	0.255	7.21			
WDS 23-8	<0.005	<0.005	<0.005	<0.050	<0.100	<0.500	<0.100	49.8	<0.050	0.265	7.55			
WDS 23-28	<0.005	<0.005	<0.005	<0.050	<0.100	<0.500	<0.100	117	<0.050	0.169	7.56			
WDS 23-60	<0.005	<0.005	<0.005	<0.050	<0.100	<0.500	0.100	252	<0.050	0.083	7.39			
WDS 23-88	<0.005	<0.005	<0.005	0.050	<0.100	<0.500	0.100	382	<0.050	0.041	7.31			
WDS 23-1 Duplicate	<0.005	<0.005	<0.005	<0.050	<0.100	<0.500	<0.100	41.5	<0.050	0.241	8.03			
WDS 23-8 Duplicate	<0.005	<0.005	<0.005	<0.050	<0.100	<0.500	<0.100	48.3	<0.050	0.260	7.67			
WDS 23-28 Duplicate	<0.005	<0.005	<0.005	<0.050	<0.100	<0.500	<0.100	114	<0.050	0.168	7.87			
WDS 23-60 Duplicate	<0.005	<0.005	<0.005	<0.050	<0.100	<0.500	0.100	272	<0.050	0.091	7.62			
WDS 23-88 Duplicate	<0.005	<0.005	<0.005	<0.050	<0.100	<0.500	0.200	407	<0.050	0.048	7.34			

Appendix 8 WDS 45, Inundated water data

Sample Name	Ca	Mg	Na	K	HCO ₃ ⁻	Cl ⁻	SO ₄ ²⁻	NO ₃ ⁻	Br ⁻	NO ₂ ⁻	HPO ₄ ²⁻	F ⁻	NPOC	Total P
	mg l ⁻¹	mg l ⁻¹	mg l ⁻¹	mg l ⁻¹	mg l ⁻¹	mg l ⁻¹	mg l ⁻¹	mg l ⁻¹	mg l ⁻¹	mg l ⁻¹				
WDS 45-1	41.8	7.67	8.80	4.00	76.0	12.9	68.6	0.675	0.025	<0.010	<0.100	1.88	4.22	<0.010
WDS 45-8	39.8	7.76	8.80	4.30	69.1	13.2	73.9	0.718	0.042	0.030	<0.100	2.02	6.11	<0.010
WDS 45-28	38.7	8.08	8.90	4.30	57.8	13.4	77.7	3.88	0.031	<0.010	<0.100	1.94	5.93	<0.010
WDS 45-60	39.0	8.56	8.90	4.10	48.2	13.5	81.9	5.41	0.032	<0.010	<0.100	1.94	6.27	<0.010
WDS 45-88	39.1	8.61	8.90	3.90	43.7	13.5	85.9	6.41	0.035	<0.010	<0.100	1.94	7.40	<0.010
WDS 45-1 Duplicate	40.4	8.08	8.80	4.20	77.6	13.0	69.7	0.739	0.029	<0.010	<0.100	1.79	5.22	0.010
WDS 45-8 Duplicate	37.7	7.74	8.60	4.30	62.1	13.1	74.3	0.846	0.044	0.019	<0.100	1.98	10.7	<0.010
WDS 45-28 Duplicate	38.0	8.05	8.80	4.30	54.8	12.9	77.8	3.56	0.056	0.289	<0.100	1.92	5.56	<0.010
WDS 45-60 Duplicate	38.3	8.50	8.80	4.10	50.0	13.1	83.1	6.08	0.039	0.044	<0.100	1.91	6.00	<0.010
WDS 45-88 Duplicate	39.5	8.68	8.80	3.90	44.2	13.2	87.3	7.40	0.040	0.038	<0.100	2.00	9.80	<0.010
	Total S	Si	SiO ₂	Ba	Sr	Mn	Total Fe	Li	Be	B	Al	Ti	V	Cr
	mg l ⁻¹	mg l ⁻¹	mg l ⁻¹	µg l ⁻¹	µg l ⁻¹	µg l ⁻¹	µg l ⁻¹	µg l ⁻¹	µg l ⁻¹	µg l ⁻¹	µg l ⁻¹	µg l ⁻¹	µg l ⁻¹	µg l ⁻¹
WDS 45-1	26.0	2.17	4.64	24.7	146	219	32.0	8.00	0.143	<20.0	14.0	0.100	<0.100	<0.100
WDS 45-8	22.0	2.16	4.62	24.4	139	125	32.0	7.00	0.139	<20.0	20.0	0.200	<0.100	0.100
WDS 45-28	23.0	2.04	4.36	23.0	130	3.30	12.0	6.00	0.131	<20.0	33.0	0.100	<0.100	0.100
WDS 45-60	25.0	1.96	4.19	24.2	130	2.40	5.00	5.00	0.134	<20.0	31.0	0.200	<0.100	0.100
WDS 45-88	26.0	1.90	4.06	23.9	126	2.60	5.00	6.00	0.119	20.0	31.0	0.100	<0.100	0.200

	Total S	Si	SiO ₂	Ba	Sr	Mn	Total Fe	Li	Be	B	Al	Ti	V	Cr
	mg l ⁻¹	mg l ⁻¹	mg l ⁻¹	μg l ⁻¹										
WDS 45-1 Duplicate	21.0	2.18	4.66	30.9	143	386	25.0	12.0	0.134	20.0	16.0	0.100	<0.100	<0.100
WDS 45-8 Duplicate	23.0	2.14	4.58	26.5	128	152	26.0	10.0	0.164	21.0	25.0	0.200	<0.100	0.100
WDS 45-28 Duplicate	26.0	2.29	4.90	23.5	122	2.70	8.00	7.00	0.160	20.0	43.0	0.100	<0.100	0.100
WDS 45-60 Duplicate	25.0	1.97	4.21	23.7	126	3.10	4.00	6.00	0.138	<20.0	37.0	0.200	<0.100	0.100
WDS 45-88 Duplicate	27.0	1.86	3.98	24.0	125	1.60	5.00	6.00	0.114	<20.0	33.0	0.200	<0.100	0.200
	Co	Ni	Cu	Zn	Ga	As	Se	Rb	Y	Zr	Nb	Mo	Ag	Cd
	μg l ⁻¹													
WDS 45-1	0.390	4.50	3.10	65.0	<0.050	0.330	0.110	13.5	0.087	0.040	<0.050	<0.200	<0.005	0.270
WDS 45-8	0.140	5.40	3.40	65.0	<0.050	0.480	0.180	16.4	0.122	0.130	<0.050	<0.200	<0.005	0.310
WDS 45-28	0.080	4.10	3.30	69.0	<0.050	0.520	0.170	8.54	0.128	0.030	<0.050	<0.200	<0.005	0.190
WDS 45-60	0.070	4.40	3.40	78.0	<0.050	0.490	0.150	8.36	0.117	0.040	<0.050	<0.200	<0.005	0.200
WDS 45-88	0.070	4.40	3.20	87.0	<0.050	0.430	0.120	7.29	0.103	0.060	<0.050	<0.200	0.015	0.200
WDS 45-1 Duplicate	0.700	5.40	3.40	84.0	<0.050	0.400	0.130	14.4	0.099	0.040	<0.050	<0.200	<0.005	0.390
WDS 45-8 Duplicate	0.220	6.60	4.00	89.0	<0.050	0.590	0.170	16.7	0.142	0.050	<0.050	<0.200	<0.005	0.410
WDS 45-28 Duplicate	0.080	4.50	3.90	81.0	<0.050	0.550	0.180	8.44	0.143	0.040	<0.050	<0.200	<0.005	0.220
WDS 45-60 Duplicate	0.060	4.40	3.60	83.0	<0.050	0.470	0.130	8.03	0.118	0.040	<0.050	<0.200	<0.005	0.220
WDS 45-88 Duplicate	0.070	4.40	3.40	89.0	<0.050	0.420	0.110	7.08	0.105	0.040	<0.050	<0.200	<0.005	0.210

	Sn	Sb	Cs	La	Ce	Pr	Nd	Sm	Eu	Tb	Gd	Dy	Ho	Er
	$\mu\text{g l}^{-1}$													
WDS 45-1	<0.100	0.564	0.280	0.019	0.030	0.007	0.034	0.012	0.007	<0.005	0.017	0.013	<0.005	0.007
WDS 45-8	<0.100	0.596	0.380	0.027	0.050	0.010	0.052	0.020	0.010	<0.005	0.025	0.019	<0.005	0.009
WDS 45-28	<0.100	0.729	0.150	0.025	0.040	0.010	0.061	0.020	0.010	<0.005	0.026	0.020	<0.005	0.011
WDS 45-60	<0.100	1.03	0.160	0.025	0.030	0.009	0.055	0.018	0.009	<0.005	0.024	0.016	<0.005	0.009
WDS 45-88	<0.100	1.08	0.130	0.024	0.030	0.008	0.045	0.014	0.009	<0.005	0.021	0.014	<0.005	0.008
WDS 45-1 Duplicate	<0.100	0.578	0.310	0.022	0.040	0.008	0.042	0.016	0.009	<0.005	0.021	0.017	<0.005	0.008
WDS 45-8 Duplicate	<0.100	0.620	0.380	0.030	0.060	0.012	0.067	0.023	0.011	<0.005	0.030	0.022	<0.005	0.012
WDS 45-28 Duplicate	<0.100	0.682	0.150	0.030	0.040	0.011	0.069	0.023	0.011	<0.005	0.029	0.021	<0.005	0.011
WDS 45-60 Duplicate	<0.100	0.887	0.150	0.025	0.030	0.009	0.054	0.021	0.010	<0.005	0.026	0.020	<0.005	0.009
WDS 45-88 Duplicate	<0.100	0.933	0.120	0.023	0.030	0.008	0.048	0.016	0.008	<0.005	0.023	0.015	<0.005	0.008
	Tm	Yb	Lu	Hf	Ta	W	Tl	Pb	Th	U	pH			
	$\mu\text{g l}^{-1}$													
WDS 45-1	<0.005	<0.005	<0.005	<0.050	<0.100	<0.500	<0.100	3.40	<0.050	0.139	7.41			
WDS 45-8	<0.005	0.007	<0.005	<0.050	<0.100	<0.500	<0.100	3.60	<0.050	0.058	7.46			
WDS 45-28	<0.005	0.007	<0.005	<0.050	<0.100	<0.500	<0.100	2.80	<0.050	0.026	7.59			
WDS 45-60	<0.005	0.006	<0.005	<0.050	<0.100	<0.500	<0.100	3.40	<0.050	0.019	7.31			
WDS 45-88	<0.005	<0.005	<0.005	<0.050	<0.100	<0.500	<0.100	3.60	<0.050	0.017	7.14			
WDS 45-1 Duplicate	<0.005	0.006	<0.005	<0.050	<0.100	<0.500	<0.100	3.50	<0.050	0.144	7.78			
WDS 45-8 Duplicate	<0.005	0.008	<0.005	<0.050	<0.100	<0.500	<0.100	4.20	<0.050	0.048	7.40			
WDS 45-28 Duplicate	<0.005	0.008	<0.005	<0.050	<0.100	<0.500	<0.100	2.80	<0.050	0.023	7.08			
WDS 45-60 Duplicate	<0.005	0.008	<0.005	<0.050	<0.100	<0.500	<0.100	2.60	<0.050	0.017	7.24			
WDS 45-88 Duplicate	<0.005	0.007	<0.005	<0.050	<0.100	<0.500	<0.100	2.70	<0.050	0.017	7.09			

Appendix 9 WDS 46, Inundated water data

Sample Name	Ca mg l ⁻¹	Mg mg l ⁻¹	Na mg l ⁻¹	K mg l ⁻¹	HCO ₃ ⁻ mg l ⁻¹	Cl ⁻ mg l ⁻¹	SO ₄ ²⁻ mg l ⁻¹	NO ₃ ⁻ mg l ⁻¹	Br ⁻ mg l ⁻¹	NO ₂ ⁻ mg l ⁻¹	HPO ₄ ²⁻ mg l ⁻¹	F ⁻ mg l ⁻¹	NPOC mg l ⁻¹	Total P mg l ⁻¹
WDS 46-1	43.4	7.58	9.00	3.90	81.4	12.6	67.3	0.887	0.110	0.036	<0.100	1.75	4.83	0.010
WDS 46-8	42.7	7.83	9.20	4.30	74.3	13.6	71.2	0.561	0.042	0.058	<0.100	1.85	10.4	<0.010
WDS 46-28	44.8	8.56	9.30	4.20	79.2	13.0	72.8	6.63	0.048	0.070	<0.100	1.66	7.18	<0.010
WDS 46-60	47.2	9.18	9.70	4.00	88.3	13.2	74.0	7.90	0.047	0.060	<0.100	1.59	8.77	<0.010
WDS 46-88	44.5	9.04	9.20	3.60	76.0	13.3	75.2	8.92	0.052	0.050	<0.100	1.53	9.75	<0.010
WDS 46-1 Duplicate	43.0	7.81	8.90	3.90	82.6	12.4	66.7	0.849	0.033	0.028	<0.100	1.55	5.07	0.010
WDS 46-8 Duplicate	44.2	8.08	9.60	4.40	83.1	12.7	70.8	0.593	0.041	0.115	<0.100	1.78	6.35	0.020
WDS 46-28 Duplicate	45.1	8.59	9.40	4.00	77.7	11.6	68.2	6.56	0.045	0.059	<0.200	1.59	7.77	<0.010
WDS 46-60 Duplicate	45.0	9.00	9.50	3.80	77.6	12.9	73.3	7.18	0.053	0.044	<0.100	1.67	11.7	<0.010
WDS 46-88 Duplicate	44.7	9.01	9.40	3.60	77.2	13.0	74.7	8.05	0.059	0.043	<0.100	1.51	9.57	<0.010
	Total S mg l ⁻¹	Si mg l ⁻¹	SiO ₂ mg l ⁻¹	Ba µg l ⁻¹	Sr µg l ⁻¹	Mn µg l ⁻¹	Total Fe µg l ⁻¹	Li µg l ⁻¹	Be µg l ⁻¹	B µg l ⁻¹	Al µg l ⁻¹	Ti µg l ⁻¹	V µg l ⁻¹	Cr µg l ⁻¹
WDS 46-1	25.0	2.19	4.69	27.1	151	200	37.0	11.0	0.145	<20.0	18.0	0.300	<0.100	<0.100
WDS 46-8	22.0	2.10	4.49	27.7	144	72.7	31.0	8.00	0.174	20.0	22.0	0.200	<0.100	0.100
WDS 46-28	22.0	2.11	4.51	26.5	145	2.40	11.0	6.00	0.178	<20.0	38.0	0.200	<0.100	0.200
WDS 46-60	23.0	2.15	4.60	26.6	156	1.40	8.00	5.00	0.154	<20.0	37.0	0.200	<0.100	0.200
WDS 46-88	24.0	2.21	4.73	26.4	144	1.80	7.00	4.00	0.133	<20.0	25.0	<0.100	<0.100	0.200

	Total S	Si	SiO ₂	Ba	Sr	Mn	Total Fe	Li	Be	B	Al	Ti	V	Cr
	mg l ⁻¹	mg l ⁻¹	mg l ⁻¹	µg l ⁻¹										
WDS 46-1 Duplicate	22.0	2.18	4.66	27.9	149	198	36.0	11.0	0.146	<20.0	10.0	<0.100	<0.100	<0.100
WDS 46-8 Duplicate	23.0	2.09	4.47	28.5	150	60.4	29.0	8.00	0.166	<20.0	16.0	<0.100	<0.100	0.100
WDS 46-28 Duplicate	23.0	2.13	4.56	26.9	148	2.10	10.0	6.00	0.181	<20.0	33.0	<0.100	<0.100	0.200
WDS 46-60 Duplicate	23.0	2.19	4.69	27.2	149	1.80	8.00	5.00	0.157	<20.0	28.0	<0.100	<0.100	0.200
WDS 46-88 Duplicate	24.0	2.20	4.71	25.9	148	3.80	6.00	4.00	0.134	<20.0	25.0	<0.100	<0.100	0.200
	Co	Ni	Cu	Zn	Ga	As	Se	Rb	Y	Zr	Nb	Mo	Ag	Cd
	µg l ⁻¹													
WDS 46-1	0.29	3.10	3.40	49.0	<0.050	0.440	0.110	12.2	0.086	0.0	<0.050	<0.200	0.006	0.180
WDS 46-8	0.11	4.20	3.90	53.0	<0.050	0.740	0.180	22.2	0.127	0.1	<0.050	<0.200	<0.005	0.190
WDS 46-28	0.08	4.20	4.00	71.0	<0.050	0.700	0.170	7.64	0.140	0.0	<0.050	<0.200	<0.005	0.170
WDS 46-60	0.09	4.30	4.00	74.0	<0.050	0.600	0.140	7.41	0.129	0.1	<0.050	<0.200	0.010	0.180
WDS 46-88	0.08	3.80	3.50	70.0	<0.050	0.390	0.120	6.41	0.121	0.1	<0.050	<0.200	<0.005	0.150
WDS 46-1 Duplicate	0.31	3.40	3.40	49.0	<0.050	0.460	0.110	12.7	0.088	0.0	<0.050	<0.200	<0.005	0.190
WDS 46-8 Duplicate	0.10	4.30	3.90	55.0	<0.050	0.690	0.170	23.2	0.127	0.1	<0.050	<0.200	<0.005	0.180
WDS 46-28 Duplicate	0.07	4.30	3.80	73.0	<0.050	0.670	0.150	7.93	0.145	0.0	<0.050	<0.200	<0.005	0.150
WDS 46-60 Duplicate	0.08	4.20	3.80	73.0	<0.050	0.510	0.130	7.19	0.134	0.1	<0.050	<0.200	<0.005	0.160
WDS 46-88 Duplicate	0.08	3.80	3.60	72.0	<0.050	0.400	0.110	6.14	0.119	0.0	<0.050	<0.200	<0.005	0.160

	Sn	Sb	Cs	La	Ce	Pr	Nd	Sm	Eu	Tb	Gd	Dy	Ho	Er
	$\mu\text{g l}^{-1}$													
WDS 46-1	<0.100	0.553	0.240	0.020	0.030	0.007	0.036	0.013	0.008	<0.005	0.017	0.014	<0.005	0.007
WDS 46-8	<0.100	0.579	0.560	0.028	0.050	0.010	0.057	0.018	0.010	<0.005	0.028	0.021	<0.005	0.010
WDS 46-28	<0.100	0.526	0.130	0.031	0.040	0.011	0.067	0.021	0.011	<0.005	0.029	0.023	<0.005	0.011
WDS 46-60	<0.100	0.568	0.130	0.028	0.030	0.010	0.059	0.023	0.010	<0.005	0.027	0.020	<0.005	0.011
WDS 46-88	<0.100	0.610	0.100	0.099	0.150	0.015	0.070	0.017	0.010	<0.005	0.023	0.020	<0.005	0.009
WDS 46-1 Duplicate	<0.100	0.572	0.250	0.020	0.030	0.007	0.037	0.013	0.009	<0.005	0.017	0.013	<0.005	0.007
WDS 46-8 Duplicate	<0.100	0.601	0.570	0.027	0.050	0.010	0.058	0.018	0.012	<0.005	0.026	0.020	<0.005	0.010
WDS 46-28 Duplicate	<0.100	0.519	0.120	0.028	0.040	0.011	0.061	0.021	0.011	<0.005	0.028	0.021	<0.005	0.011
WDS 46-60 Duplicate	<0.100	0.552	0.120	0.030	0.030	0.010	0.059	0.019	0.010	<0.005	0.026	0.020	<0.005	0.010
WDS 46-88 Duplicate	<0.100	0.574	0.100	0.027	0.030	0.010	0.055	0.018	0.009	<0.005	0.023	0.017	<0.005	0.009
	Tm	Yb	Lu	Hf	Ta	W	Tl	Pb	Th	U	pH			
	$\mu\text{g l}^{-1}$													
WDS 46-1	<0.005	<0.005	<0.005	<0.050	<0.100	<0.500	<0.100	2.50	<0.050	0.170	7.88			
WDS 46-8	<0.005	0.007	<0.005	<0.050	<0.100	<0.500	<0.100	2.20	<0.050	0.084	7.56			
WDS 46-28	<0.005	0.008	<0.005	<0.050	<0.100	<0.500	<0.100	1.60	<0.050	0.043	7.71			
WDS 46-60	<0.005	0.007	<0.005	<0.050	<0.100	0.800	<0.100	1.60	<0.050	0.036	7.69			
WDS 46-88	<0.005	0.007	<0.005	0.060	<0.100	<0.500	<0.100	2.00	<0.050	0.031	7.06			
WDS 46-1 Duplicate	<0.005	<0.005	<0.005	<0.050	<0.100	<0.500	<0.100	2.70	<0.050	0.170	7.97			
WDS 46-8 Duplicate	<0.005	0.008	<0.005	<0.050	<0.100	<0.500	<0.100	2.30	<0.050	0.075	7.66			
WDS 46-28 Duplicate	<0.005	0.010	<0.005	<0.050	<0.100	<0.500	<0.100	1.70	<0.050	0.043	7.46			
WDS 46-60 Duplicate	<0.005	0.007	<0.005	<0.050	<0.100	<0.500	<0.100	1.60	<0.050	0.032	7.41			
WDS 46-88 Duplicate	<0.005	0.007	<0.005	<0.050	<0.100	<0.500	<0.100	2.10	<0.050	0.030	7.16			

Appendix 10 WDS 47, Inundated water data

Sample Name	Ca	Mg	Na	K	HCO ₃ ⁻	Cl ⁻	SO ₄ ²⁻	NO ₃ ⁻	Br ⁻	NO ₂ ⁻	HPO ₄ ²⁻	F ⁻	NPOC	Total P
	mg l ⁻¹	mg l ⁻¹	mg l ⁻¹	mg l ⁻¹	mg l ⁻¹	mg l ⁻¹	mg l ⁻¹	mg l ⁻¹	mg l ⁻¹	mg l ⁻¹				
WDS 47-1	48.4	7.27	9.10	3.90	91.6	12.6	68.7	1.78	0.037	0.037	<0.100	1.47	4.59	0.010
WDS 47-8	55.8	7.80	9.30	4.30	111	12.8	79.6	1.23	0.044	0.091	<0.100	1.75	5.53	<0.010
WDS 47-28	66.7	8.36	9.20	4.00	127	12.9	86.3	8.72	0.052	0.045	<0.100	1.75	6.84	<0.010
WDS 47-60	76.4	8.91	9.10	4.00	138	13.0	108	8.85	0.048	0.052	<0.100	1.52	4.63	<0.010
WDS 47-88	84.3	9.51	9.00	4.00	132	13.0	135	8.06	0.038	<0.010	<0.100	1.37	6.98	<0.010
WDS 47-1 Duplicate	48.0	7.08	8.70	3.80	79.9	12.4	68.2	1.59	<0.020	0.023	<0.100	1.45	4.72	0.010
WDS 47-8 Duplicate	55.6	7.48	9.10	4.30	103	12.7	78.3	1.14	0.047	0.182	<0.100	1.70	12.1	<0.010
WDS 47-28 Duplicate	71.1	8.65	9.70	4.30	129	12.9	86.7	7.86	0.049	0.055	<0.100	1.69	5.59	<0.010
WDS 47-60 Duplicate	76.7	8.80	9.20	4.10	141	12.9	105	6.48	0.058	0.101	<0.100	1.56	5.57	<0.010
WDS 47-88 Duplicate	85.6	9.45	9.20	4.00	139	13.0	127	6.40	0.050	0.037	<0.100	1.42	9.19	<0.010
	Total S	Si	SiO ₂	Ba	Sr	Mn	Total Fe	Li	Be	B	Al	Ti	V	Cr
	mg l ⁻¹	mg l ⁻¹	mg l ⁻¹	µg l ⁻¹	µg l ⁻¹	µg l ⁻¹	µg l ⁻¹	µg l ⁻¹	µg l ⁻¹	µg l ⁻¹	µg l ⁻¹	µg l ⁻¹	µg l ⁻¹	µg l ⁻¹
WDS 47-1	22.0	2.15	4.60	23.0	181	47.0	33.0	11.0	0.122	<20.0	8.00	<0.100	<0.100	<0.100
WDS 47-8	25.0	2.08	4.45	30.3	212	218	12.0	10.0	0.089	<20.0	7.00	<0.100	<0.100	<0.100
WDS 47-28	27.0	2.14	4.58	41.8	269	785	5.00	8.00	0.071	<20.0	14.0	0.100	<0.100	<0.100
WDS 47-60	34.0	2.35	5.03	59.0	312	1.60	3.00	9.00	0.067	<20.0	13.0	0.200	<0.100	0.100
WDS 47-88	42.0	2.48	5.31	77.5	345	2.60	3.00	9.00	0.059	<20.0	14.0	0.200	<0.100	0.200

	Total S	Si	SiO ₂	Ba	Sr	Mn	Total Fe	Li	Be	B	Al	Ti	V	Cr
	mg l ⁻¹	mg l ⁻¹	mg l ⁻¹	µg l ⁻¹										
WDS 47-1 Duplicate	22.0	2.13	4.56	21.7	177	43.5	31.0	10.0	0.097	<20.0	14.0	0.200	<0.100	0.100
WDS 47-8 Duplicate	25.0	2.09	4.47	29.1	213	131	9.00	9.00	0.083	<20.0	11.0	0.100	<0.100	<0.100
WDS 47-28 Duplicate	27.0	2.16	4.62	40.0	283	2.90	2.00	8.00	0.069	<20.0	13.0	0.200	<0.100	<0.100
WDS 47-60 Duplicate	33.0	2.32	4.96	58.1	314	2.20	2.00	8.00	0.063	<20.0	13.0	0.200	<0.100	<0.100
WDS 47-88 Duplicate	40.0	2.39	5.11	75.7	343	2.10	2.00	9.00	0.058	<20.0	13.0	0.200	<0.100	0.100
	Co	Ni	Cu	Zn	Ga	As	Se	Rb	Y	Zr	Nb	Mo	Ag	Cd
	µg l ⁻¹													
WDS 47-1	0.180	2.20	6.20	32.0	<0.050	0.440	0.130	10.3	0.046	0.010	<0.050	<0.200	<0.005	0.150
WDS 47-8	0.360	3.10	7.00	48.0	<0.050	0.690	0.180	18.5	0.049	0.010	<0.050	0.200	<0.005	0.280
WDS 47-28	0.400	5.50	6.80	123	<0.050	0.770	0.180	6.52	0.043	0.020	<0.050	<0.200	<0.005	0.690
WDS 47-60	0.130	4.40	6.00	156	<0.050	0.720	0.130	6.12	0.036	0.040	<0.050	<0.200	0.009	0.490
WDS 47-88	0.140	6.80	5.30	469	<0.050	0.530	0.110	5.40	0.037	0.050	<0.050	<0.200	<0.005	1.44
WDS 47-1 Duplicate	0.160	2.40	6.10	32.0	<0.050	0.490	0.110	10.1	0.045	0.030	<0.050	<0.200	<0.005	0.150
WDS 47-8 Duplicate	0.260	2.90	6.50	44.0	<0.050	0.690	0.200	17.5	0.046	0.040	<0.050	0.200	<0.005	0.270
WDS 47-28 Duplicate	0.130	4.30	6.30	73.0	<0.050	0.810	0.180	6.83	0.039	0.020	<0.050	<0.200	<0.005	0.220
WDS 47-60 Duplicate	0.140	5.20	5.90	190	<0.050	0.750	0.150	6.22	0.039	0.030	<0.050	<0.200	<0.005	0.720
WDS 47-88 Duplicate	0.180	7.20	5.30	468	<0.050	0.530	0.110	5.51	0.040	0.040	<0.050	<0.200	<0.005	1.60

	Sn	Sb	Cs	La	Ce	Pr	Nd	Sm	Eu	Tb	Gd	Dy	Ho	Er
	$\mu\text{g l}^{-1}$													
WDS 47-1	<0.100	1.32	0.130	0.012	0.020	<0.005	0.017	0.006	0.005	<0.005	0.009	0.006	<0.005	<0.005
WDS 47-8	<0.100	2.80	0.340	0.015	0.020	<0.005	0.016	0.006	0.006	<0.005	0.009	0.006	<0.005	<0.005
WDS 47-28	<0.100	3.34	0.070	0.012	0.010	<0.005	0.014	<0.005	0.006	<0.005	0.006	0.005	<0.005	<0.005
WDS 47-60	<0.100	5.48	0.080	0.016	0.010	<0.005	0.016	<0.005	0.007	<0.005	0.005	<0.005	<0.005	<0.005
WDS 47-88	<0.100	5.45	0.060	0.017	0.010	<0.005	0.015	0.006	0.009	<0.005	<0.005	<0.005	<0.005	<0.005
WDS 47-1 Duplicate	<0.100	1.39	0.120	0.013	0.020	<0.005	0.017	0.006	<0.005	<0.005	0.008	0.008	<0.005	<0.005
WDS 47-8 Duplicate	<0.100	2.82	0.320	0.014	0.020	<0.005	0.017	0.005	<0.005	<0.005	0.007	0.006	<0.005	<0.005
WDS 47-28 Duplicate	<0.100	3.59	0.070	0.010	<0.010	<0.005	0.011	<0.005	0.006	<0.005	0.005	<0.005	<0.005	<0.005
WDS 47-60 Duplicate	<0.100	5.93	0.080	0.016	<0.010	<0.005	0.017	<0.005	0.007	<0.005	0.006	<0.005	<0.005	<0.005
WDS 47-88 Duplicate	<0.100	5.84	0.060	0.022	0.020	<0.005	0.019	<0.005	0.009	<0.005	0.006	<0.005	<0.005	<0.005
	Tm	Yb	Lu	Hf	Ta	W	Tl	Pb	Th	U	pH			
	$\mu\text{g l}^{-1}$													
WDS 47-1	<0.005	<0.005	<0.005	<0.050	<0.100	<0.500	<0.100	18.9	<0.050	0.277	8.00			
WDS 47-8	<0.005	<0.005	<0.005	<0.050	<0.100	<0.500	<0.100	15.9	<0.050	0.381	7.90			
WDS 47-28	<0.005	<0.005	<0.005	<0.050	<0.100	<0.500	<0.100	3.70	<0.050	0.393	7.60			
WDS 47-60	<0.005	<0.005	<0.005	<0.050	<0.100	<0.500	<0.100	5.70	<0.050	0.428	7.74			
WDS 47-88	<0.005	<0.005	<0.005	<0.050	<0.100	<0.500	<0.100	14.7	<0.050	0.384	7.54			
WDS 47-1 Duplicate	<0.005	<0.005	<0.005	<0.050	<0.100	<0.500	<0.100	17.9	<0.050	0.267	7.88			
WDS 47-8 Duplicate	<0.005	<0.005	<0.005	<0.050	<0.100	<0.500	<0.100	12.3	<0.050	0.376	7.49			
WDS 47-28 Duplicate	<0.005	<0.005	<0.005	<0.050	<0.100	<0.500	<0.100	1.30	<0.050	0.404	7.91			
WDS 47-60 Duplicate	<0.005	<0.005	<0.005	<0.050	<0.100	<0.500	<0.100	12.8	<0.050	0.428	7.59			
WDS 47-88 Duplicate	<0.005	<0.005	<0.005	<0.050	<0.100	<0.500	<0.100	39.1	<0.050	0.435	7.60			

Appendix 11 Residual bulk pore-water data

Sample	Ca	Mg	Na	K	HCO ₃ ⁻	Cl ⁻	SO ₄ ²⁻	NO ₃ ⁻	Br ⁻	NO ₂ ⁻	HPO ₄ ²⁻	F ⁻	NPOC	Total P
	mg l ⁻¹	mg l ⁻¹	mg l ⁻¹	mg l ⁻¹	mg l ⁻¹	mg l ⁻¹	mg l ⁻¹	mg l ⁻¹	mg l ⁻¹	mg l ⁻¹	mg l ⁻¹	mg l ⁻¹	mg l ⁻¹	mg l ⁻¹
WDS 16	72.7	10.62	10.5	4.30	182	14.7	80.1	9.66	0.057	0.261	<0.200	1.30	14.3	<0.100
WDS 16 Duplicate	67.5	9.93	9.70	4.00	172	13.9	75.8	8.33	0.044	1.18	<0.100	1.23	16.8	<0.100
WDS 23	81.4	9.77	9.80	5.00	29.3	11.3	199	4.12	<0.200	<0.100	<1.00	1.94	<12.0	<0.100
WDS 23 Duplicate	81.5	9.67	9.80	5.00	34.3	11.6	198	2.52	<0.200	<0.100	<1.00	2.05	<12.0	<0.100
WDS 45	37.1	8.44	9.40	4.30	35.7	11.5	72.8	4.54	<0.200	0.167	<1.00	2.26	<12.0	<0.100
WDS 45 Duplicate	36.1	8.38	9.30	4.40	31.0	11.9	86.5	7.53	<0.040	<0.020	<0.200	2.20	12.1	<0.100
WDS 46	39.6	8.22	9.60	4.10	50.3	12.2	72.9	9.19	0.064	0.149	<0.200	1.71	9.64	<0.100
WDS 46 Duplicate	41.2	8.31	9.90	4.20	49.9	12.4	73.0	8.47	0.064	0.049	<0.200	1.69	15.2	<0.100
WDS 47	91.2	10.13	10.6	5.20	114	12.0	147	8.10	0.046	0.130	<0.200	1.35	14.5	<0.100
WDS 47 Duplicate	85.2	9.63	9.50	4.60	121	12.0	138	6.40	0.047	0.089	<0.200	1.44	13.2	<0.100
	Total S	Si	SiO₂	Ba	Sr	Mn	Total Fe	Li	Be	B	Al	Ti	V	Cr
	mg l ⁻¹	mg l ⁻¹	mg l ⁻¹	µg l ⁻¹	µg l ⁻¹	µg l ⁻¹	µg l ⁻¹	µg l ⁻¹	µg l ⁻¹	µg l ⁻¹	µg l ⁻¹	µg l ⁻¹	µg l ⁻¹	µg l ⁻¹
WDS 16	29.0	2.69	5.75	38.2	305	1371	82.0	<10.0	0.130	<200	31.0	<1.00	<1.00	<1.00
WDS 16 Duplicate	30.0	2.54	5.43	32.4	292	437	22.0	<10.0	0.158	<200	22.0	<1.00	<1.00	<1.00
WDS 23	84.0	2.12	4.54	160	323	5356	351	<10.0	0.167	<200	27.0	<1.00	<1.00	<1.00
WDS 23 Duplicate	88.0	2.19	4.69	156	336	6545	63.0	<10.0	0.115	<200	47.0	<1.00	<1.00	<1.00
WDS 45	42.0	2.17	4.64	26.0	116	10.9	124	<10.0	0.154	<200	73.0	<1.00	<1.00	<1.00
WDS 45 Duplicate	36.0	1.90	4.06	25.5	119	8.7	114	<10.0	0.150	<200	63.0	<1.00	<1.00	<1.00
WDS 46	31.0	2.38	5.09	28.1	133	137	86.0	<10.0	0.180	<200	58.0	<1.00	<1.00	<1.00
WDS 46 Duplicate	32.0	2.41	5.16	29.6	132	104	49.0	<10.0	0.131	<200	57.0	<1.00	<1.00	<1.00
WDS 47	59.0	2.81	6.01	93.1	373	3262	106	11.0	0.053	<200	44.0	<1.00	<1.00	<1.00
WDS 47 Duplicate	56.0	2.70	5.78	87.6	352	2554	88.0	11.0	0.062	<200	53.0	<1.00	<1.00	<1.00

	Co	Ni	Cu	Zn	Ga	As	Se	Rb	Y	Zr	Nb	Mo	Ag	Cd
	µg l ⁻¹													
WDS 16	4.79	6.30	<5.00	102	<0.500	0.550	0.380	8.29	0.117	0.610	<0.500	<2.00	0.130	0.540
WDS 16 Duplicate	2.19	4.60	<5.00	73.0	<0.500	<0.500	0.180	7.70	0.079	0.630	<0.500	<2.00	<0.050	0.250
WDS 23	19.4	18.6	7.00	1305	<0.500	<0.500	0.140	10.1	0.061	0.740	<0.500	<2.00	0.074	7.02
WDS 23 Duplicate	21.4	17.7	15.3	1044	<0.500	0.630	<0.100	10.1	0.081	0.900	<0.500	<2.00	0.148	6.48
WDS 45	0.120	5.40	<5.00	91.0	<0.500	0.620	<0.100	8.58	0.179	0.820	<0.500	<2.00	<0.050	0.230
WDS 45 Duplicate	0.110	5.20	<5.00	90.0	<0.500	<0.500	0.130	8.82	0.182	1.02	<0.500	<2.00	<0.050	0.220
WDS 46	1.07	4.40	<5.00	73.0	<0.500	0.540	0.150	7.28	0.163	1.16	<0.500	<2.00	<0.050	0.300
WDS 46 Duplicate	0.960	5.10	<5.00	78.0	<0.500	<0.500	0.120	8.05	0.124	1.14	<0.500	<2.00	<0.050	0.300
WDS 47	9.02	8.80	11.8	304	<0.500	0.700	0.160	6.18	0.111	1.39	<0.500	<2.00	<0.050	1.71
WDS 47 Duplicate	5.59	7.20	11.7	248	<0.500	0.840	0.140	6.62	0.107	2.24	<0.500	<2.00	<0.050	1.29
	Sn	Sb	Cs	La	Ce	Pr	Nd	Sm	Eu	Tb	Gd	Dy	Ho	Er
	µg l ⁻¹													
WDS 16	<1.00	0.619	0.130	0.063	<0.100	<0.050	0.060	<0.050	<0.050	<0.050	<0.050	<0.050	<0.050	<0.050
WDS 16 Duplicate	<1.00	0.661	0.120	<0.050	<0.100	<0.050	<0.050	<0.050	<0.050	<0.050	<0.050	<0.050	<0.050	<0.050
WDS 23	<1.00	6.54	0.180	<0.050	<0.100	<0.050	<0.050	<0.050	<0.050	<0.050	<0.050	<0.050	<0.050	<0.050
WDS 23 Duplicate	<1.00	7.09	0.340	0.332	0.550	<0.050	0.103	<0.050	<0.050	<0.050	<0.050	<0.050	<0.050	<0.050
WDS 45	<1.00	1.34	0.280	0.059	0.110	<0.050	0.103	<0.050	<0.050	<0.050	0.054	<0.050	<0.050	<0.050
WDS 45 Duplicate	<1.00	1.39	0.170	0.057	0.110	<0.050	0.086	<0.050	<0.050	<0.050	<0.050	<0.050	<0.050	<0.050
WDS 46	<1.00	0.701	0.140	0.237	0.410	<0.050	0.140	<0.050	<0.050	<0.050	<0.050	<0.050	<0.050	<0.050
WDS 46 Duplicate	<1.00	0.686	0.140	<0.050	<0.100	<0.050	0.083	<0.050	<0.050	<0.050	<0.050	<0.050	<0.050	<0.050
WDS 47	<1.00	6.58	<0.100	<0.050	0.110	<0.050	0.055	<0.050	<0.050	<0.050	<0.050	<0.050	<0.050	<0.050
WDS 47 Duplicate	<1.00	6.79	<0.100	0.051	0.100	<0.050	0.085	<0.050	<0.050	<0.050	<0.050	<0.050	<0.050	<0.050

	Tm	Yb	Lu	Hf	Ta	W	Tl	Pb	Th	U	pH			
	$\mu\text{g l}^{-1}$													
WDS 16	<0.050	<0.050	<0.050	<0.500	<1.00	<5.00	<1.00	7.00	<0.500	0.471	7.66			
WDS 16 Duplicate	<0.050	<0.050	<0.050	<0.500	<1.00	<5.00	<1.00	3.70	<0.500	0.466	8.07			
WDS 23	<0.050	<0.050	<0.050	<0.500	<1.00	<5.00	<1.00	509	<0.500	<0.050	7.41			
WDS 23 Duplicate	<0.050	<0.050	<0.050	<0.500	<1.00	<5.00	<1.00	473	<0.500	<0.050	7.54			
WDS 45	<0.050	<0.050	<0.050	<0.500	<1.00	<5.00	<1.00	15.1	<0.500	<0.050	7.31			
WDS 45 Duplicate	<0.050	<0.050	<0.050	<0.500	<1.00	<5.00	<1.00	14.9	<0.500	<0.050	7.42			
WDS 46	<0.050	<0.050	<0.050	<0.500	<1.00	<5.00	<1.00	11.6	<0.500	<0.050	7.46			
WDS 46 Duplicate	<0.050	<0.050	<0.050	<0.500	<1.00	<5.00	<1.00	7.40	<0.500	<0.050	7.52			
WDS 47	<0.050	<0.050	<0.050	<0.500	<1.00	<5.00	<1.00	154	<0.500	0.303	8.06			
WDS 47 Duplicate	<0.050	<0.050	<0.050	<0.500	<1.00	<5.00	<1.00	124	<0.500	0.401	8.09			

Appendix 12 Release rate curves for analysed elements in the study where sediment information has been determined

ALUMINIUM

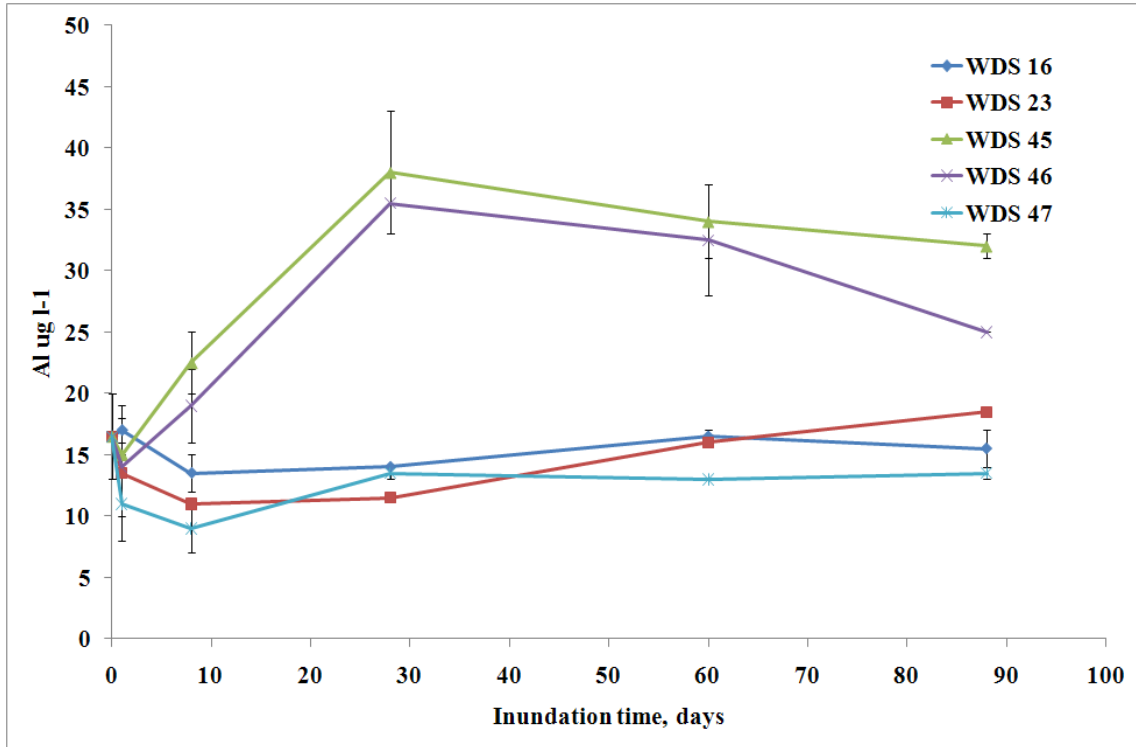


Figure 26 Aluminium rate release curve, $\mu\text{g l}^{-1}$

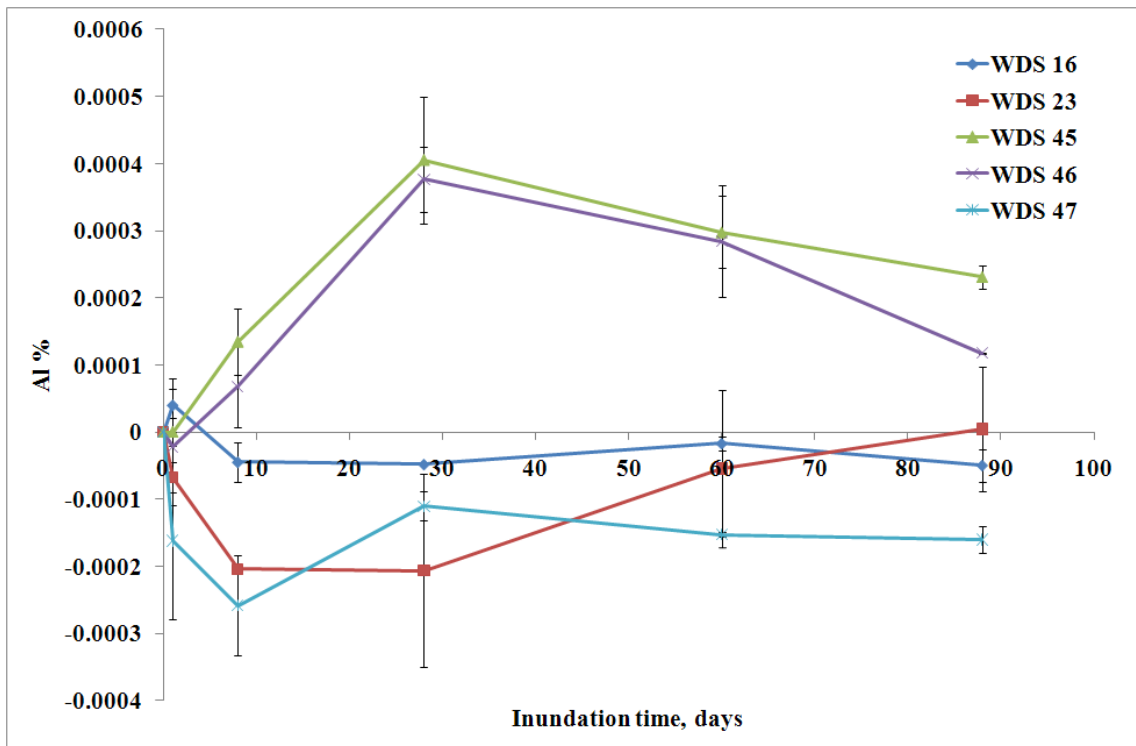


Figure 27 Aluminium release rate curve, % of the original sediment concentration

ARSENIC

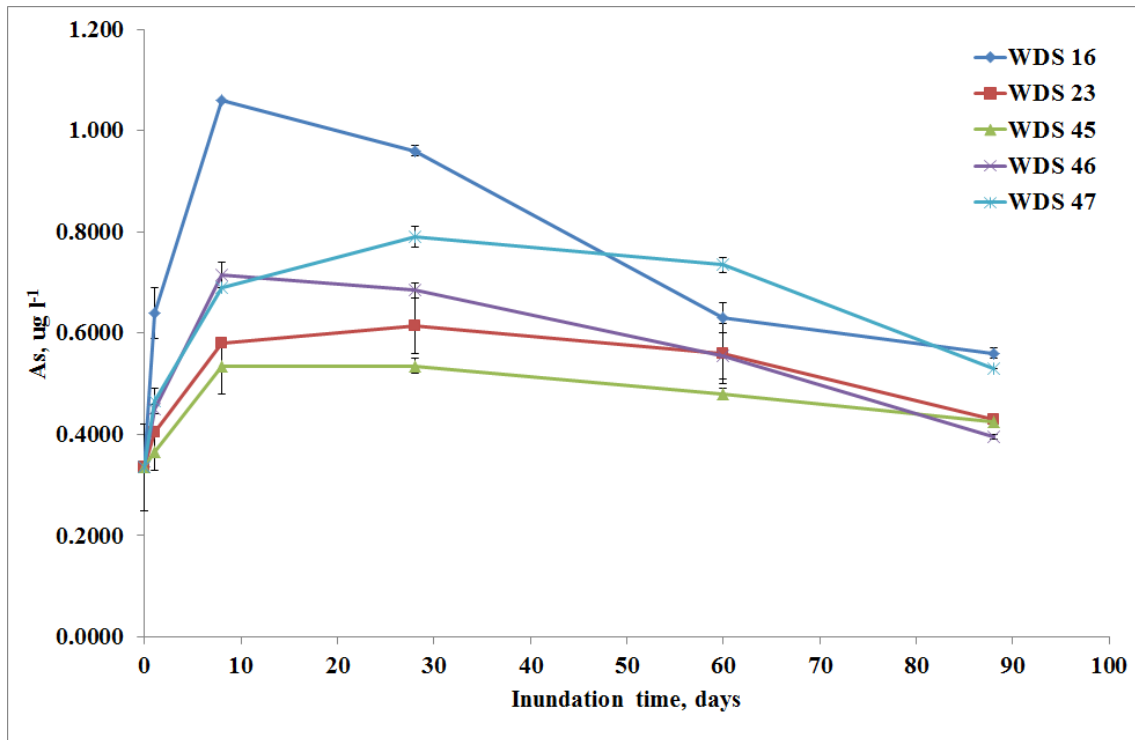


Figure 28 Arsenic rate release curve, µg l⁻¹

BARIUM

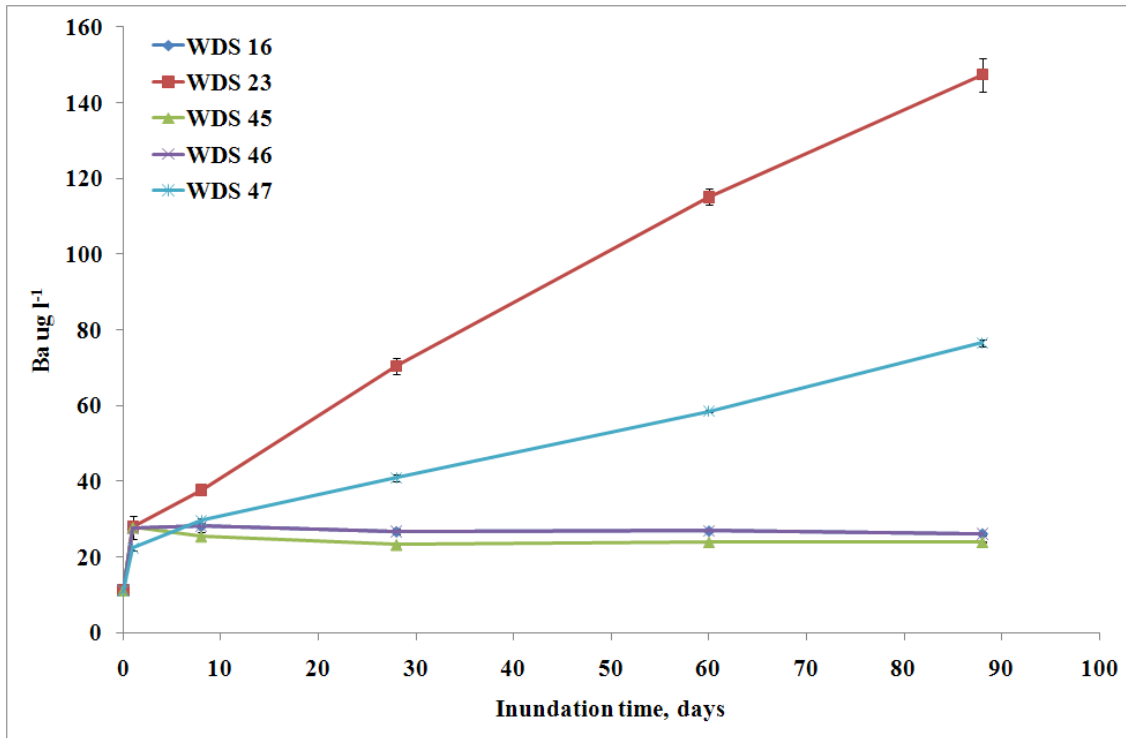


Figure 29 Barium release rate curve, $\mu\text{g l}^{-1}$

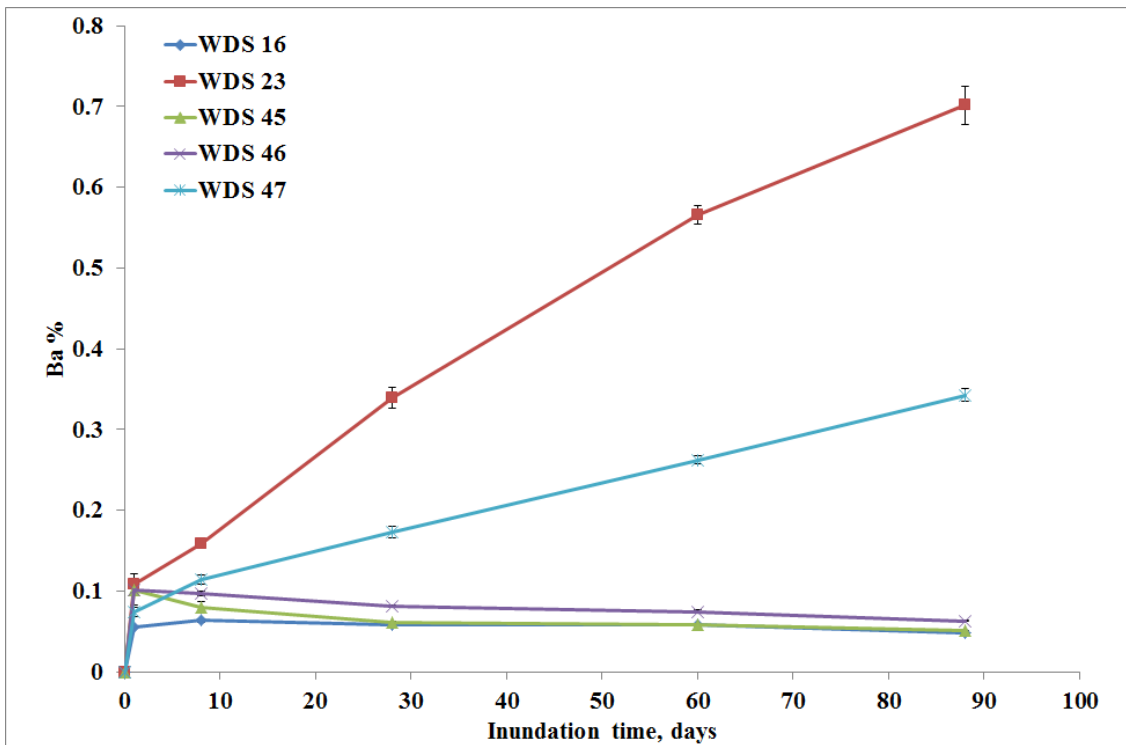


Figure 30 Barium rate release curve, % of the original sediment concentration

CALCIUM

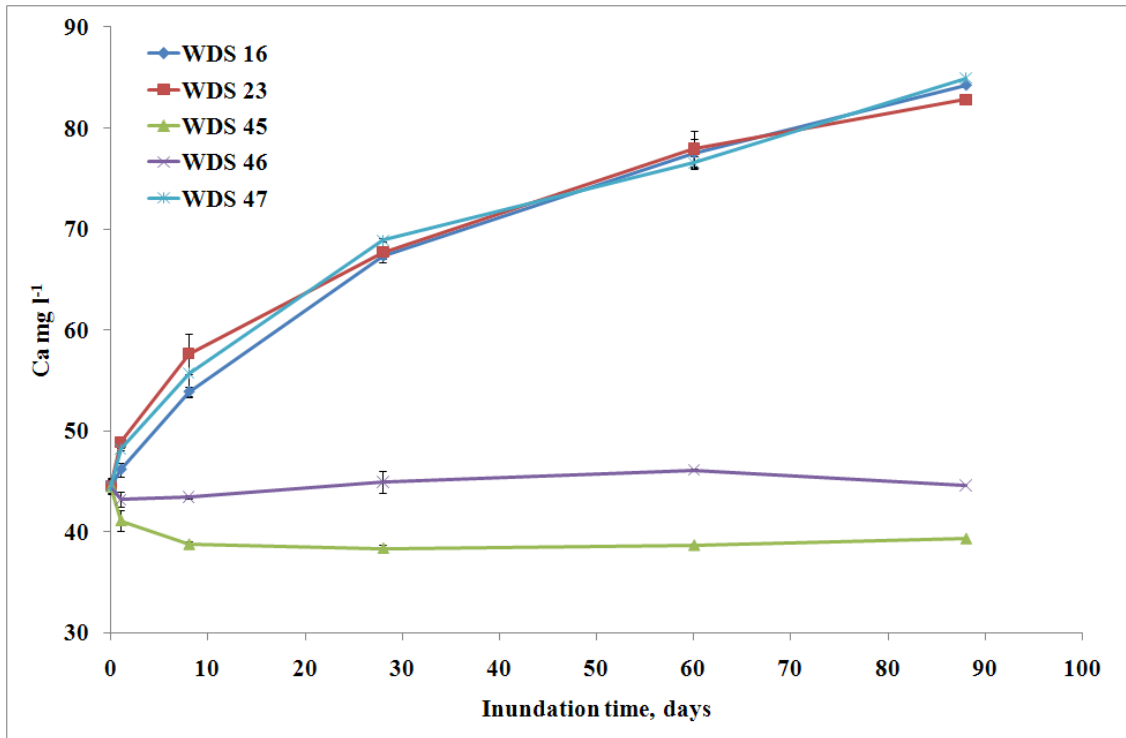


Figure 31 Calcium release rate curve, mg l⁻¹

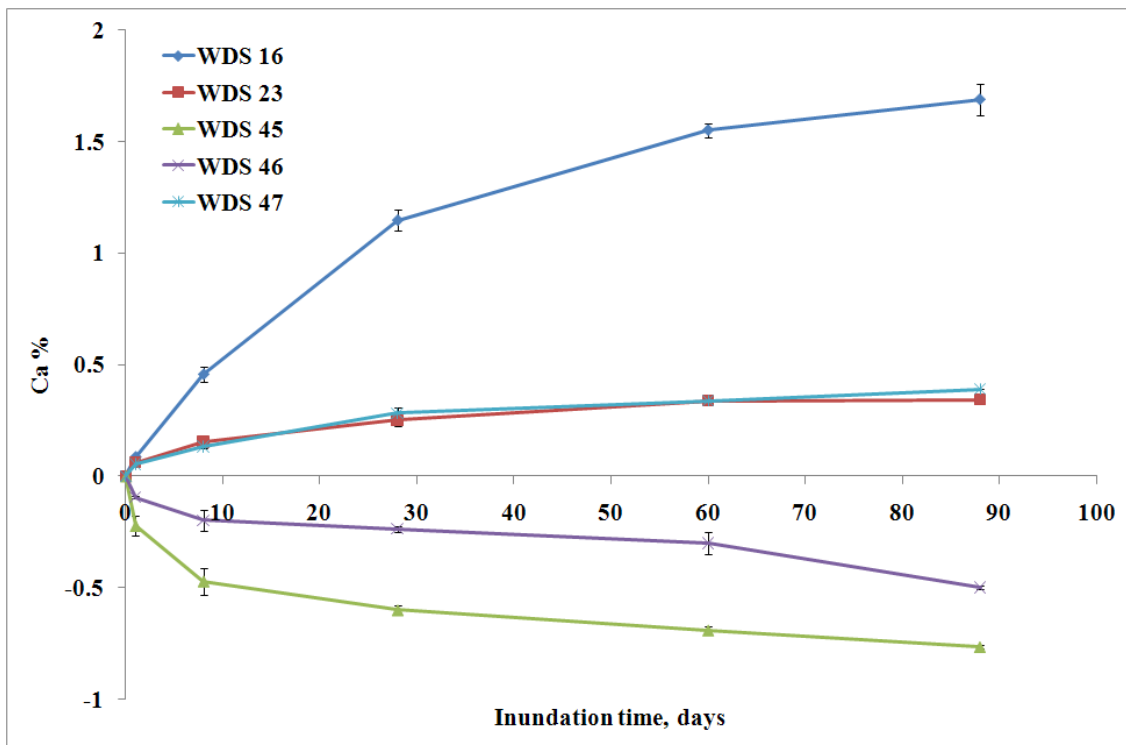


Figure 32 Calcium release rate curve, % of the original sediment concentration

CADMIUM

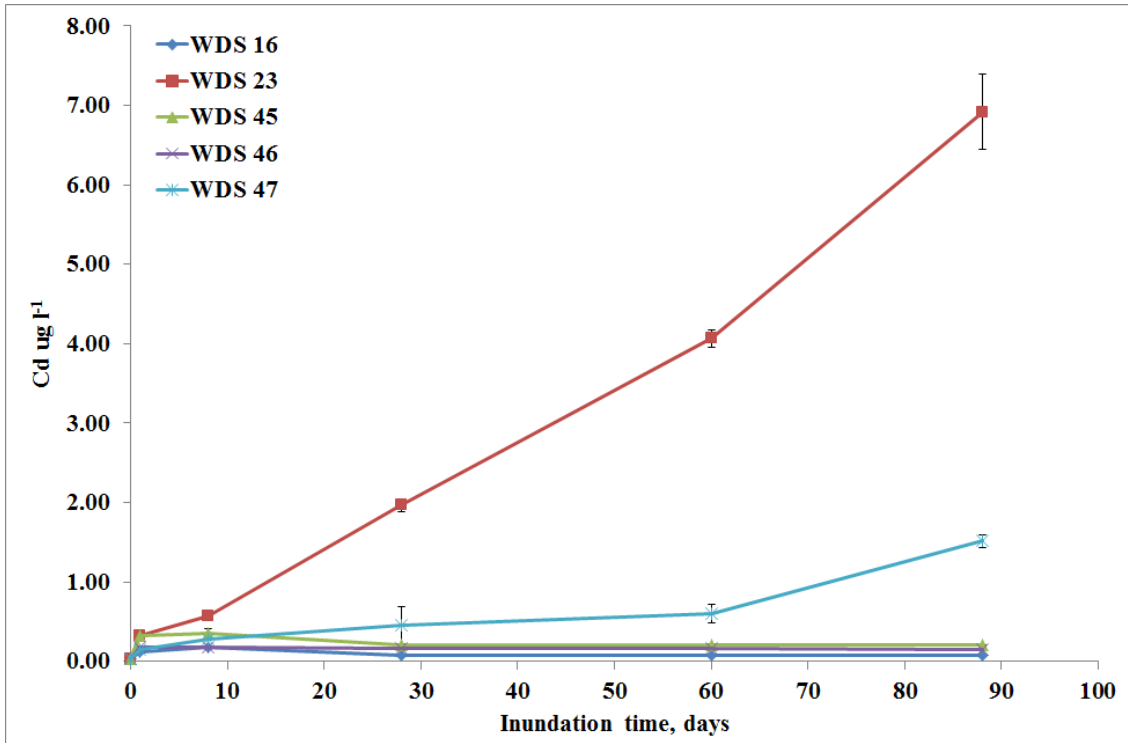


Figure 33 Cadmium release rate curve, mg l^{-1}

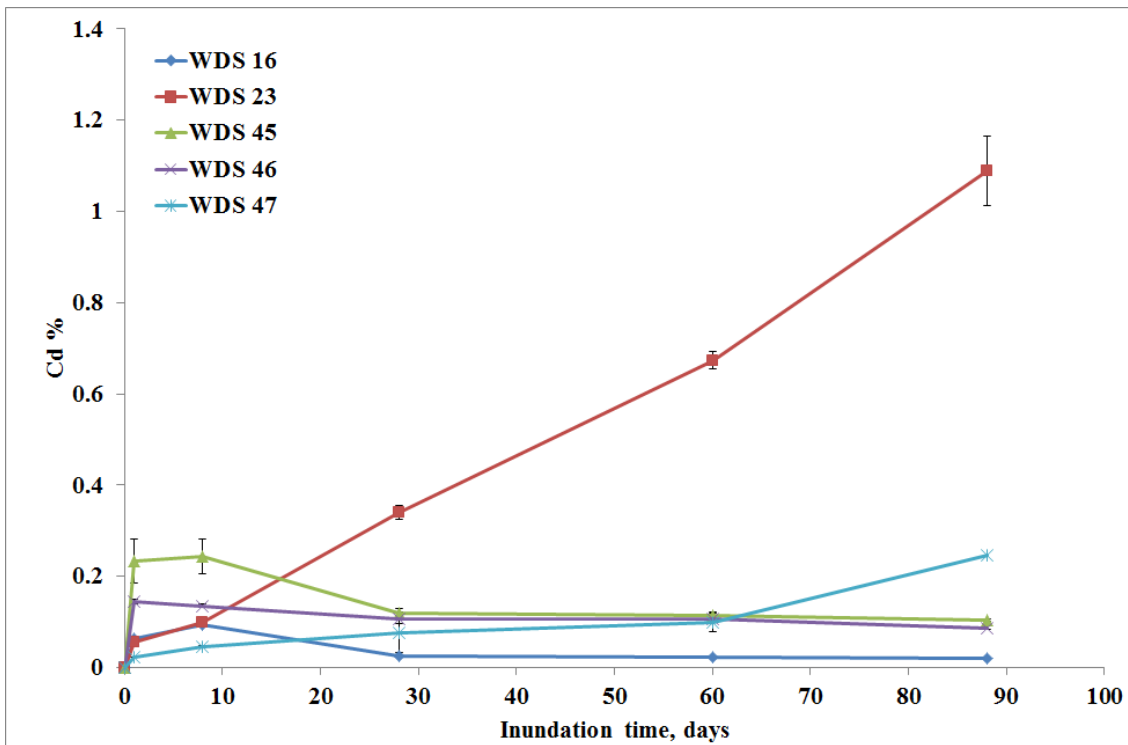


Figure 34 Cadmium release rate curve, % of the original sediment concentration

COBALT

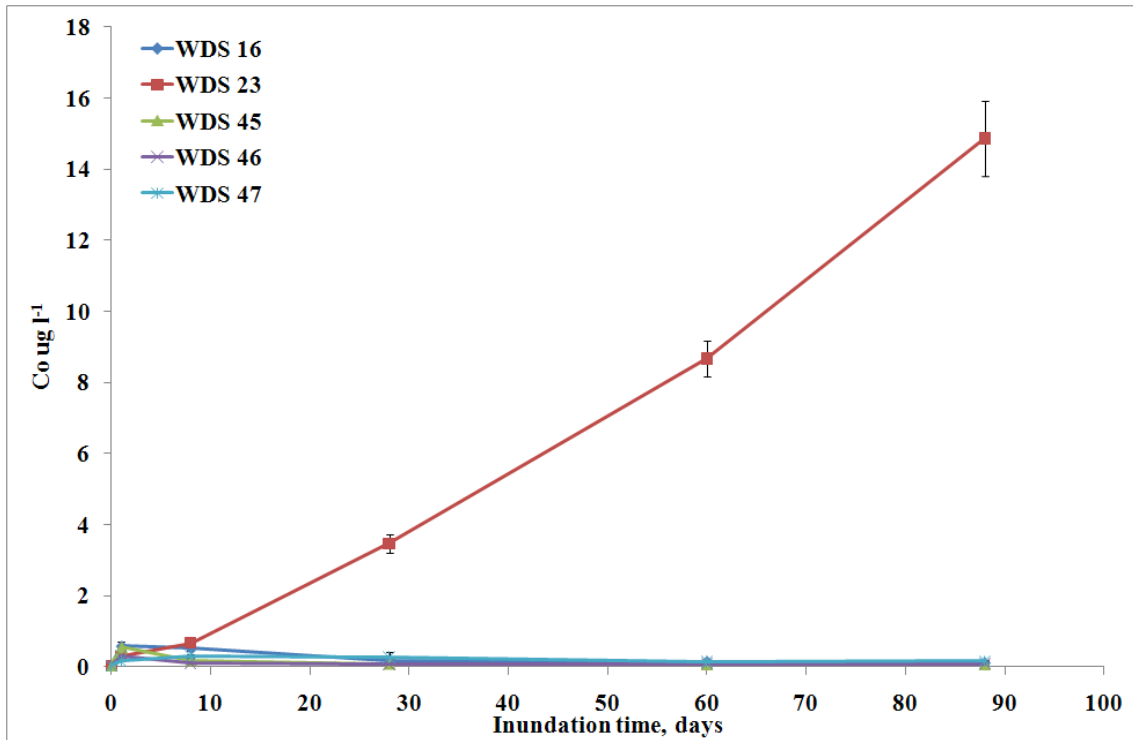


Figure 35 Cobalt release rate curve, $\mu\text{g l}^{-1}$

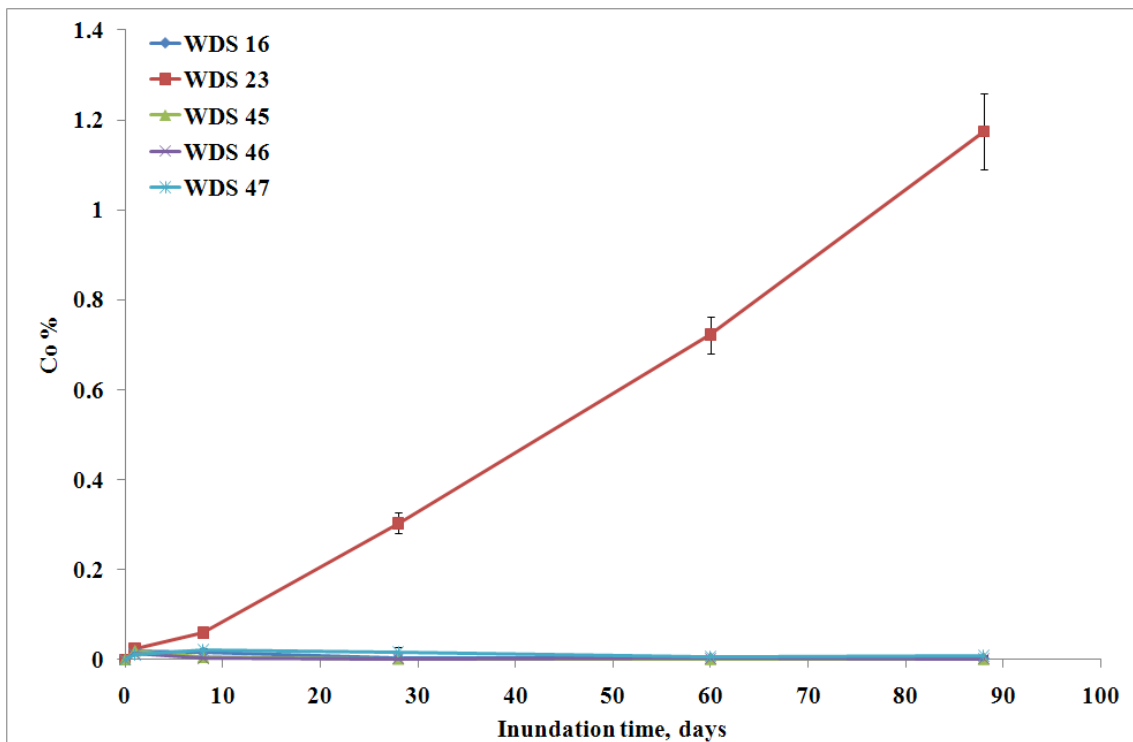


Figure 36 Cobalt release rate curve, % of the original sediment concentration

CHROMIUM

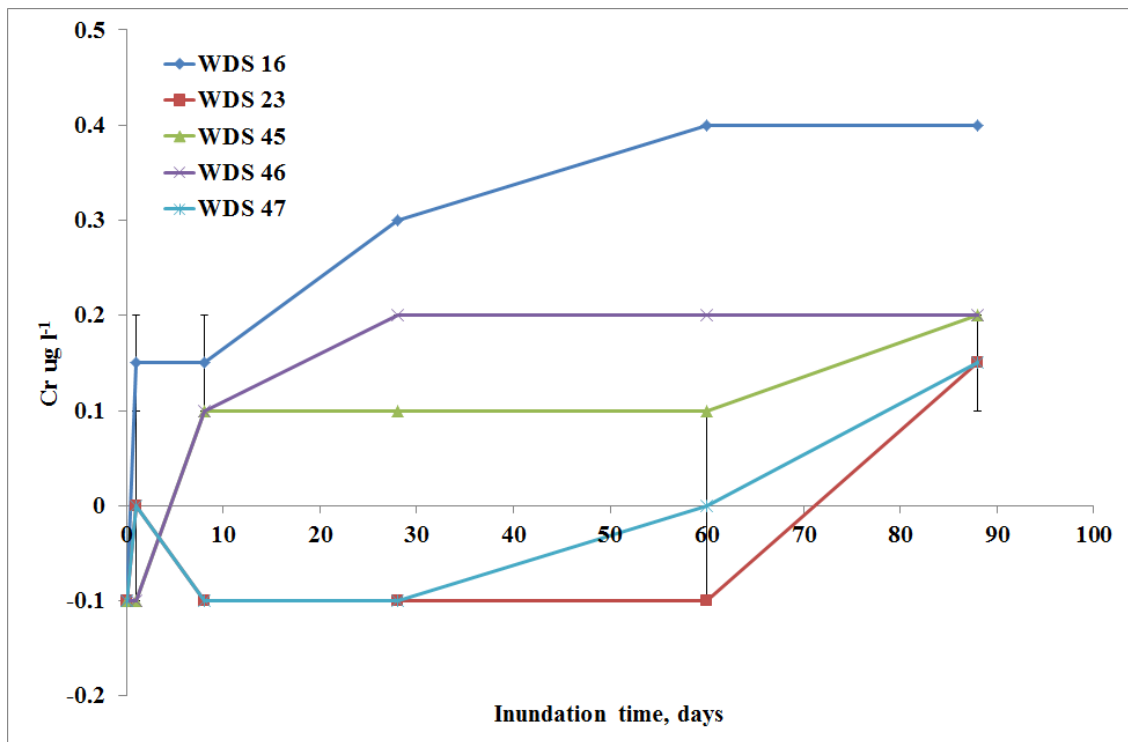


Figure 37 Chromium release rate curve, µg l⁻¹

LITHIUM

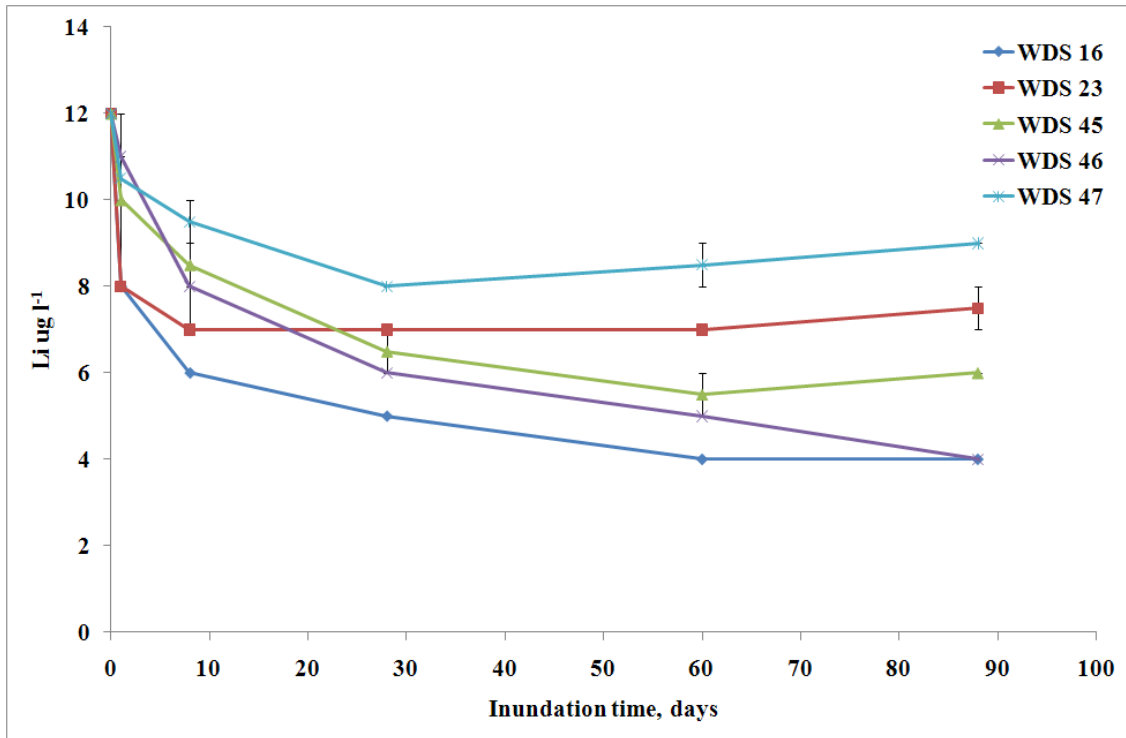


Figure 38 Lithium release rate curve, $\mu\text{g l}^{-1}$

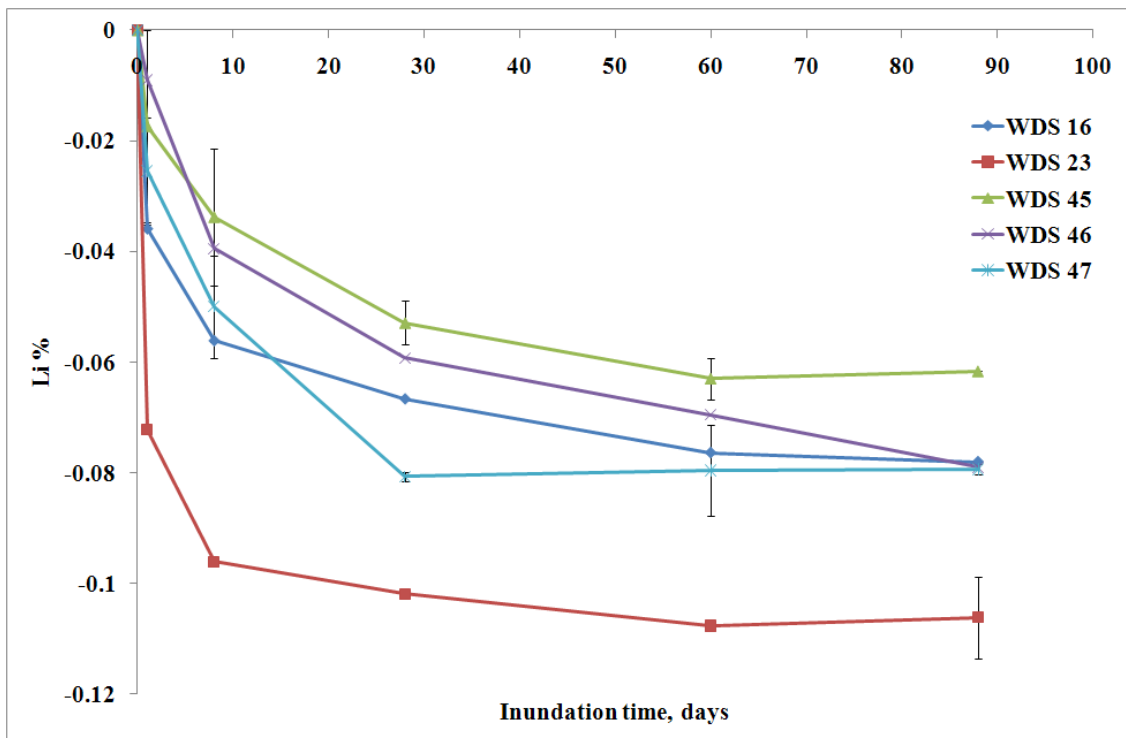


Figure 39 Lithium release rate curve, % of the original sediment concentration

MAGNESIUM

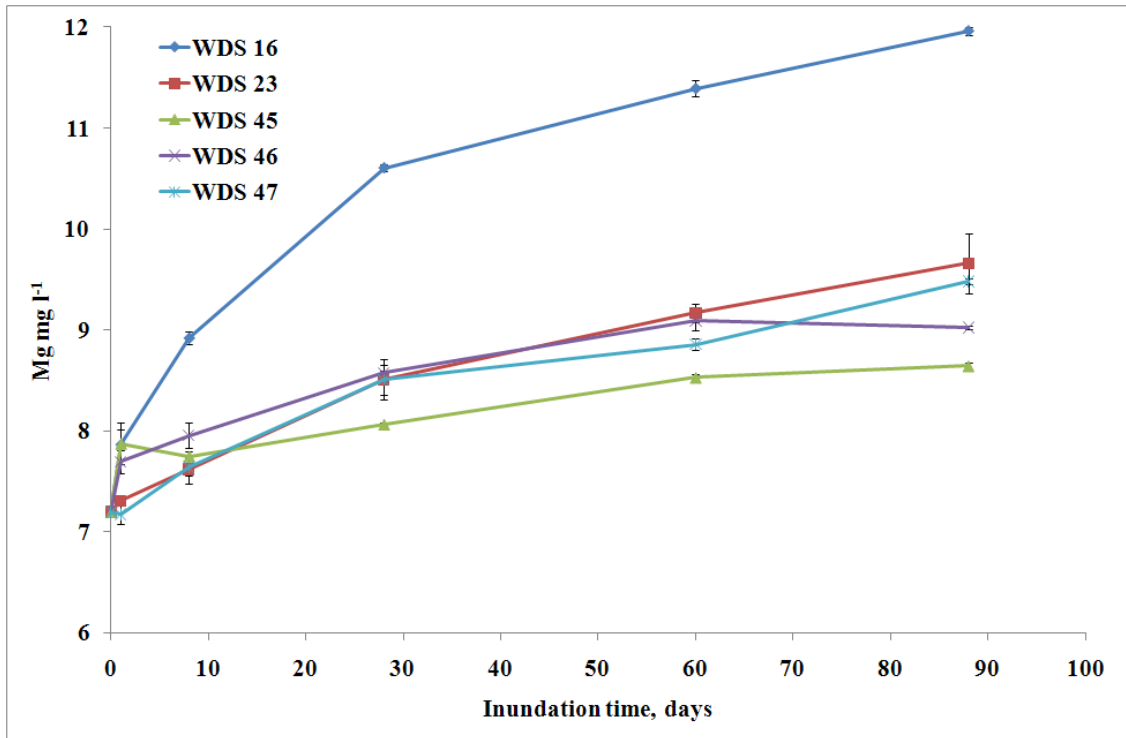


Figure 40 Magnesium release rate curve, mg l⁻¹

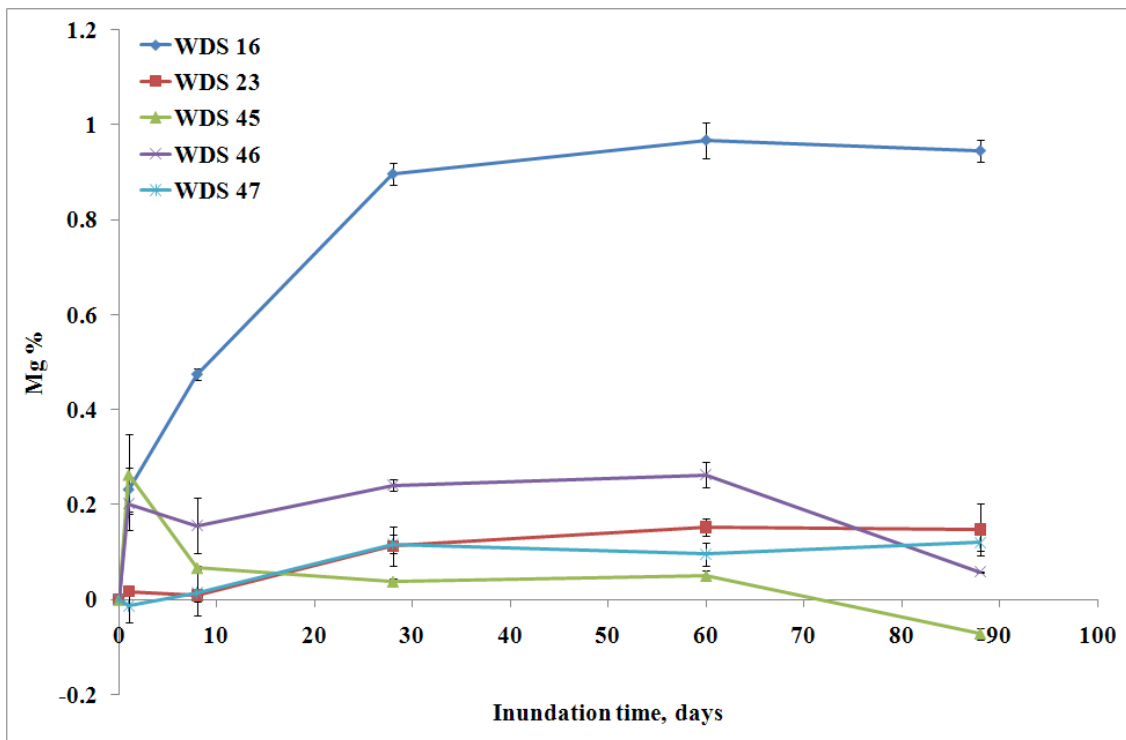


Figure 41 Magnesium release rate curve, % of the original sediment concentration

NICKEL

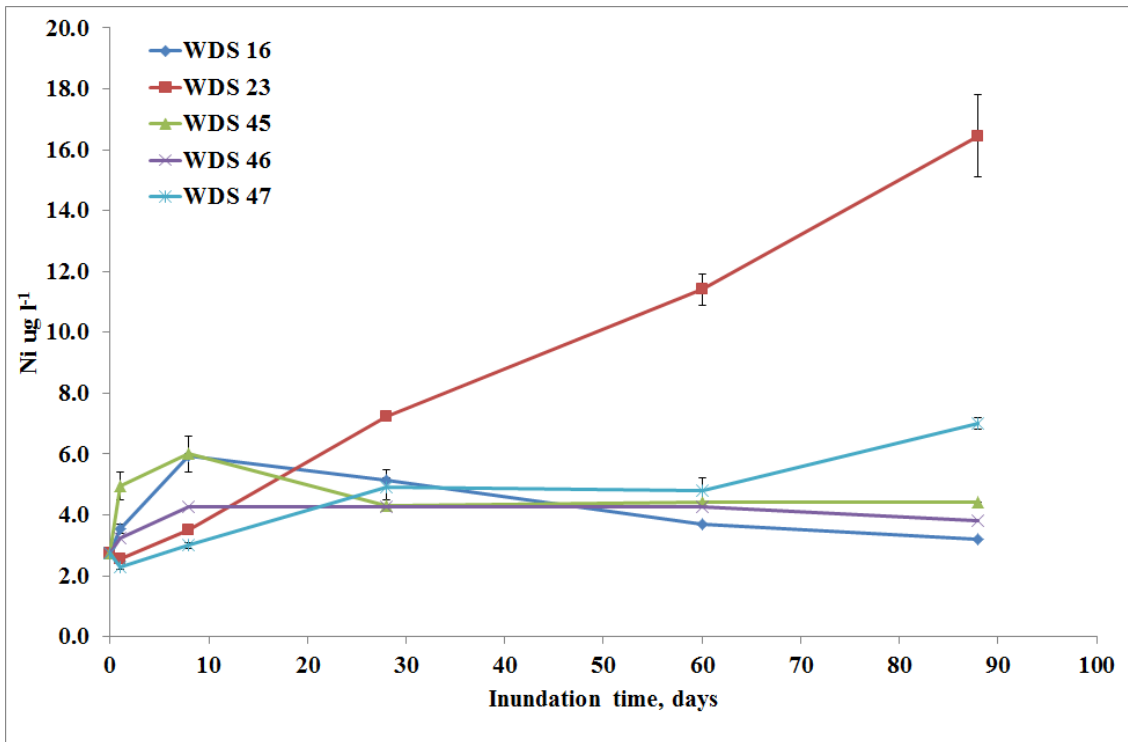


Figure 42 Nickel release rate curve, mg l^{-1}

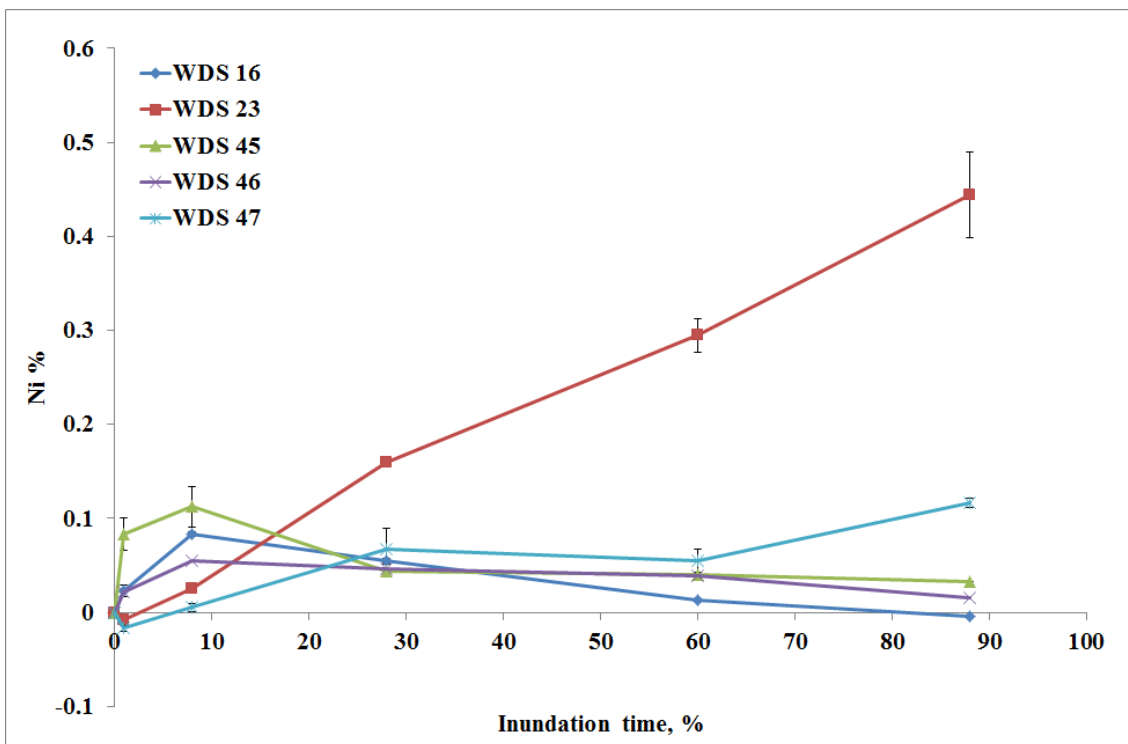


Figure 43 Nickel release rate curve, % of the original sediment concentration

POTASSIUM

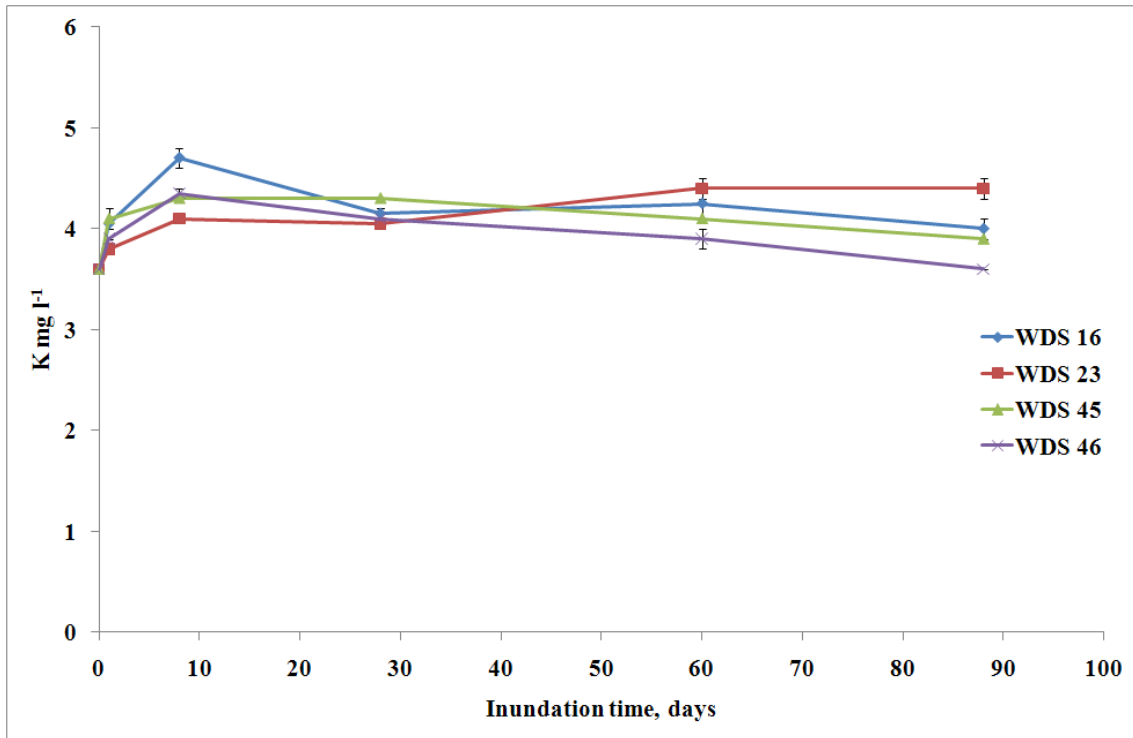


Figure 44 Potassium release rate curve, mg l⁻¹

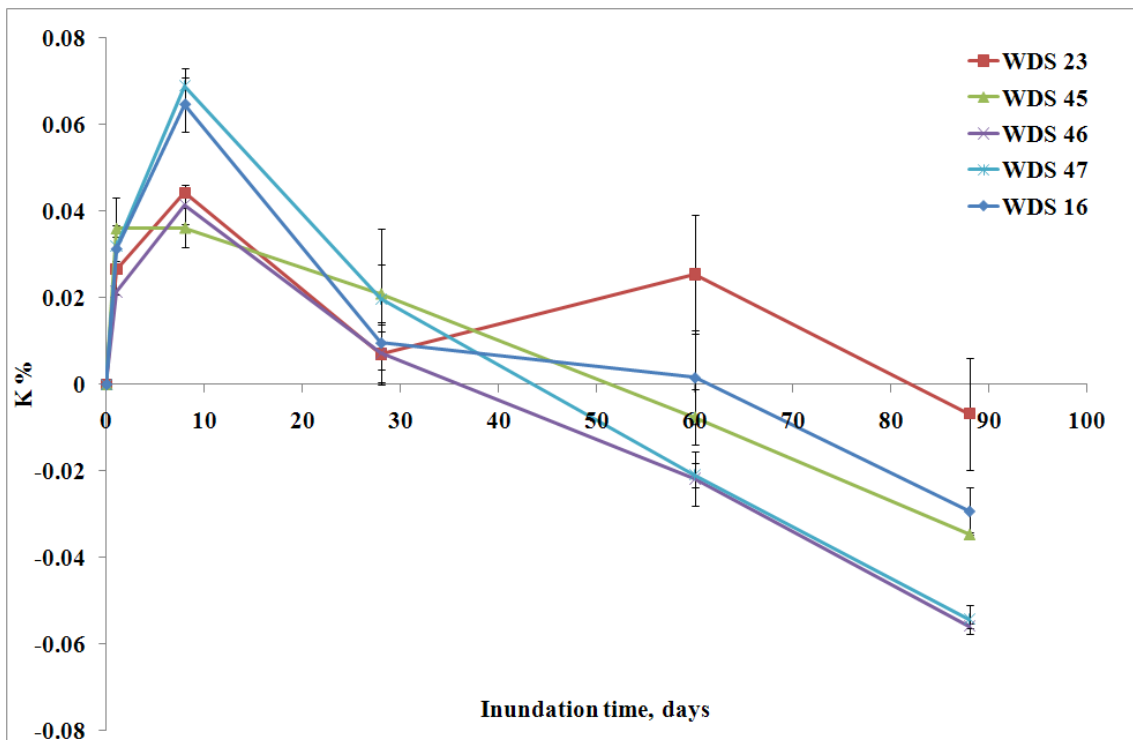


Figure 45 Potassium release rate curve, % of the original sediment concentration

SELENIUM

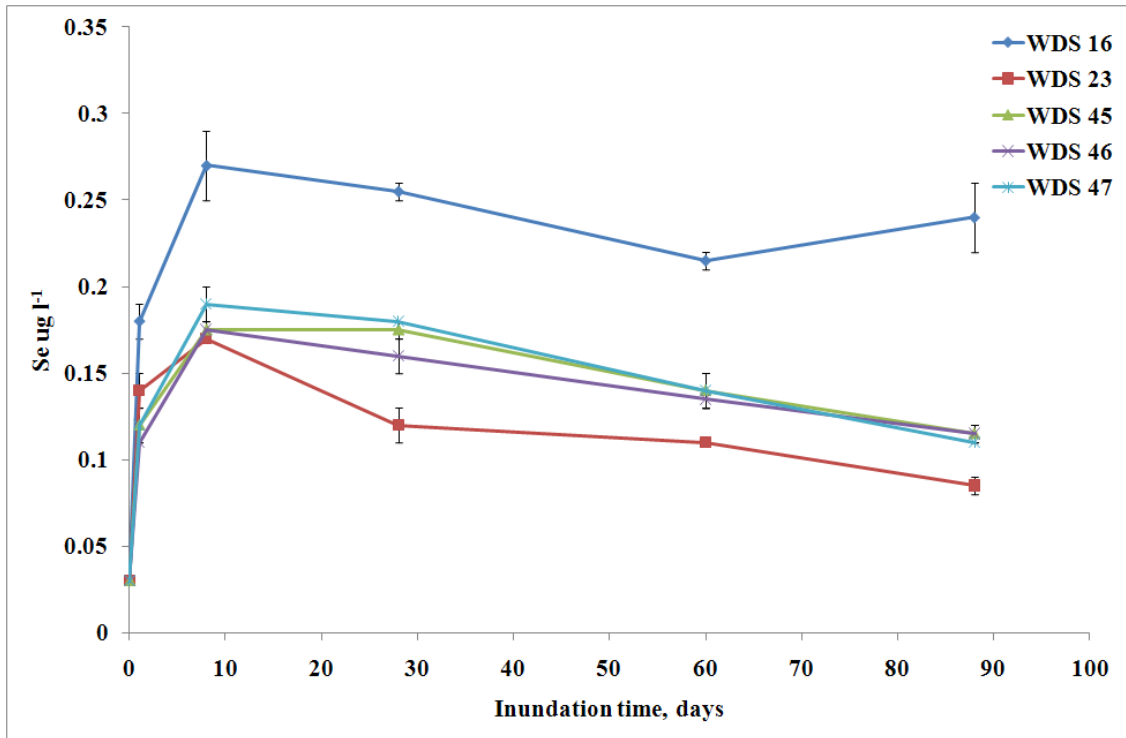


Figure 46 Selenium release rate curve, mg l⁻¹

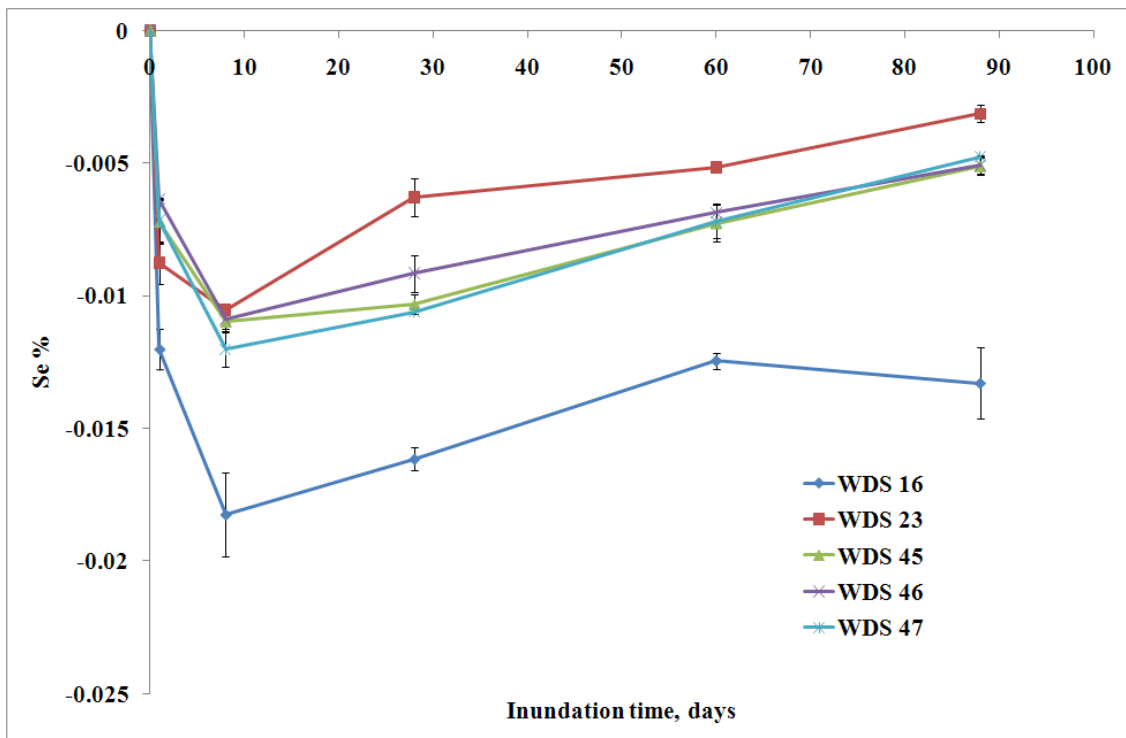


Figure 47 Selenium release rate curve, % of the original sediment concentration

SODIUM

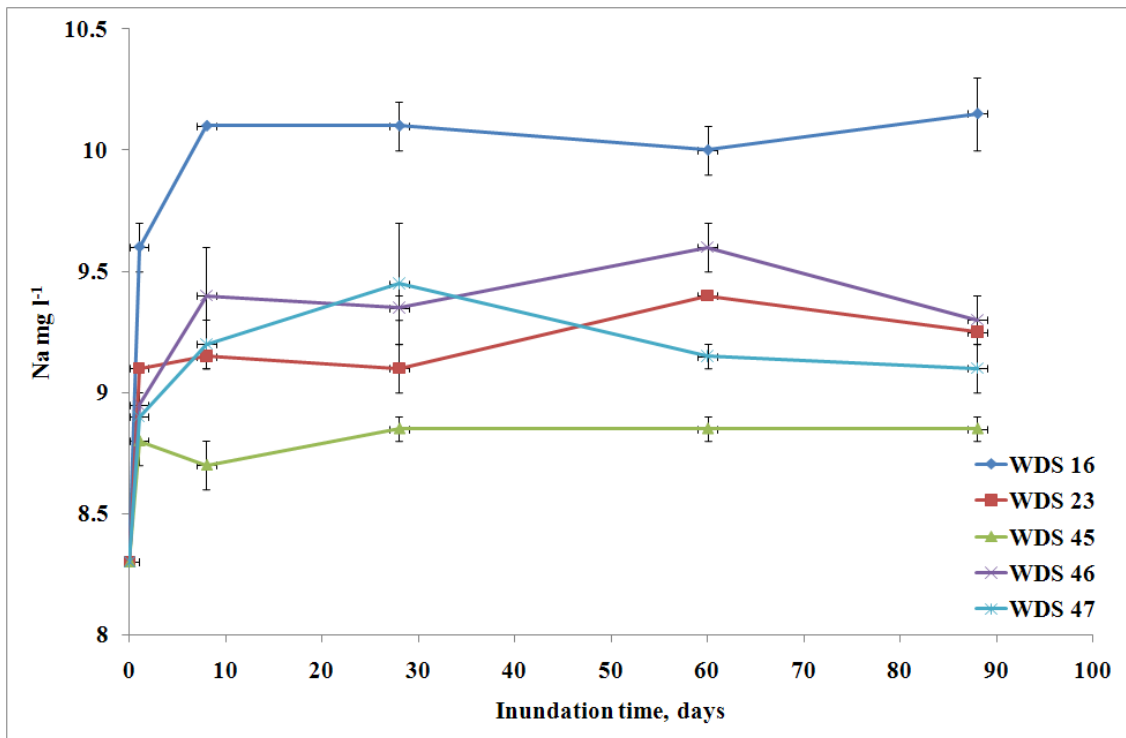


Figure 48 Sodium release rate curve, mg l⁻¹

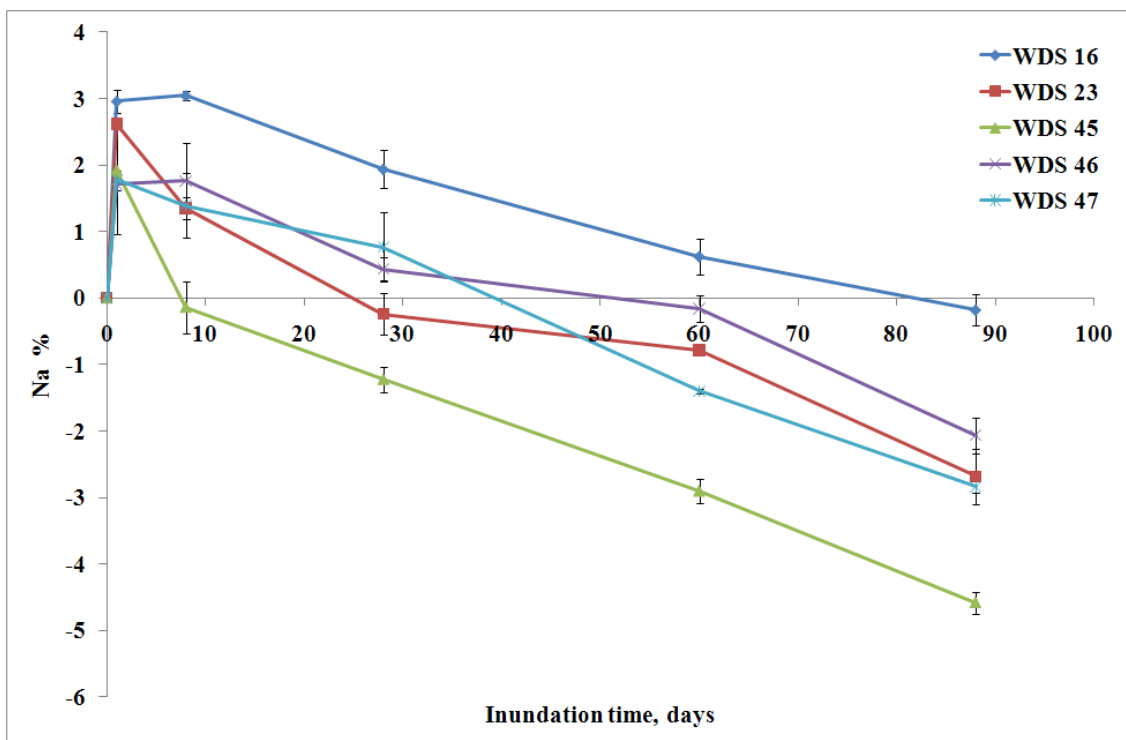


Figure 49 Sodium release rate curve, % of the original sediment concentration

STRONTIUM

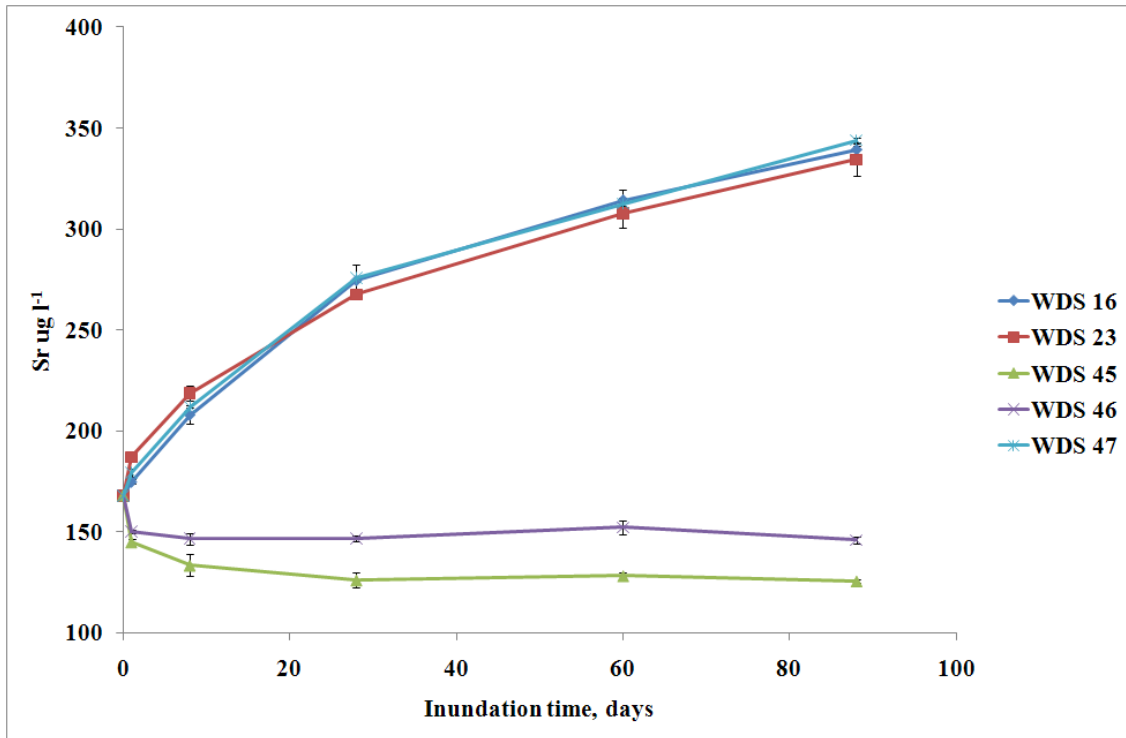


Figure 50 Strontium release rate curve, $\mu\text{g l}^{-1}$

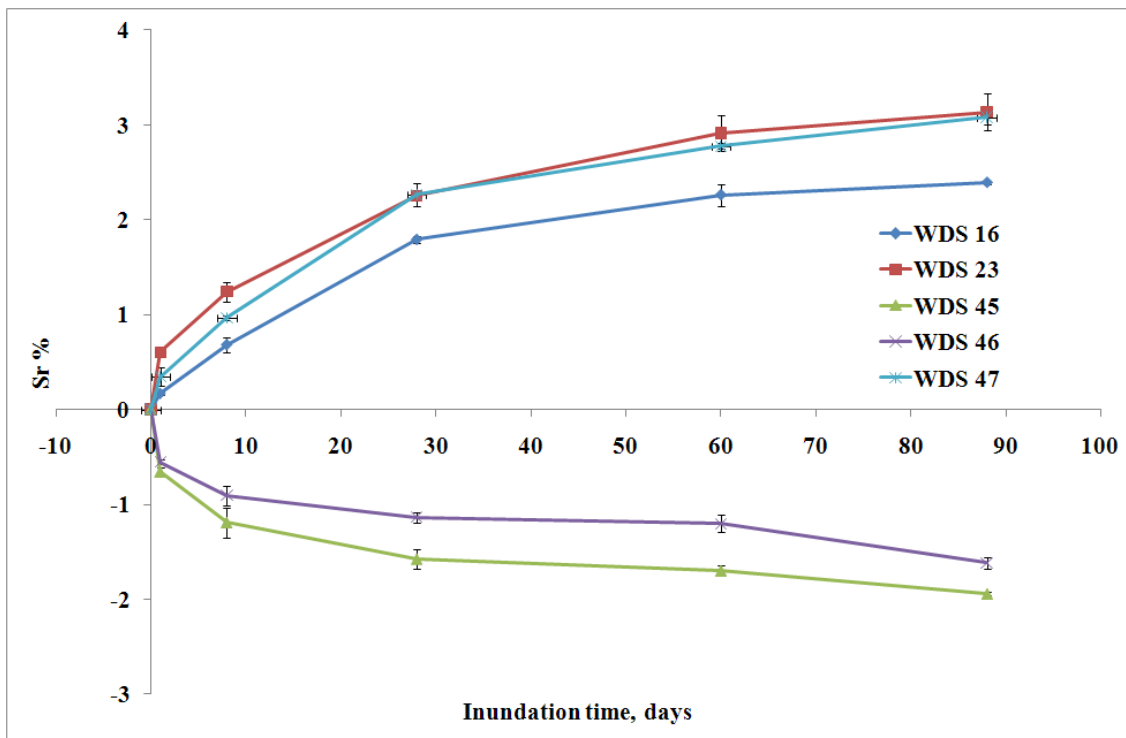


Figure 51 Strontium release rate curve, % of the original sediment concentration

SULPHUR

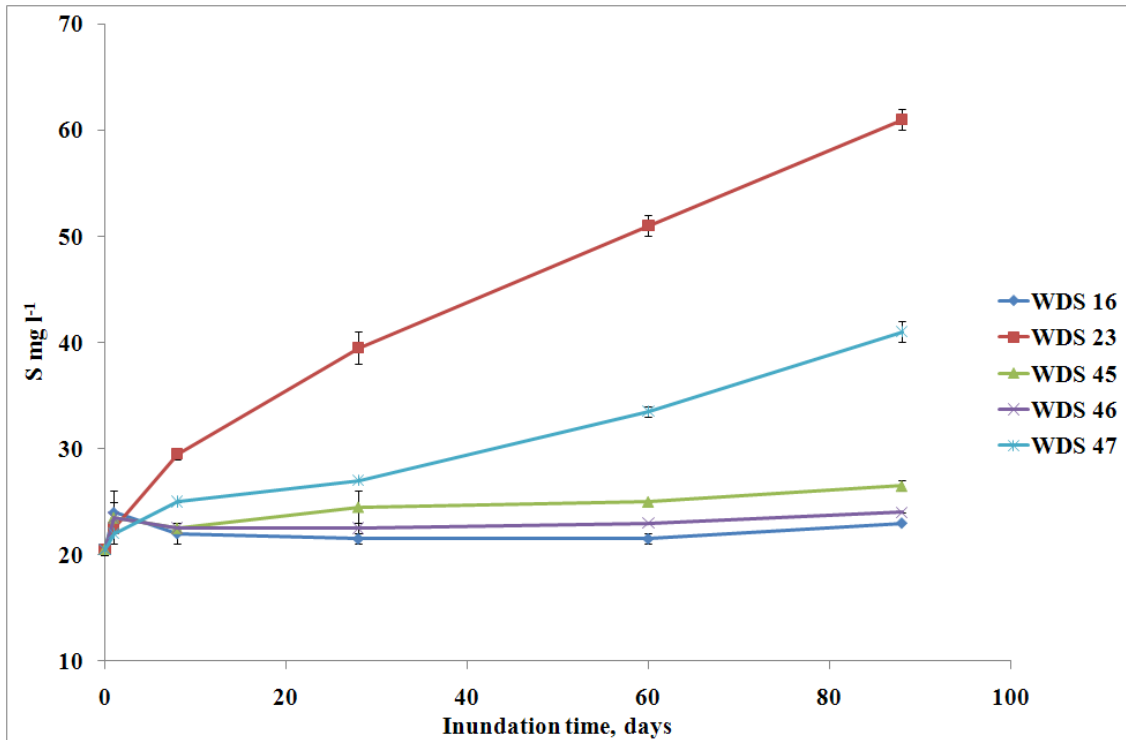


Figure 52 Sulphur release rate curve, mg l⁻¹

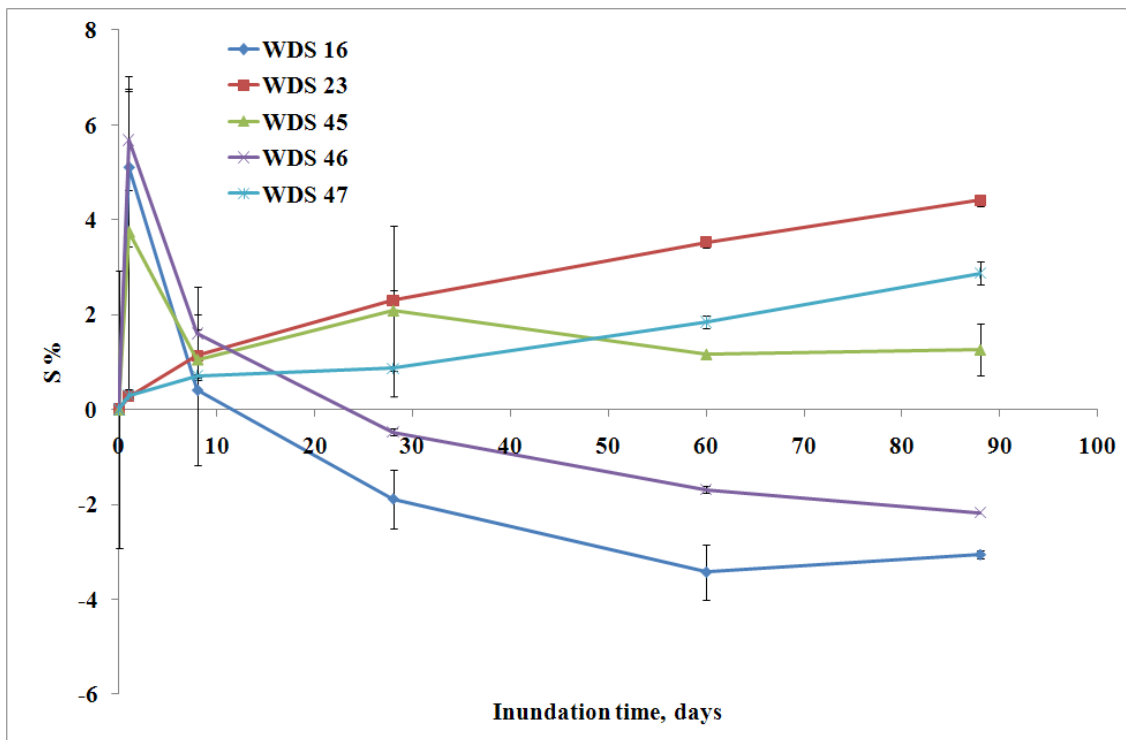


Figure 53 Sulphur release rate curve, % of the original sediment concentration

VANADIUM

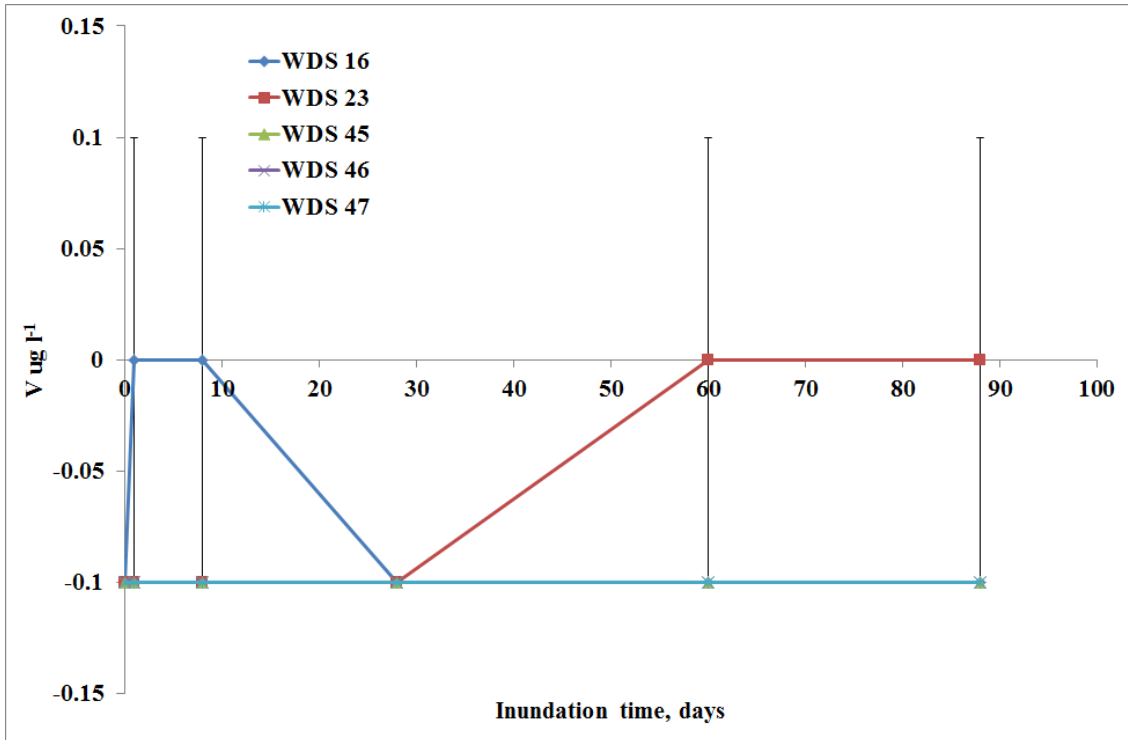


Figure 54 Vanadium release rate curve, mg l⁻¹

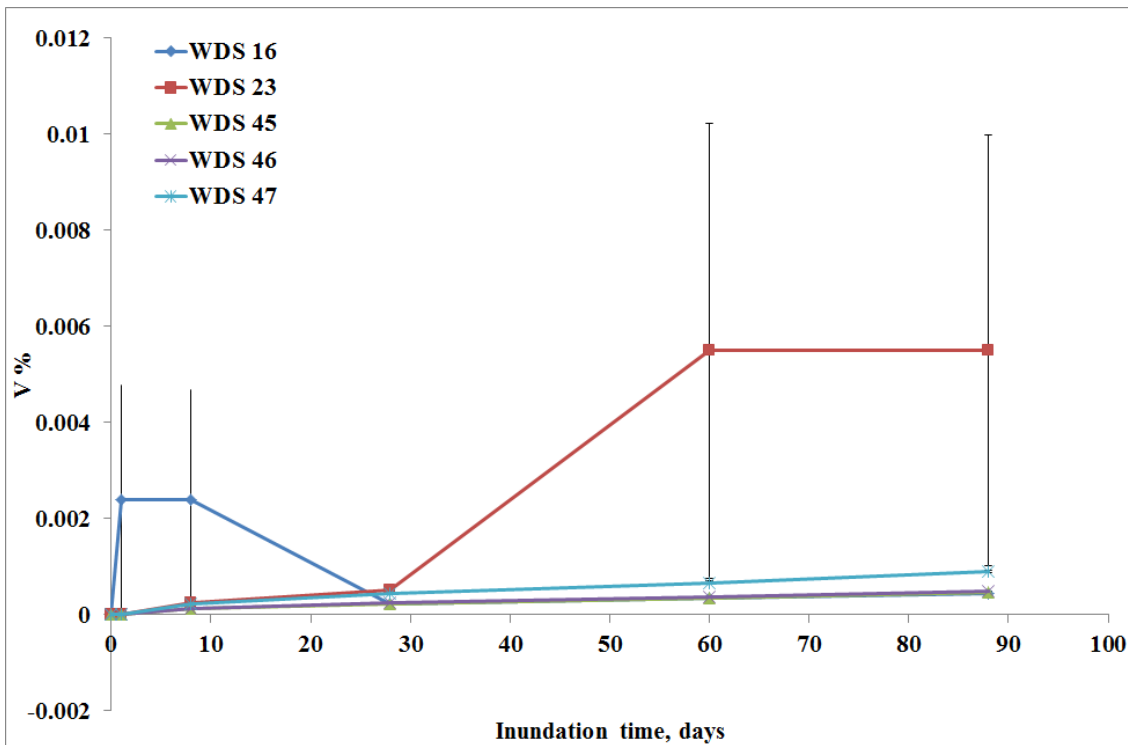


Figure 55 Vanadium release rate curve, % of the original sediment concentration

References

British Geological Survey holds most of the references listed below, and copies may be obtained via the library service subject to copyright legislation (contact libuser@bgs.ac.uk for details). The library catalogue is available at: <http://geolib.bgs.ac.uk>.

- BALL, J. W., and NORDSTROM, D. K. 1991. User's manual for WATEQ4F, with revised thermodynamic data base and test cases for calculating speciation of major, trace, and redox elements in natural waters. U.S. Geological Survey Open-File Report 91-183.
- BANKS, V.J. AND PALUMBO-ROE, B. 2010. Synoptic monitoring as an approach to discriminating between point and diffuse source contributions to zinc loads in mining impacted catchments. *Journal of Environmental Monitoring*, 12 (9), 1684-1698.
- BARGAR, J.R., FULLER, C.C., MARCUS, M.A., BREARLEY, PEREZ DE LA ROSA, A.J.M., Webb, S.M., CALDWELL, W.A. 2009. Structural characterization of terrestrial microbial Mn oxides from Pinal Creek, AZ, *Geochimica et Cosmochimica Acta*, 73 (4), 889-910.
- BATSON, V.L., BERTSVH, P.M. AND HERBERT, B.E. 1996. Transport of anthropogenic uranium from sediments to surface waters during episodic storm events. *Journal of Environmental Quality*. 25 (5), 1129-1137.
- BERT, V., SEUNTJENS, P., DEJONGHE, W., LACHAREZ, S., THUY, HTT AND VANDECASTEELE E, B. 2009. Phytoremediation as a management option for contaminated sediments in tidal marshes, flood control areas and dredged sediment landfill sites. *Environmental Science and Pollution Research*, 16 (7), 745-764.
- BBC. 2007. Homes and transport hit by flood. Accessed at <http://news.bbc.co.uk/1/hi/uk/6755571.stm>
- BEGUM, M., JURAIMI, A.S., AMARTALINGAM, R., BIN MAN, A. AND RASTANS, S.O.B. 2006. The effects of sowing depth and flooding on the emergence, survival and growth of *Fimbristylis miliacea* (L) Vahl. *Weed Biology and Management*, 6, 3, 157-164.
- BILLET, M F., LOWE, J A H., BLACK, K E. AND CRESSER, M S. 1997. The Influence of parent material on small-scale spatial changes in streamwater chemistry in Scottish upland catchments. *Journal of Hydrology*, Vol 187, 311-331.
- BOARDMAN, J., SHEPHEARD, M.L., WALKER, E. AND FOSTER, I.D.L. 2009. Soil erosion and risk assessment for on- and off-farm impacts: A test case using the Midhurst area, West Sussex, UK. *Journal of Environmental Management*, 90, 2578-2588.
- BOWES, P., and WALL, T. 1995. Rookhope's Landscape Legacies. North Pennines Heritage Trust, pp 32. ISBN 0951353527
- BREWARD, K. M., CHENERY, S. R. N. and BARLOW, T. S. 2009. Validation report for the analysis of aqueous solutions by the Agilent 7500 series ICP-MS. British Geological Survey, Internal Report IR/09/049.
- BYRNE, P., REID, I. AND WOOD, P.J. 2010. Sediment geochemistry of streams draining abandoned lead/zinc mines in central Wales: the Afon Twymyn. *Journal of Soils and Sediments*, 10, 683-697.
- CAMICI, S., TARPANELLI, A., Brocca, L., MELONE, F. AND MORAMARCO, T. 2011. Design soil moisture estimation by comparing continuous and storm based rainfall-runoff modelling. *Water Resources Research*, 47, Article Number W05527.
- CHAPMAN, B.M., JONES, D.R., JUNG, R.F. 1983. Processes controlling metal ion attenuation in acid mine drainage streams. *Geochim Cosmochim Acta*, 47, 1957-1973.
- CHARLATCHKA, R. AND CAMBIER, P. 2000. Influence of reducing conditions on solubility of trace metals in contaminated soils. *Water Air and Soil Pollution*, Vol 118, 143-167.
- CHARLTON, B. D., REEDER, S., ENTWISLE, D.C., CAVE, M.R., SHAW, R., TAYLOR, H AND WRAGG, J. 2003. Extraction and Characterisation of Interstitial Pore-Waters from the SCK-CEN Ophelie Mock-Up. Commissioned Report, CR/04/001.
- CHATAIN, V., SANCHEZ, F., BAYARD, R., MOSZKOWICZ, P. AND GOURDON, R. 2005. Effect of experimentally induced reducing conditions on the mobility of arsenic from mining soil. *Journal of Hazardous Materials*, 119-128
- CIRTAİN, M.C., FRANKLIN, S.B. AND PEZESHKI, S.R., 2004. Effects of nitrogen and moisture regimes on *Arundinaria gigantea* (Walt.) Muhl. seedling growth. *Nat. Areas J.* 24, 251-257.
- CODLING, E E. AND DAO, T H. 2007. Short term effect of lime, phosphorous and iron amendments on water-extractable lead and arsenic in orchard soils. *Communications in Soil Science and Plant Analysis*, Vol 38, 903-918.
- COMBER, D.D.W., MERRINGTON, G., STURDY, L., DELBEKE, K. AND VAN ASSCHE, F. 2008. Copper and zinc water quality standards under the EU Water Framework Directive: The use of a tiered approach to estimate the levels of failure. *Science of the Total Environment*, 403, 12-22.
- COURTWRIGHT, J. AND FINDLAY, S.E.G. 2011. Effects of microtopography on Hydrology, Physiochemistry and Vegetation in a Tidal Swamp of the Hudson River. *Wetlands*, 31 (2), 239-249.
- CUMMINGS, D.E., MARCH, A.E., BOSTICK, B., SPRING, S., CACCAVO, F., FENDORF, S. AND ROSENZWEIG, R.F. 2000. Evidence for microbial Fe(III) reduction in anoxic, mining impacted lake sediments (Lake Coeur d'Alene, Idaho). *Applied Environmental Microbiology*, 66 (1), 154-162.
- DENNIS, I.A., MACKLIN, M.G., COULTHARD, T.J. AND BREWER, P.A. 2003. The impact of the October-November 2000 floods on contaminants metal dispersal in the River Swale catchment, North Yorkshire, UK. *Hydrological Processes*, 17 (8), 1641-1657.

- DU LAING, G., VAN DE MOORTEL, A., LASAGE, E., TACK, F.M.G. AND VERLOO, M.G. 2008. Factors affecting metal accumulation, mobility and availability in intertidal wetlands of the Scheldt Estuary (Belgium). *Wastewater Treatment Plant Dynamics and Management in Constructed and Natural Wetlands*, 121-133.
- EC Dangerous Substances Directive (76/464/EEC).
- ENVIRONMENT AGENCY. 2008. Assessment of metal mining contaminated river sediments in England and Wales. *Science Report SC030136/SR4*.
- ENVIRONMENT AGENCY. 2009. Using Soil Guideline Values, *Science Report SC050021/SGV* introduction.
- EMMERSON, R.H.C., BIRKETT, J.W., SCRIMSHAW, M. AND LESTER, J.N. 2000. Solid phase partitioning of metals in managed retreat soil: field changes over the first year of tidal inundation. *The Science of the Total Environment*, 254, 75-92.
- ERBER, C AND FELIX-HENNINGSEN, P. 2001. Heavy metal contents and mobility of artificially inundated grasslands along river Weser, Germany. *Water, Science and Technology*, VOL 44 504-514.
- FORDYCE, F M., BROWN, S E., ANDER, E L., RAWLINS, B G., O'DONNELL, K E., LISTER, T R., BREWARD, N. AND JOHNSON, C C. 2005. GSUE: Urban geochemical mapping in Great Britain. *Geochemistry Exploration Environment Analysis*, VOL 5, 325-336.
- FUGE, R., PEARCE, F.M., PEARCE, N. J. G. AND PERKINS, W. T. 1993. Geochemistry of Cd in the secondary environment near abandoned metalliferous mines, Wales, *Applied Geochemistry*, Volume 8, Supplement 2, Pages 29-35, ISSN 0883-2927, 10.1016/S0883-2927(09)80006-1.
- GOLDEN, D C., TURNER, F T., SITTERTZBHATKAR, H AND DIXON, J B. 1997. Seasonally precipitated iron oxides in a vertisol of southwest Texas. *Soil Science Society of America Journal*, VOL 61, 958-964.
- HERNANDEZ, J.G., BRAUCHLI, T., BOILLAT, J.L. AND SCLEISS, A.J. 2011. Flood management in the Upper Rhone River basin: from forecast to decision. *Houille Blanche-Revue Internationale De L'Eau*. 2, 69-75.
- HILL, S. J., FISHER, A. AND CAVE, M. (2004) *In Soil and Environmental Analysis, Modern Instrumental Techniques* (Eds, Smith, K. A. and Cresser, M. S.) Marcell Dekker, New York, pp. 53-110.
- HILLIER, S., SUZUKI, K. AND COTTER-HOWELLS, J. 2001. Quantitative determination of Cerussite (lead carbonate) by X-ray powder diffraction and inferences for lead speciation and transport in stream sediments from a former lead mining area of Scotland. *Applied Geochemistry*, 16, 597-608.
- HUDSON-EDWARDS, K.A., 2003. Sources, mineralogy, chemistry and fate of heavy metal-bearing particles in mining-affected river systems. *Mineralogical Magazine*, 67, 205-217.
- HUDSON-EDWARDS, K.A., MACKLIN, M.G., BREWER, P.A., DENNIS, I.A. 2008. Assessment of Metal Mining-Contaminated River Sediments in England and Wales. Environmental Agency Science Report SC030136/SR4.
- HOLDGATE, M.W. 1979. A Perspective on Environmental Pollution, Cambridge University Press, Cambridge.
- HOWE, J, AND WHITE, I. 2002. The geography of the autumn 2000 floods in England and Wales: Causes and solutions. *Geography*, Vol 87, 116-124.
- KOBAYASHI, T., RYDER, D.S., RALPH, T.J., MAZUMDER, D., SAINTILA, N., ILES, J., KNOWLES, L., THOMAS, R. AND HUNTER, S. 2011. Longitudinal spatial variation in ecological conditions in an in-channel floodplain river system during flow pulses. *River Research and Applications*, 27 (4), 461-472.
- JOHNSON, K. and YOUNGER, P.L. 2002. Hydrogeological and geochemical consequences of the abandonment of Frazer's Grove carbonate hosted Pb/Zn fluor spar mine, North Pennines, UK. In: Younger, P.L. and Robins, N.S. (Editors). 2002. Mine water hydrogeology and geochemistry. Geological Society of London Special Publication, 198, 347-363.
- JOHNSON, C C., BREWARD, N., ANDER, E L. AND AULT, L. 2005. G-BASE: Baseline geochemical mapping of Great Britain and Northern Ireland. *Geochemistry Exploration Environment Analysis*, Vol 5, 347-357.
- JOHNSTON, S.G., KEENE, A.F., BURTON, E.D., BUSH, R.T. AND SULLIVA, L.A. 2011. Iron and Arsenic cycling in Intertidal Surface Sediments during Wetland Remediation. *Environmental Science & Technology*. 45 (6), 2179-2185
- JORGENSEN, N., LAURSEN, J., VIKSNA, A., PIND, N. AND HOLM, P E. 2005. Multi-elemental EDXRF mapping of polluted soil from former horticultural land. *Environment International*. Vol 31, 43-52.
- KENNEDY, A., ROGERS, S., SALLENGER, A., GRAVOIS, U., ZACHRY, B., DOSA, M. AND ZARAMA, F. 2011. Building destruction from waves and surge on the Bolivar Peninsula during hurricane Ike. *Journal of Waterway Port Coastal and Ocean Engineering – ASCE*. 137 (3), 132-141.
- LACAL, J., DA SILVA, M P., GARCIA, R, SEVILLA, M T., PROCOPIO, J R. AND HERNANDEZ, L. 2003. Study of fractionation and potential mobility of metal in sludge from pyrite mining and affected river sediments: changes in mobility over time and use of artificial aging as a tool in environmental impact assessment. *Environmental Pollution*, Vol 124, 291-305.
- LLOYD, J.R. AND OREMLAND, R.S. 2006. Microbial transformations of arsenic in the environment: From soda lakes to aquifers. *Elements*, 2, 85-90.
- LOEB, R., VAN DAALLEN, E., LAMERS, L.P.M. AND ROELOFS, J.G.M. 2007. How soil characteristics and water quality influence the biogeochemical response to flooding in riverine wetlands. *Biogeochemistry*, 85, 3, 289-302.
- MA, L Q. AND DONG, Y. 2004. Effects of incubation on solubility and mobility of trace metals in two contaminated soils. *Environmental Pollution*, Vol 130, 301-307.

- MACKLIN, M.G., BREWER, P.A., HUDSON-EDWARDS, K.A., BIRD, G., COULTHARD, T.J., DENNIS, I.A., LECHLER, P.J., MILLER, J.N AND TURNER, J.N. 2006. A geomorphological approach to the management of rivers contaminated by metal mining. *Geomorphology*, 79, 423-447.
- MACKLIN, M G. AND RUMSBY, B T. 2007. Changing climate and extreme floods in the British uplands. *Transaction of the Institute of British Geographers*, Vol 32, 168-186.
- MCGEECHAN, S L. 1996. Arsenic sorption and redox reactions: relevance to transport and remediation. *Journal of Environmental Science and Health Part A- Environmental Science and Engineering & Toxic and Hazardous Substance Control*. Vol 31, 2319-2336.
- MOALLA, S N. AND PULFORD, I D. 1995. Mobility of metals in Egyptian desert soils subject to inundation by Lake Nasser. *Soil Use and Management*. Vol 11, 94-98.
- NAGASAKA, S., KONO, E., WALLENDER, W.W., KANG, D-J., UEDA, S., ISHIKAWA, S. AND VIJARNSORN, P. 2009. Improvement of leaching methods for acid sulphate soil. 2009 ASABE Annual International Meeting, Reno, Nevada, June 21-June 24 2009.
- NAFTZ, D L., YAHNKE, J., MILLER, J. AND NOYES, S. 2005. Selenium mobilization during a flood experiment in a contaminated wetland: Stewart Lake Waterfowl Management Area, Utah. *Applied Geochemistry*, Vol 20, 569-585.
- NEUMEISTER, H., KRUGER, A. AND SCHNEIDER, B. 1997. Problems associated with the artificial flooding of floodplain forests in an industrial region in Germany. *Global Ecology and Biogeography Letters*, Vol 6, 197-209.
- NEWMAN, S. AND PIETRO, K. 2001. Phosphorous storage and release in response to flooding: implications for Everglades stormwater treatment areas. *Ecological Engineering*, Vol 18, 23-38.
- NORDSTROM, D.K. 2011. Hydrogeochemical processes governing the origin, transport and fate of major and trace elements from mine wastes and mineralized rock to surface waters, *Applied Geochemistry*, Volume 26, Issue 11, Pages 1777-1791, ISSN 0883-2927, 10.1016/j.apgeochem.2011.06.002
- OLDE VENTERINK, H., DAVIDSSON, T.E., KIEHL, K. AND LEONARDSON, L. 2002. Impact of drying and re-wetting on N, P and K dynamics in a wetland soil. *Plant and Soil*, 243, 119-130.
- PAGNEUX, E., GISLADOTTIR, G. AND JONSDOTTIR, S. 2011. Public perception of flood hazard and flood risk in Iceland: a case study in a watershed prone to ice-jam floods. *Natural Hazards*. 57 (1), 269-287.
- PANT, H K., NAIR, V D., REDDY, K R., GRAETZ, D A. AND VILLAPANDO, R R. 2002. Influence of flooding on phosphorous mobility in manure impacted soil. *Journal of Environmental Quality*. 31, 1399-1405.
- PAPPENBERGER, F., THIELEN, J. AND DEL MEDICO, M. 2011. The impact of weather forecast improvements on large scale hydrology: analysing a decade of forecasts of the European Flood Alert System. *Hydrological Processes*. 25 (7), 1091-1113
- PHIPPS, G.C., BOYLE, D.R. AND CLARK, I.D. 2004. Groundwater geochemistry and exploration methods: Myra Falls volcanic massive-sulphide deposits, Vancouver Island, British Columbia, Canada. *Geochemistry: Exploration, Environment, Analysis*, 4 (4), 329-340.
- PARKHURST, D. L., AND APPELO, C. A. J. 1999. Users guide to PHREEQC (Version 2). A computer program for speciation, batch-reaction, one dimensional transport, and inverse geochemical calculations. U.S. Geological Survey Water-Resources Investigations Report 99-4259, 312 p.
- PULFORD, I.D., MACKENZIE, A. B. DONATELLO, S., AND HASTINGS, L. 2009. Source term characterisation using concentration trends and geochemical associations of Pb and Zn in river sediments in the vicinity of a disused mine site: Implications for contaminant metal dispersion processes, *Environmental Pollution*, 157 (5), 1649-1656.
- REYNOLDS, J.G., NAYLOR, D.V. FENDORF, S.E. 1999. Arsenic sorption in phosphate-amended soils during flooding and subsequent aeration. *Soil Science Society of America Journal*, Vol 63, 1149-1156.
- ROBINS, P.E., DAVIES, A.G. AND JONES, R. 2011. Application of a coastal model to simulate present and future inundation and aid coastal management. *Journal of Coastal Conservation*. 15 (1), 1-14
- ROMANESCU, G AND NISTOR, I. 2011. The effects of the July 2005 catastrophic inundations in the Siret River's Lower Watershed, Romania. *Natural Hazards*. 57 (2), 345-368.
- ROTKIN-ELLMAN, M., SOLOMA, G., GONZALES, C.R., LOVELL, A. AND MIELKE, H.W. 2009. Arsenic contamination in New Orleans soil: Temporal changes associated with flooding. *Environmental Research*, 110, 19-25.
- ROWLAND, H.A.L., PENDRICK, R.L., POLYA, D.A., PANCOST, R.D., VAN DONGEN, B.E., GUALT, A.G., VAUGHAN, D.J., BRYANT, C., ANDERSEN, B AND LLOYD, J. 2007. The control of organic matter on microbially mediated iron reduction and arsenic release in shallow alluvial aquifers, Cambodia. *Geobiology*, 5 (3), 281-292.
- SCHREIBER, M., OTTO, M., FEDOTOV, P S. AND WENNRICH, R. 2005. Dynamic studies of the mobility of trace elements in soil and sediment samples influenced by dumping of residues of the flood in the Mulde river region in 2002. *Chemosphere*, Vol 61, 107-115.
- SIMPSON, P R., EDMUNDS, W M., BREWARD, N., COOK, J M., FLIGHT, D M F., HALL, G E M. AND LISTER, T R. 1993. Geochemical mapping of streamwater for environmental studies and mineral exploration in the UK. *Journal of Geochemical Exploration*, Vol 49, 63-89.
- SIMPSON, P R., BREWARD, N., FLIGHT, D M F., LISTER, T R., COOK, J M, SMITH, B. AND HALL, G E M. 1996. High resolution hydrogeochemical baseline mapping of streamwater of Wales, the welsh borders and west midlands region. *Applied Geochemistry*, Vol 11 (5), 621-632.

- SIMPSON, S, FITZPATRICK, R, SHAND, P, ANGEL, B, SPANARO, D, MERRY, R AND THOMAS, M. 2008. Acid, Metal and Nutrient Mobilisation following rewetting of acid sulphate soils in the Lower Murray. CSIRO Land and Water Report Number CLW27/08
- SMIT, M P J., GROTENHUIS, T., BRUNING, T., BRUNING, H. AND RULKENS, W H. 2008. Desorption of dieldrin from field aged sediments: Simulating flood events. *Journal of soils and sediments*, 8, 2, 80-85.
- SNYDER, R.L. AND BISH, D.L. 1989. Quantitative analysis. In: Bish, D.L., Post, J.E. (Eds), *Modern Powder Diffraction, Reviews in Mineralogy*, Volume 20, Mineralogical Society of America, USA, pp. 101-144 (Chapter 5).
- STRIKER, G.G. 2008. Visiting the methodological aspects of flooding experiments: Quantitative evidence from agricultural and ecophysical studies. *Journal of Agronomy and Crop Science*, 194, 4, 249-255.
- SMITH, K.S., 1999, Metal sorption on mineral surfaces: an overview with examples relating to mineral deposits, in Plumlee, G.S., and Logsdon, M.J., eds., *The environmental geochemistry of mineral deposits*: Society of Economic Geologists, Inc.
- TACK, F., JANSSEN, C. AND MEIRE, P. 2006. Changes in metal biogeochemistry resulting from wetland creation: bioavailability, toxicity and risk "WETMAT": final report. Belgian Science Policy: Brussel, Belgium.
- THOMPSON, M. AND WALSH, J. M. (1983) In *A Handbook of Inductively Coupled Plasma Spectrometry*, Vol. 144-145 Blackie, Glasgow and London.
- DI TORO, D.M., MAHONY, J.D., HANSEN, D.J., AND BERRY, W.J. 1996. A model of the oxidation of iron and cadmium sulfide in sediments. *Environ. Toxicol. Chem.* 15, 2168-2186.
- UNGER, I.M., KENNEDY, A.C. AND MUZIKA, R.M. 2009. Flooding effects on soil microbial communities, *Applied soil ecology*, 42, 1, 1-8.
- VAN DEN BERG, G A., LOCH, J P G. AND WINKELS, H J. 1998. Effect of fluctuating hydrological conditions on the mobility of heavy metals in soils of a freshwater estuary in the Netherlands. *Water Air and Soil Pollution*, Vol 102, 377-388.
- VAN DER GEEST, G.G. AND LEON PAUMAN, M. 2008. Dynamics of metal availability and toxicity in historically polluted floodplain sediments. *Science of the Total Environment*, 406, 419-425.
- WAKITA, H. AND SCHMITT, R.A. 1970. Cadmium. In *Handbook of Geochemistry*. WEDEPOHL K.H.(editor), Vol. 2, Ch. 48, Springer.
- WEBER, F.A., VOEGELIN, A. AND KRETZSCHMAR, R. 2009. Multi-metal contaminated dynamics in temporarily flooded soil under sulphate limitation. *Geochimica et Cosmochimica Acta*. 73 (19), 5513-5527.
- WEBER, F.A., HOFACKER, A.F., VOEGELIN, A. AND KRETZSCHMAR, R. 2010. Temperature Dependence and Coupling of Iron and Arsenic Reduction and Release during Flooding of a Contaminated Soil. *Environmental Science & Technology*, 44 (1), 116-122.
- WEBSTER, J, WEBSTER, K, NELSON, P AND WATERHOUSE, E. 2002. The behaviour of residual contaminants at a former station site, Antarctica. *Environmental Pollution*, 123, 163-179.
- WILBY, R.L., NICHOLLS, R.J., WARREN, R., WHEATER, H.S., CLARKE, D. AND DAWSON, R.J. 2011. Keeping nuclear and other coastal sites safe from climate change. *Proceedings of the Institution of Civil Engineers-Civil Engineering*. 164 (3), 129-136
- WRAGG, J. 2009. BGS Guidance Material 102, Ironstone Soil, Certificate of Analysis. *British Geological Survey Internal Report*, IR/09/006.
- YIN, Z.E., YIN, J., XU, S.Y. and WEN, J.H. 2011. Community based scenarion modelling and disaster risk assessment of urban rainstorm waterlogging. *Journal of Geographical Sciences*. 21 (2), 274-284.
- ZHAO, Y, K., ZHANG, X, Q. AND MARRIOT, S. 2009. Phase change and remobilisation of heavy metals in floodplain sediments of UK river systems after frequent flooding. *Progress in Environmental Science and Technology*, Vol II, parts A and B, 979-985.